

Operation considerations for pre-tensioning mooring systems

Thesis report

Hugo Kerckhoffs

Analysis of current pre-tensioning operations by analysing static and dynamic loads



Operation considerations for pre-tensioning mooring systems

Thesis report

by

Hugo Kerckhoffs

preparation to obtain the degree of Master of Science

at the Delft University of Technology and the Norwegian University of Science and Technology.

To be defended publicly on Wednesday 6th of July, 2022 at 10:00.

Student number TU Delft:	4436962
Student number NTNU Trondheim:	557406
Project duration:	September 28, 2021 – July, 2022
Thesis Supervisors:	dr. ir. G. Lavidas, TU Delft Prof. dr. ir. K. Halse NTNU Ir. J. Dijkstra Huisman Dr. Ing. S. Schreier TU Delft Prof. dr. ir. K. Larsen NTNU

An electronic version of this thesis is available at the TU Delft repository.
Huisman internal information is censored. Full version is available upon request.



Preface

This thesis is the result of my internship at Huisman and was the final requirement for obtaining a master's degree in European Wind Energy at Delft University of Technology (TU Delft) and Norges Teknisk Naturvitenskapelige Universitet (NTNU). I could not have done it without several people's help and support, and I would like to thank them sincerely for their contributions. First and foremost, I would like to thank my supervisors, Jeroen Dijkstra and George Lavidas for their insightful assistance. Jeroen Dijkstra has been very helpful, especially with regard to his knowledge of the offshore industry and he gave me invaluable guidance in solving critical issues. Similarly, George Lavidas, has my gratitude for all his efforts, expertise and constructive criticism, all of which were of great help. It has brought lots of guidance in structuring the project and the final report. Thirdly, I would like to express my gratitude to Prof. Karl H. Halse for his helping hand and for giving me so confidence in times when I needed it. Furthermore, I would like to thank Prof. Sebastian Schreier for supervising this project. Critical questions during meetings helped to challenge my own thought process and keep the main objective in mind. This academic expertise and feedback were of great help during the process. Finally, I would like to thank Kjell Larsen for his insights into the industry and lectures on marine operations.

*Hugo Kerckhoffs
Delft, June 2022*

Abstract

In recent years, the demand for renewable energy has increased significantly because of its lower environmental impact than conventional energy technologies. As a result, wind power is one of the most important renewable energy sources. As land-based turbines have reached their maximum potential, recent market trends are moving into deeper waters with higher capacity turbines.

The design of a floating offshore wind turbine (FOWT) foundation poses technical challenges. Mooring design, installation operations and the fact that it is a new engineering field, to name a few. Moreover, as mooring design for FOWT is still at an early stage of development, cost-effective installation remains one of the critical issues. After the FOWT is towed to the site, the mooring lines are hooked up, and one line is usually shortened. This can be performed in three ways: By seabed tensioning, inline tensioning or tensioning at the fairlead. In this investigation, details about mooring installation processes are collected from interviews, academic papers, manuals and videos to investigate differences between mooring system installations and ultimately figure out how pre-tensioning these systems can be carried out most effectively.

This work presents a comparison between these three existing methods for the final phase of mooring installation. To perform a quantitative study, the Umaine VoltturnUS-S 15MW floater is considered. Current modelling techniques are expanded to allow for the static simulation of the rotations or sliding at the tensioning device. The model framework is used to find the static equilibrium and tensions at different phases in the installation operations. Additionally, an alternative mooring configuration is proposed with synthetic inserts to verify whether the tension is dependent on the mooring configuration. Finally, the dynamics between the anchor handling vessel(AHV), the FOWT and the mooring chains are modelled as a linear mass-spring system.

Vessel responses and work wire tensions are compared against each other for identical environmental conditions and equipment specifications. Based on simulation results, it is found that the seabed tensioner causes little dynamic relation between the AHV and the floater and was not further investigated. Inline tensioning showed to be the method that requires the lowest tensions in the AHV work wire. Fairlead tensioning was found to be discouraged since the high required bollard pull forces. This issue is mitigated by a proposed new concept of fairlead tensioning. When the chain is hauled in from above the fairlead by a vessel crane or A-frame, it is possible to tension effectively without fuel-intense bollard pull.

Nomenclature

Abbreviations

AHV	Anchor handling vessel
COG	Center of gravity
DNV	Det Norske Veritas
DOF	Degree of freedom
FEM	Finite element method
FOWT	Floating offshore wind turbine
kn	knots; Nautical miles per hour
LCOE	Levelized costs of energy
NM	Nautical mile
O&G	Oil and gas
RAO	Response amplitude operator
ROV	Remotely operated underwater vehicle, technically ROUV
TLP	Tension leg platform
Tn)	Metric tonne force
TRL	Technology Readiness Level
UMaine	University of Maine

Symbols

ω Wave frequency

ϕ	Phase shift
ρ	Water density
ζ	Wave height
A	Cable cross-sectional area
CB	Seabed contact friction coefficient
E	Young's modulus
g	Acceleration due to gravity
H	Horizontal fairlead force
h	Vertical fairlead excursion
H_a	Horizontal anchor force
L	Unstretched line length
l	Horizontal fairlead excursion
L_B	Line length resting on the seabed
s	Unstretched distance from the anchor ($0 \leq s \leq L$)
V	Vertical fairlead force
V_a	Vertical anchor force
W	Cable weight-per-unit length in fluid
X_0	Horizontal force transition point for $H(s) > 0$

Contents

Preface	i
Abstract	ii
1 Introduction	1
1.1 Background	1
1.2 Problem statement	2
1.3 Objectives	2
1.4 Approach to research	3
1.5 Document structure	3
2 Literature analysis	5
2.1 Floating Wind Turbines	5
2.2 Mooring systems	7
2.2.1 Mooring examples	8
2.3 Installation of semi-submersible floating turbines	11
2.3.1 Base case introduction	11
2.3.2 Anchor deployment	12
2.3.3 Proof loading	13
2.3.4 Mooring line pre-lay	13
2.3.5 Towing and line transfer	14
2.3.6 Hook-up	14
2.3.7 Pre-tensioning using seabed tensioner	15
2.4 Variation in pre-tensioning	15
2.5 Simulation of catenary systems	17
2.6 Conclusion literature analysis	20
3 Model description for a semi-submersible based FOWT	22
3.1 Model architecture	22
3.2 The main script: The user interface	23
3.3 System builder: Structured configuring of mooring systems	23
3.3.1 Pre-build	24
3.3.2 Tensioner specific builds	24
3.3.3 Finish-build	25
3.4 Systems class: Storing models of mooring configurations	25
3.4.1 Lines	25
3.4.2 Points	25
3.4.3 Bodies	26
3.4.4 Finding the system equilibrium	26
3.5 Floating Bodies	26
3.6 The 'addWheel' module: Simulating the pre-tensioner	26
3.7 Description of modelled scenarios	28
3.7.1 Floating turbine	28
3.7.2 Mooring system	30
3.7.3 Vessel	31
3.7.4 Tensioning equipment	32
3.8 Conclusion	33
4 Static simulation results	34
4.1 Modelling of the installed floating turbine as validation	34
4.2 Results for the three pre-tensioning concepts	35

4.3	Line tensions	35
4.4	Load development	37
4.5	Sensitivity study: Advanced mooring system with inserts	38
4.5.1	Setting up the mooring system.	38
4.5.2	Pre-tension load development results	39
4.6	Conclusions on static modelling	41
5	Model extension for dynamic simulation	42
5.1	Dynamic simulation methodology	42
5.2	Dynamic modelling components	43
5.2.1	Floating turbine	44
5.2.2	Tensioning equipment	46
5.2.3	Vessel	47
5.2.4	Combined equation of motion	48
5.2.5	Mooring system.	48
5.3	Solving the equation of motions	50
5.4	Natural frequencies.	52
5.5	Code structure	53
6	Results and validation	54
6.1	Validation of dynamic model	54
6.1.1	Generation of equivalent mooring stiffness and natural frequency.	54
6.1.2	Motion comparison for the installed case without pre-tensioner	55
6.2	Dynamic responses while inline tensioning	56
6.3	Dynamic responses while fairlead tensioning	57
6.4	Assessment of spring linearity	59
6.4.1	Unexpected high stiffness during the finish of fairlead tensioning	59
6.4.2	Assumption of catenary shape verification	61
7	Practical implications and pre-tension trade-off	63
7.1	Seabed tensioning	63
7.2	Inline tensioning	63
7.3	Fairlead tensioning	64
7.4	Trade off	65
8	Conclusion and recommendations	66
8.1	Conclusion	66
8.1.1	Characteristics and problems of pre-tensioning.	66
8.1.2	Environmental conditions and potentially critical events	67
8.1.3	Suggested improvements for pre-tensioning	68
8.2	Recommendations	69
8.2.1	Recommendations for scientific research	69
8.2.2	Recommendations for Huisman	69
8.3	Discussion	69
8.3.1	Limitations	69
8.3.2	Scientific contributions	70
	Bibliography	71
	List of Figures	74
	List of Tables	76
A	Complete RAO descriptions	77
A.1	FOWT	77
A.2	AHV	79
B	Matrix specifications	80
B.1	Inline tensioning	80
B.2	Fairlead tensioning	81

Introduction

1.1. Background

Energy is a topic of great concern in human societies, where fossil fuels like oil and gas continue to dominate. However, the growing awareness that fossil fuels are at the heart of many environmental problems, such as the greenhouse effect and air pollution, has led to the ever-increasing interest in renewable energy, like that which can be derived from wind.

The wind industry has developed very fast in recent years. Having begun with primarily onshore wind turbines, in recent years, offshore turbines have increased in popularity, first in shallow water and then in deep water. The reason for this progressive change is that the available site for onshore wind energy is depleting because turbines near inhabited regions are often seen as visual pollution. Besides, not every area has a high enough wind energy potential for turbines to be economically viable. Hence the shift to offshore wind farms.

The offshore environment solves the issue of visual pollution and has a higher potential energy yield than onshore turbines due to higher and more constant wind speeds [1]. However, offshore wind energy also brings challenges. The turbines are subject to more severe environmental loading offshore than onshore, and the foundations experience higher loads due to the hydrodynamic pressure of waves. In addition, current wind turbine technology means that they can only be installed in relatively shallow waters in order to be viable. If deepwater wind farms are to grow, more robust and/or inventive turbine designs are required. One of the solutions that have been put forward is the deployment of floating offshore wind farms.

Floating offshore wind energy is still a relatively new concept and has not been done on a large scale [2]. Therefore, many of the criteria of wind farm performance are based on small examples. As a result, the floating wind energy industry is missing critical field data for actual power production and has little to go on when making projections and plans.

In order to generate the necessary data and gain experience, full-scale model floating wind farms are currently being developed and tested. The first fully operational floating offshore wind farms are also being deployed. The three biggest wind farms have 11, 5 and 3 turbines, with larger quantities of turbines per farm expected in the near future [2]. It is expected that the cost of floating wind energy will reduce when the number of produced floaters increases and the fabrication matures. However, with the wide variety of concepts and stakeholders, this quantity advantage is far from being found.

Within the many concepts that are being investigated, there are a couple of similarities. One similarity is that all floating structures (Semi-submersible, Spar, and TLP) are positioned by a station-keeping system. Mooring systems and thrusters are the traditional ways of station keeping, but for floating wind turbines, mooring systems are favoured. A mooring system consists of several cables with their upper ends attached to different positions of the floater and their lower ends anchored to the seabed. Different types of mooring systems exist, but current prototypes are quite similar overall. The mooring system is designed to avoid collisions with adjacent structures and stretch electrical export cables. [3].

Installation of mooring systems for floating wind is currently complex and project-specific, often based on available resources and experiences from the oil and gas industries. For instance, dedicated vessels have been built for the oil and gas industry to deploy anchors, and a large fleet exists that can perform such operations. Wind turbine installation is new, and such a standardised fleet is not present. As a result, wind farm owners are secretive about the exact method and costs involved in setting up and maintaining a deep water wind farm. However, it is a given that offshore operations are costly, and any opportunity to decrease installation costs should be investigated.

One such investigation was conducted by the Energy Research Centre of the Netherlands, which presented a breakdown of the modelled capital expenditure (CAPEX) for the Gemini wind farm off the Dutch coast [4]. Both bottom-fixed and floating substructures were modelled, and the differences in cost origins can be observed. While the exact breakdown of costs varies from project to project depending on the site-specific conditions and technologies adopted, the research showed a 31% increase in installation costs.

The data of the Gemini farm shows that the mooring system alone accounts for 10% of the cost, and the complete installation accounts for a further 10% of the cost. Myhr [5], analysed and compared the costs of floating wind farm concepts. Using a model, Myhr could vary parameters like farm size and depth to see how costs might change. The model was based on a simplified mooring system in order to estimate costs, thus making it possible to simulate the installation and make a cost estimate, assuming onshore assembly, towing and hook-up. The result of the study was that the mooring system and installation account for between 4 and 15% of the total cost. Therefore, investigating potential improvements to mooring installations was key to the growth of the deep water floating wind farm sector.

1.2. Problem statement

The installation of a floating offshore wind farm involves the careful consideration of numerous operations. Many approaches to installation can be adopted and can influence early design decisions.

In the future, wind turbines are expected to continue to grow, reaching up to 15 MW. The costs of installation and the cost of the mooring system are expected to grow accordingly. For a more economical and faster installation procedure, new installation technologies are required. Operations from oil and gas need to be closely analysed and tailored to effectively apply to the wind industry.

To optimise the installation, it is necessary to understand the available options. For example, options that are currently expensive might benefit from being manufactured at a larger scale, leading to a cost reduction. What's more, the installation methods chosen for any given wind farm project need to be appropriate for the specific requirements of each farm and sufficiently flexible to make space for a range of anticipated concepts.

While mooring equipment is typically pre-installed on the seabed before the floating turbine is towed to the site, mooring installation processes can be divided into multiple sub-operations, all of which can be thoroughly analysed. Once on-site, the floating turbine is hooked up to the mooring system. To facilitate this operation, one of the mooring lines has extra slack to lower the tensions while hooking up. This extra slack can extend over a distance of up to 100 meters. This slack chain is hauled in to get the required mooring stiffness and maximum offset. In the oil and gas industry, floating rigs usually have chain windlasses or jacks that haul in the chain, and the rigs can be repositioned multiple times in their lifespan. For floating wind, mooring lines generally only need to be pre-tensioned once. The heavy and expensive equipment on the floater is useless for the rest of its lifespan.

Generally, three different concepts exist to pre-tension a mooring system. The main difference lies in where the mooring leg is shortened: On the seabed, somewhere suspended or at the floater fairlead. The requirements of this operation are very different than for the installation within oil & gas. It is to investigate the differences to determine how pre-tensioning could be done most effectively in the future.

1.3. Objectives

The objective of this research is to investigate the different pre-tensioning approaches and ultimately develop a proposal for a more efficient pre-tensioning methodology. To bound the scope of the research, the following research questions were chosen:

"How do procedures and required equipment influence the pre-tensioning operation to ultimately reduce the duration and cost of installing mooring systems for floating wind?"

This question is broken down into three sub-questions:

- What are the details for a typical FOWT pre-tension operation, what critical events must one account for, and how is this different from the oil and gas industry?
- What is the relationship between environmental conditions and potentially critical events? What are the corresponding limiting (response) parameters?
- To decrease the overall installation time of a mooring system, what type of pre-tensioning improvements show the highest potential?

The questions result from a literature study performed in preparation for the research. The approach to how the questions are answered is described in the following section.

1.4. Approach to research

This section describes the approach to answering the research questions. First, fundamental introductory knowledge on floating wind energy and on mooring equipment is reviewed. A stand-alone literature review has been written about floating wind, mooring equipment and installation in preparation for the empirical research. It was concluded that the study would require a base case to perform a quantitative comparison between pre-tensioning methods. An investigation was conducted to select a base case by comparing the different types of substructure and mooring configurations for floating offshore wind turbines. The goal of this base case is to represent as many varieties of future floating installations as possible. For this base case, three static model pre-tension methodologies were simulated and compared, with the mooring configurations modelled as stand-alone and while they were being pre-tensioned. The goal of such static modelling is to identify which pre-tension methods require high tensions. A sensitivity analysis was then performed to see how alternative mooring systems influence the static loads.

While static modelling helps form a baseline, pre-tension methods might behave differently when exposed to the more erratic pressure of waves. To get a better insight into vulnerability into resonance, the dynamic tensions due to waves were thus investigated. Finally, further practical considerations are explored in detail to present a complete comparison of static and dynamic tensions and their practical implications.

1.5. Document structure

The following is a summarised overview of the structure of this dissertation to provide a clear idea of which subjects are addressed in which chapters.

Chapter 1 introduces the background of the floating wind turbine development, the knowledge gap around pre-tensioning and objectives as well as approaches of this project.

Chapter 2 provides a brief overview of the mooring system for FOWTs and moreover presents installation details of an example floating turbine.

Chapter 3 presents the static model to compare the pre-tensioning concepts on static loads. It describes the floating turbine, mooring system, installation vessel and tensioning equipment. The inclusion of the sliding elements in catenary systems is developed.

Chapter 4 contains the results of the static load modelling. The load developments within the pre-tensioning are compared.

Chapter 5 provides details and results of a dynamic simulation and answers the question of whether the pre-tensioning operations could lead to critical dynamic situations.

Chapter 6 highlights the key findings. A complete comparison of the techniques is presented.

Chapter 7 concludes the research and provides recommendations and discussion.

All chapters in this thesis are ordered to obtain a structured step-wise build-up to draw the final conclusions. General background information, verification of methods and extensive descriptions and results of all simulation load cases that are not specifically addressed in the main report are presented in the appendices. At the end of the report, references, a list of figures and a list of tables are included.

2

Literature analysis

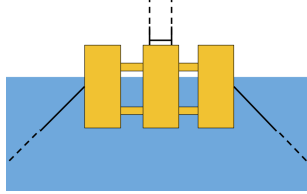
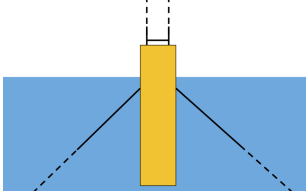
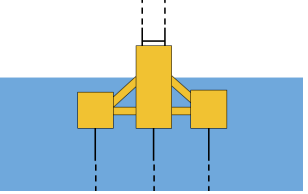
This chapter is designed to fulfil three purposes. Firstly, existing concepts of floating wind substructures and mooring systems are introduced. Secondly, the installation processes of mooring systems are presented. One typical FOWT is used as an example; for that turbine, the installation is laid out step by step with a high level of detail. Thirdly, this chapter draws on the existing literature to elaborate on the theory needed to create a model that can be used to simulate mooring line configurations.

2.1. Floating Wind Turbines

Offshore wind turbines come in a variety of shapes. A single slender tower with a horizontal axis and a three-bladed rotor is most common. Other concepts, like two turbines on one substructure or rotor grids, have a lower technology readiness level (TRL) and are not investigated here.

Within the current market, there is little convergence on which floater concepts are preferable, and floaters are being explored worldwide. In 2015, the Carbon Trust Market Report reviewed 33 different concepts[6] The three most mature concepts, based on their TRL, are selected and compared in table 2.1.

Table 2.1: Overview of floating substructure concepts

Concept	Semi-Sub	Spar	TLP
Illustration (For clarity, only two mooring lines are drawn)			
Structure	Complex structure configuration, good in shallow areas and large size structure	Simple structure, yet very large	Lightweight structure but high mooring line tensions
Installation & Transport	Can change draught for fast towing or stability. Convenient next to quays.	Towing either on it's side or stand up. Requires deep water for assembly.	Some TLPs are unstable without mooring, that greatly increases installation complexity. Challenging installation process.
Natural stability	Buoyancy devices with large arm provides stable platform	Ballast generates restoring moment when inclined	Taut mooring lines keep the platform upright.
Risks	Relatively low. Failure of mooring	Relatively low. Failure of mooring	High. Failure of mooring system leads to total loss turbine
Commercial examples for (≈10MW turbine)	Inocean designed concept for 12 MW turbines [7]. Three 8.4 MW FOWTs are supported by Windfloat developed by Principle Power with active ballast.	Hywind Tampen has eleven 8 MW turbines on spar floaters	SBM TLP platform for 8 MW turbines. Will be installed in France in 2023
TRL development:	8(Pilot) since 2020. Scheduled to be 9(Pre-commercial) in 2025/2026	8(Pilot) since 2017. Scheduled to be 9(Pre-commercial) in 2022	4(tank testing) since 2016. Scheduled to be 9 (Pre-commercial) in 2022

The table illustrates the differences and similarities between the concepts. However, this comparison is conceptual and quantifying the differences in floater mass, floater motion or mooring tension would be helpful to put the floater configurations in perspective. At the Norwegian University of Science and Technology (NTNU), three investigations were conducted into substructures to support a DTU 10MW reference turbine; a semi-submersible [8], a spar [9] and a TLP [10]. The three concepts are designed for a location on the west coast of Norway with a water depth of 200 meters. Significant differences can be observed between each case, particularly in terms of the floater offset and mooring line tensions. A very striking difference lies in the maximum mooring line tension between the TLP and the other two concepts. This is explained by the high pre-tension that is required for a TLP.

Table 2.2: Summary of the results of three NTNU researches to compare substructure types

NTNU Concept	Semi-Sub	Spar	TLP
Total mass of floater and sub-structure[Tn]	7 708	13 405	9 293
Mooring configuration	3 x catenary with 861 m 153 mm chain. 1 001 kN pretension.	Oversimplified mooring without proper clarification. Thesis does not propose suitable mooring	3 x steel tendon with 89 mm thickness and 1.35 m radius. 27 526 kN pretension.
Mean surge at rated conditions [m]	7	14	3
Max mooring line tension in extreme conditions [kN]	5 886	3 237	37 474

The thesis that described the spar floater did not propose a suitable mooring system but extrapolated and simplified a mooring system that was designed for 320 meters depth in another research. The

reason that the surge is rated wind speed and the thrust at an extreme event is that the mean thrust of the wind turbine is highest around its rated velocity. The mean surge is a good indicator for the designed offset that the mooring allows. A usual limitation of this offset is the flexibility of electrical connection [3]. The maximum mooring line tensions occur in all three cases in the most extreme wave conditions. It is typical that the tensions for the TLP concept are significantly higher since it uses continuous tension for the righting stability. On the other hand, the other two are inherently stable and use the mooring solely for station keeping [11]. From the maximum offset, it can be deduced that the mooring stiffness of the TLP is higher than those of the spar and the semi-sub. For equal environmental conditions, it is therefore logical that a stiff mooring system not only has a low offset, but also high tensions.

Although floating wind turbines are a recent development, the oil- and gas industry has been deploying floating structures since the 1960s [3]. It is beneficial for the development of FOWTs that many aspects of engineering are similar to that of oil- and gas-related projects. However, some differences exist and three main differences are pointed out: Firstly, the financial margins on wind energy are lower, therefore, the whole supply chain of the FOWT is looking for cost-effective installation. [12]. Secondly, if the FOWT industry will grow as expected, it is wise to spend resources on developing good installation techniques, since they could be performed very repetitively. [13] Finally, failure of a mooring line of manned oil and gas platforms may cause severe consequences. Oil and gas rigs are usually manned and mooring failure could lead to fatalities. In the event of a mooring failure for a platform with risers, it is likely that they will break too and hence risking oil pollution in the seawater. Therefore, mooring line requirements for oil and gas rigs are more strict.

2.2. Mooring systems

Depending on their profiles and configurations, mooring systems can be grouped into two categories: either catenary or taut. For catenary systems, the suspended line between the floating unit and the seabed is shaped like a free-hanging line with a section that lies on the seabed. By contrast, a taut leg mooring system has mooring lines that arrive at an anchor at an angle. The anchor points in a taut leg mooring system must be capable of withstanding horizontal and vertical forces. In taut leg mooring, the restoring forces are generated by the elasticity of the mooring line.

Finally, a combination of taut and catenary systems also exists. When all-chain catenary designs become too heavy in deep waters, a mooring designer might insert wire rope segments made of steel or synthetic fibres. The chain segment still provides a catenary effect, while the insert reduces the overall tension on the floater. This is often referred to as a semi-taut mooring system.

Figure 2.1 demonstrates the different types of mooring lines, their shape as seen from the side and above, and the advantages and disadvantages of each. In the following sub-sections, each type of mooring system is analysed in turn, beginning with a catenary system, to provide greater detail.

Name	Side view	Top view	Advantages	Disadvantages
taut mooring			<ul style="list-style-type: none"> + Good in deep waters + Can be designed redundant 	<ul style="list-style-type: none"> - Anchors required to withstand vertical forces - Very high mooring tensions
Spread catenary			<ul style="list-style-type: none"> + Can be redundant + Very common 	<ul style="list-style-type: none"> - Heavy in deep waters - Large seabed footprint
Semi - taut		<div style="margin-top: 5px;"> <ul style="list-style-type: none"> — Chain — Rope or wire — Tendon </div>	<ul style="list-style-type: none"> + Catenary stiffness effect + Lighter mooring leg than sole chain 	<ul style="list-style-type: none"> - Many components/ connectors

Figure 2.1: Mooring concepts: Taut moorings, catenary moorings and their combination: Semi-taut

Catenary

Catenary mooring is the oldest and yet still the most common mooring system. Its name comes from the mooring line's weight forming a curved catenary shape, which generates the necessary force to

cope with the floater's static offset and dynamic motions. Restoring force is mainly obtained by lifting and lowering the weight of the mooring line. For this system to be effective, a large part of the anchor line must lie on the sea bed to ensure that the anchors are kept in position. Clump weight or buoyancy modules can complement the catenary system. Clump weights are additional masses that increase the tension on the line and thus the restoring force applied to the floater when it moves away from its standard location[14]. Buoyancy modules make it possible to reduce the mooring line dynamics and line tension[15].

Taut

Taut mooring systems are those where mooring stiffness is primarily provided by the line's tensile stretch. The lines have a low net weight, thereby eliminating catenary action. Synthetic fibres and steel wire rope are most common for this type of mooring. Synthetic fibres emerge in deep water(300 m +) or when very high mooring stiffness is required. Steel wire has a better resistance against abrasion. In shallower water or when more flexibility is required, polyester segments can be added to act as springs.

Taut mooring can also be designed with vertical cables. Thus vertical tension mooring is a sub-category of taut systems. Vertical mooring lines, also called tendons, imply that each turbine can be installed with a smaller footprint (the space that the turbine occupies at the base of the mooring system). What's more, the platform on which the turbines are erected is more stable and the system requires less mooring line length. The platform that is purposely designed for this kind of mooring is called a Tension Leg Platform (TLP). However, the large amount of vertical tension means that more complex and costly anchors are needed, thereby limiting the anchoring options and making the installation procedure more complex. It is partly for this reason that taut mooring is rare in FOWT. 4C Offshore concluded trends in the industry based upon 278 project proposals, of which only 12 are TLPs [16]. Because the installation of TLPs and the working principle of the mooring is so different to catenary and semi-taut systems, TLPs will not be further elaborated on.

Semi-taut

The semi-taut system combines the taut mooring system and catenary mooring system, wherein some parts of the mooring system are taut, and others are catenary. The semi-taut and taut systems are better suited for use in deep water than catenary systems. The semi-taut system and taut system have shorter mooring lines and require less seafloor space or seafloor spread than the catenary system. The shorter mooring lines result in material savings.

Generally, the taut and semi-taut systems are lighter and cheaper designs than the catenary systems for deep water applications. In the following section, three operational FOWTs are analysed to gain an understanding of current standard practices.

2.2.1. Mooring examples

To understand the current developments in mooring installation, two existing and one planned farm are analysed. The goal is to identify the mooring equipment, installation methods and underlying reasoning. Many sources were consulted so as to construct complete pictures of examples of FOWT mooring as involved stakeholders are not very keen on sharing all the information at once. The lecture slides from Kjell Larsen from Equinor and complementary discussions [17] have been very helpful. Additionally, conversations with and installation documentation from Kevin Hart from Vryhof [18] [19] also contributed to finding the bigger picture. Other sources include papers that are written in collaboration with Windfloat or Stiesdal [20],[21]. For each case, a brief summary and sketch are provided. The first example listed below is Hywind Scotland.

Hywind Scotland After Equinor successfully installed a single demo floating wind turbine, they decided to scale up. They commissioned the first commercial wind farm with five wind turbines off the coast of Scotland. The mooring system that they used can be seen in figure 2.2. Each turbine has three mooring legs, and the suction anchors are not shared.

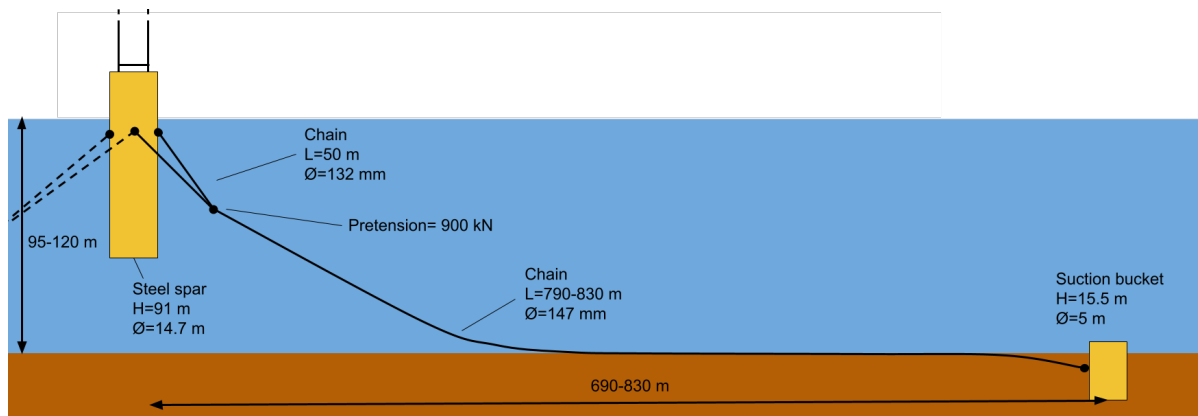


Figure 2.2: Mooring system lay-out for Hywind Scotland

Seeing as the site is relatively shallow, a chain-only mooring system was used. The suction buckets were installed separately with a short chain segment attached to quickly connect them to the rest of the system. When the mooring lines were laid, an ROV connected the mooring chain to the suction bucket as seen in figure 2.3.

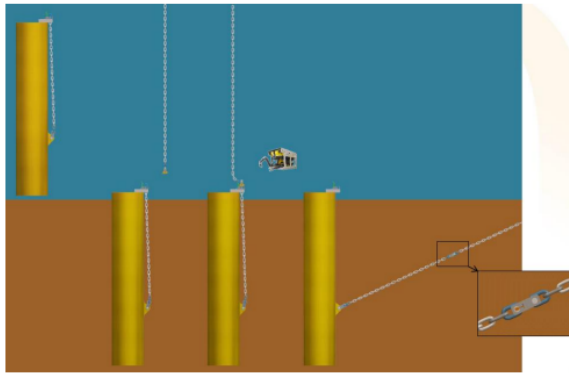


Figure 2.3: Procedure for chain attachment to the suction bucket. [22]

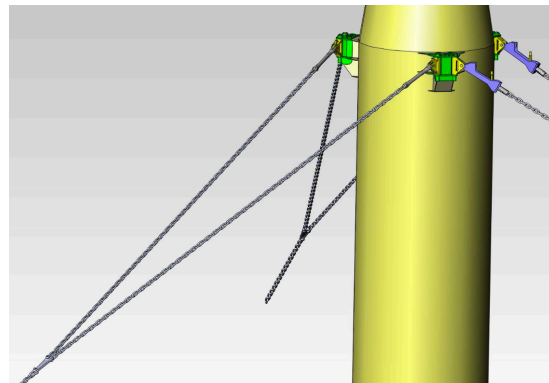


Figure 2.4: Mooring attachment detail. [23]

To prevent yaw motions of the floater, each mooring line was installed with a bridle, meaning that the mooring line from the anchor split into two 50 m chains, which in turn attached to the turbine as can be seen in figure 2.4. One of the three mooring lines was installed with a chain stopper and fairlead in place of its regular and fixed strong-point, making it adjustable. Prior to tensioning, the two standard mooring lines were hooked up. Pretension was then performed by leading the bridle chains from the third anchor chain through the fairleads to an AHV and pulling the chain through. The mating was performed by a crane vessel and not a land-based crane. Not many quays have cranes with sufficient height/weight capabilities, including the quay in Stord, where Hywind operate from.

Hywind Tampen After the Hywind Demo and the Hywind Scotland project, Equinor's next step is to increase the scale of the floating wind farms. The aim of this trilogy of floating wind projects is to develop technology to reduce costs and for the benefit of future projects. The farm shall deliver power to offshore oil and gas facilities offshore, also owned by Equinor. Parts of the Tampen project, such as the substructure are currently being built and are expected to go operational by the end of 2022. The Hywind projects scale up every time in not only capacity but also complexity. The wind turbines are bigger, the water is deeper, it is further offshore and new components are introduced. One particularly interesting innovation is the shared suction anchor. The turbine mooring line-out is visualised in figure 2.5.

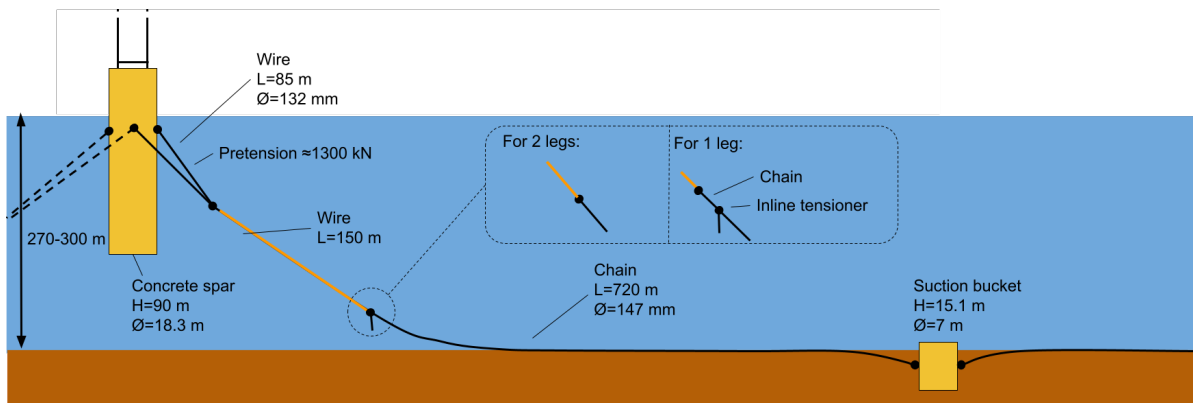


Figure 2.5: Mooring system lay-out for Hywind Tampen

The first major difference between the Scotland mooring layout and the Tampen layout is the fact that, when possible, anchors are shared between two or three turbines. 19 suction anchors are installed for 11 turbines as seen in figure.

In-line tensioners (See section 2.4) are one of the many developments within the oil&gas industry that help to reduce the cost of floating wind farms. The chain stopper and fairlead combination are moved away from the structure to an insert in the chain. Whereas the Scotland project required two fairleads and two chain stoppers, now only one is used.

What is interesting about the Tampen project is the three-fold usage of the bridle. First, the turbines need to be moored while waiting for transport to the site. This is done by attaching a temporary mooring to the bridle. Secondly, the bridle is used to tow the turbine. Finally, the bridle is used in the permanent mooring set-up as shown in figure 2.5.

WindFloat Atlantic Project Another European floating wind project is the Windfloat Atlantic project. It consists of three Vestas 8.3 MW turbines on semi-sub floaters by Principle Power. Vryhof delivered the mooring equipment. The turbines are located in relatively shallow water (95-100m). The involved parties did not release many details about the project like Equinor did. Video fragments on Youtube[24] revealed some detailed drawings that helped construct figure 2.6.

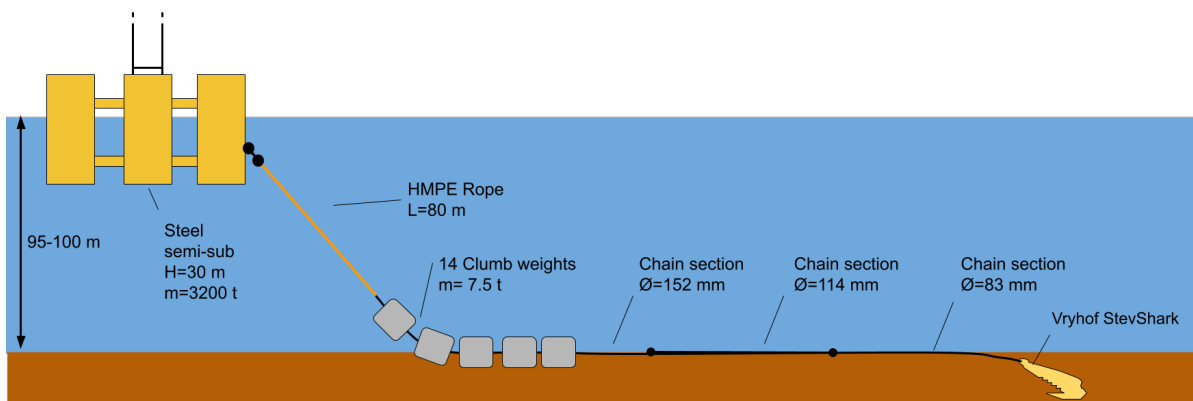


Figure 2.6: Mooring system lay-out for Windfloat Atlantic

Three interesting findings based on this figure are the use of HMPE rope, clump weights and the chain segments with varying diameters. The Hywind Scotland project has a similar depth and turbine power rating but had only chain in its mooring system. Combining rope and clump weights involves more components, and using HMPE rope requires careful handling. The main advantage of this set-up is that the mooring line is heavy, where it is beneficial to be heavy and more lightweight in sections where it is advantageous to be lightweight.

2.3. Installation of semi-submersible floating turbines

Floating wind turbine installation methods are dependent on the type of floater, depth, and available resources. Most of the found literature, including Wu [3], acknowledges three phases of installation: Anchor installation, line prelay and floater hook-up. From this high-level approach, it is not possible to identify knowledge gaps or potential efficiency gains. To structure the details and information one base case was selected for which the installation is completely worked out. There were two main requirements for this base case:

1. It should represent the majority of the future farms
2. Differences between FOWTs designs and their impact on the installation should be minimal but identified.

With the information on future wind turbines from Quest Floating Wind Energy[25], interviews with Vryhof[18] and Heerema Engineering Solutions[26] and available information in the public domain, the Stiesdal TetraSpar and its mooring system are selected to form the basis of the installation storyboard. This base case has properties that one expects to find in most future projects: A semi-submersible floater with an advanced catenary mooring with multiple components. The installation steps and potential variations are elaborated on in this section.

2.3.1. Base case introduction

Stiesdal designed a 3.6 MW semi-sub floating wind turbine and mooring system for a 220 m deep site[21]. The mooring system compositions is well documented, but no information about the installation was provided. All elements are briefly discussed.

Floater The TetraSpar floater is a flexible platform that can come with a submersible keel or with buoyant columns on the three corners. In this example, the concept with a keel is used. In figure 2.7, the floater is shown in yellow and the keel in red. They are connected through a suspension system.

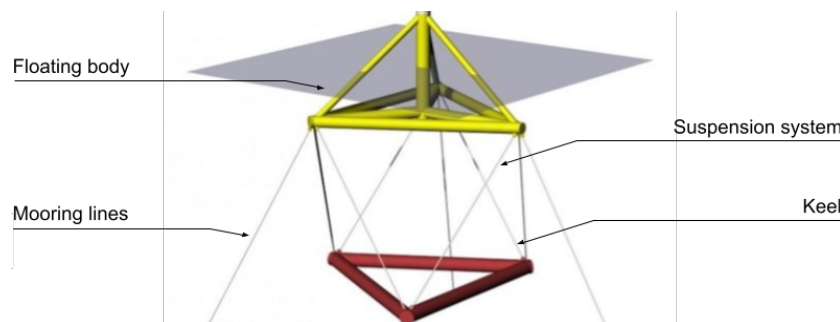


Figure 2.7: Stiesdal Tetraspar floating substructure concept. Original from Tetraspar description [21]

The Tetraspar is a unique design; no other concepts with a suspended keel are currently present in the database of 4C Offshore. [16]. However, it does not change the mooring line installation.

Catenary lines with inserts The mooring system that is designed for the TetraSpar has all the elements that can be found in the Kincardine field (with Windfloat semi-subs[24]), and the Hywind Tampen (spar type floaters)[17]. From anchor to the floater, the following components are present:

- A long ground chain is essential when using drag anchors since it has very little vertical holding power. In extreme conditions, the loading of the anchor must be horizontal.
- Clump weight section to increase the stiffness of the mooring.
- Dip chain segment, which will see most of the slamming of the seabed.
- Synthetic wire. It should not touch the seabed during its operational lifetime. The handling chain in the middle simplifies the connection, as seen in the next section.

A mooring line is visualised in figure 2.8:

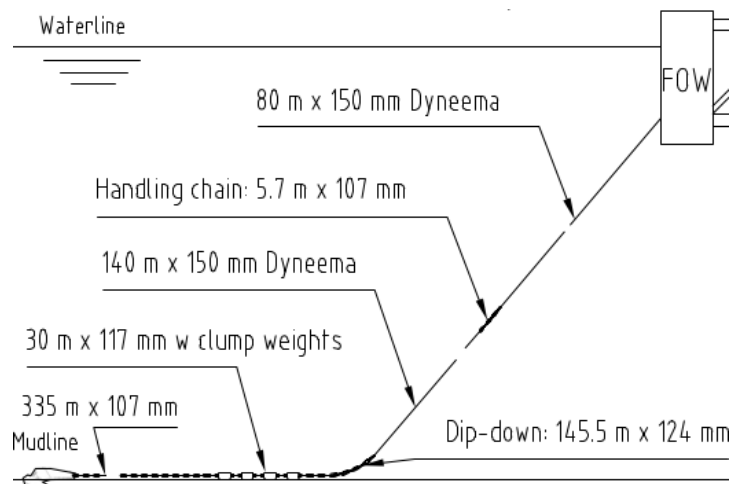


Figure 2.8: Mooring systematic overview of different components

Anchors A drag anchor is considered in this example. The anchor type hardly influences the other steps. A typical procedure adapted from O&G industry and very dependent on the type of anchor: A drag anchor is standard in situations when anchors are not shared. When another anchor type, like a suction anchor, is used, the rest of the installation remains unchanged.

Depth Depth of 220 m is within the range of what can be expected at other locations such as offshore Scotland and Norway. The range for which such systems could work is not fully bounded yet. The Kincardine farm is built in approximately 100 meters deep water, and its mooring legs similarly include clump weights and synthetic inserts.

Pre-tensioning device In this case, a seabed tensioner is used to pretension the system. It is one of the three concepts used on current FOWT systems.

Now, all information is available to work out all installation steps.

2.3.2. Anchor deployment

The first step in mooring installation is the anchor installation. Anchors are stored upside down on the deck, and usually sea fastened with a 20 mm chain. The middle path must be clear for work wires and moving equipment. Tugger winches and a movable crane help move equipment around the deck.

Once at the location, an anchor is positioned at the stern roller and pulled overboard by aft winches. The anchor chain is slowly released, and it can be that the chain is fully suspended above the deck between the anchor and the reel.

AHV lowers the anchor to just above the seabed and positions it approximately 50/ 100 meters away from the target box, such that when the anchor is proof-loaded, it digs itself into the target box. The AHV typically moves forward while the anchor touches down to ensure proper orientation. An ROV monitors the touch-down to validate the orientation of the anchor.

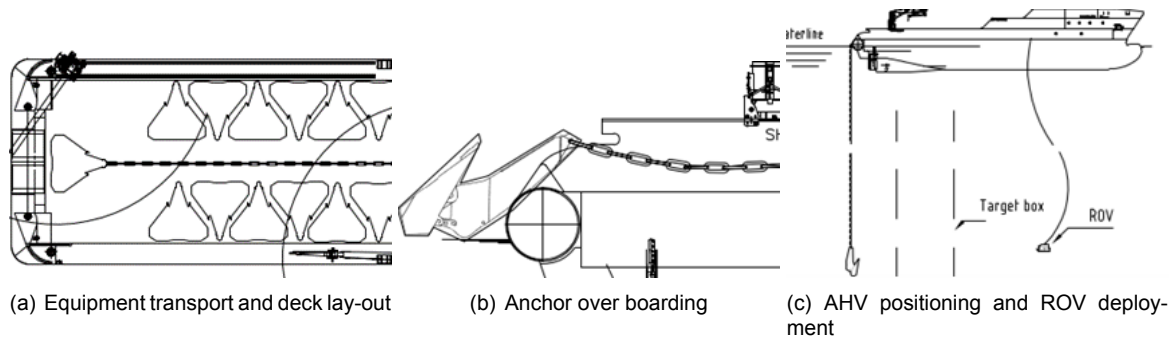


Figure 2.9: Drag anchor installation

t

2.3.3. Proof loading

Once the anchor touches down on the seabed, the AHV slowly pays out the anchor chain in the correct orientation while moving forward. A constant bollard pull force of around 15 Tn is applied to ensure a straight chain laying on the seabed.

When the entire ground chain is paid out, the AHV connects its work wire to the last ground chain shackle. The purpose of this work wire is to ensure the anchor does not undergo any uplift while being proof loaded. During the proof loading, the vessel uses thrust to dig the anchor into the ground. Generating the required thrust for proof loading requires high engine power and is also a field of development for future wind farms [18].

After proof loading, the work wire is reeled back in until the anchor chain is in the shark jaws. Shark jaws are retractable chain stoppers on the aft of the AHV. Based on the exact and final location of the anchor, the chain can be cut to a precise length. The mooring line pre-lay can be done directly after the proof loading or in a separate campaign. In the latter case, the mooring chain needs to be abandoned. This can be done in two ways, and both methods are illustrated in figure 2.10(c):

- (A) Buoy off with surface buoy: Requires a temporary wire and surface buoy. More suitable for shallow sites
- (B) Leave chain at the seabed with an ROV pick up rigging in the last link.

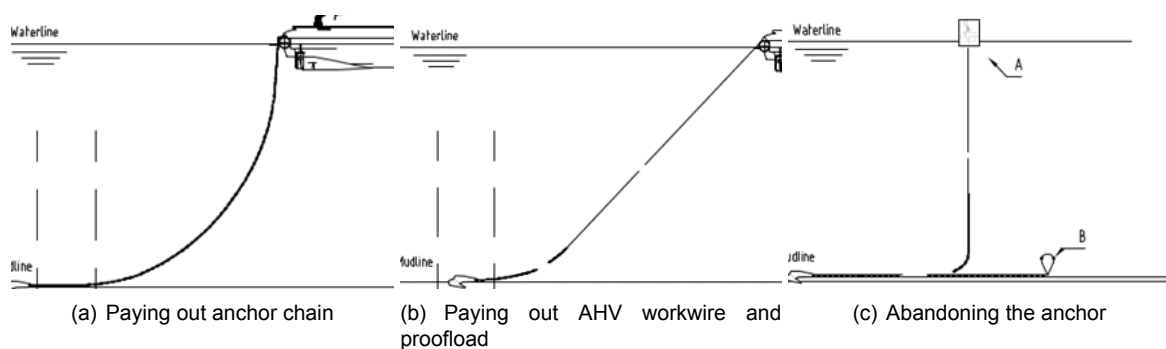


Figure 2.10: Ground chain lay out on the seabed and proof loading of anchor

2.3.4. Mooring line pre-lay

At this point, the anchor and ground chain are in place, and the clump weight section, dip chain section and synthetic bottom section are ready to be installed. This operation can start directly after the proof loading if the required mooring equipment is on board. If the chain was abandoned, the chain could

be retrieved by either a hook and a floating loop in case of a surface buoy(A) or an ROV in case of a submerged buoy(B).

Once the end of the ground chain is in the shark jaw, the clump weight assembly is connected and paid out until the last few links are on deck and stopped off. These last few links are connected to the dip chain segment, which is paid out too. Finally, the Dyneema rope is attached and paid out. The ropes are stored on reels of AHV or deck reels. The chains are stored on deck or in AHV lockers.

During all paying out, a constant bollard pool of 15 metric tonne force (Tn) is applied to ensure the correct direction of the mooring leg. During the installation of one of the three legs, the seabed tensioner is deployed to haul in a section of the ground chain.

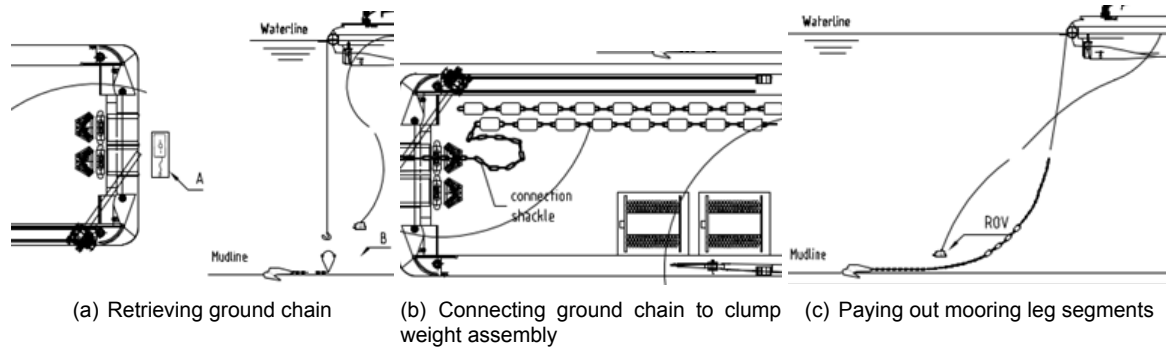


Figure 2.11: Prelay operation of mooring line. For one of the three legs, the seabed tensioner is deployed too.

2.3.5. Towing and line transfer

Now that the mooring lines are pre-installed, the floater is towed to the site. Different towing configurations exist based on the sea state, floater size and required accuracy while manoeuvring. Towing configurations generally change once the vessel is outside constricted waters, from a controllable set-up to a more efficient towing set-up. Fewer vessels imply smaller costs; typically, two vessels are enough to keep the floater in position while hooking up offshore. More vessels could increase the station-keeping capabilities but also the complexity. [26]

One section of synthetic mooring line is pre-installed in the previous step, the remaining synthetic line is stored on the floater. While two (or more) vessels keep the floater in position, an AHV, approaches the floater. From the floater, a messenger wire is thrown towards the AHV so that the synthetic mooring line can be pulled onto the AHV. Other towing/station keeping configurations of the tugs and bridles can create more safe area for the AHV to manoeuvre but come at the cost of an extra tug boat and extra bridles.

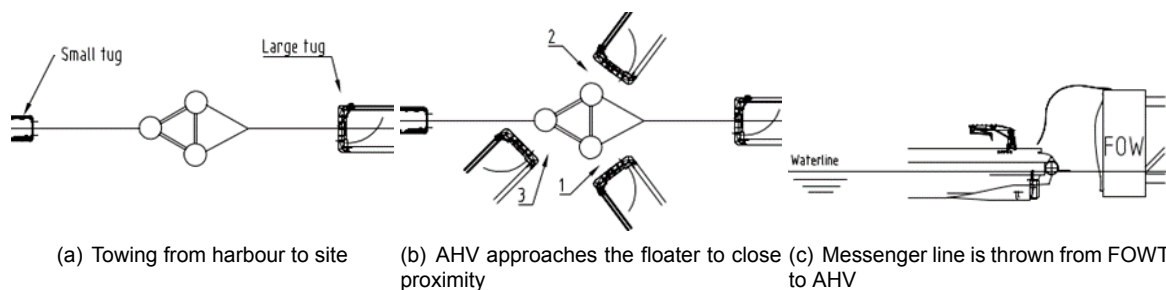


Figure 2.12: Towing of the FOWT, arrival at site and transfer of messenger line to prepare hook-up.

2.3.6. Hook-up

Both ends can be connected, as seen in the first image when the line was thrown from the FOWT to the AHV holding the mooring line. The AHV work wire with a release mechanism is attached to the

mooring line for gently lowering. Slowly, the AHV pays out the work wire so that the mooring line can find an equilibrium.

To ease the process, the tugboats can move the FOWT closer to the anchor it is hooking up to. After all three mooring lines are attached, the FOWT can be considered 'storm safe'. Although one of the mooring lines still contains too much chain and needs to be pre-tensioned, the FOWT will remain in position. Having 'too much' mooring line reduces the mooring stiffness and will be further elaborated upon in the next chapter. Additionally, the electrical cables are often the limiting factor to offset the FOWT, so pre-tensioning of the mooring system is required.

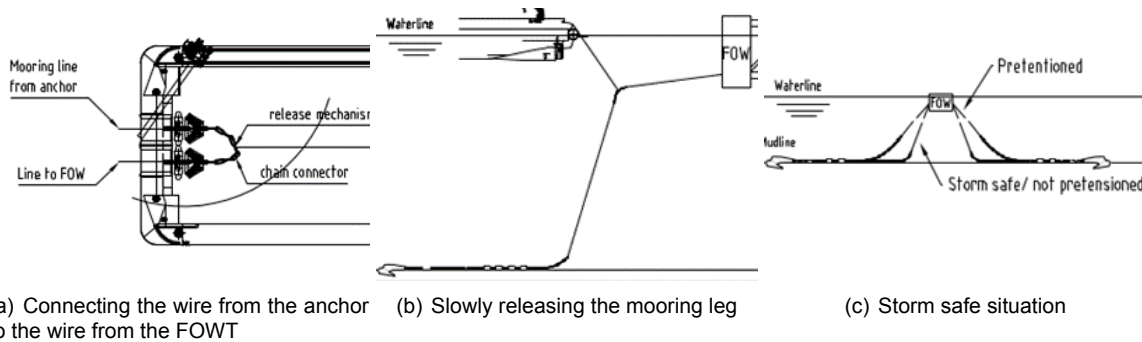


Figure 2.13: Hooking up the three mooring lines to the FOWT to create a storm-safe situation

2.3.7. Pre-tensioning using seabed tensioner

In one of the mooring legs, approximately 300 meters from the anchor, the seabed tensioner sits on the seabed. As shown in the first picture, the AHV positions itself above it and deploys an ROV. Secondly, the ROV connects a work wire to the chain end (A), as illustrated in the centre image. Subsequently, another work wire is connected to the locking mechanism of the tensioner (B).

The activation wire (B) is pulled to deactivate the cam and allow tensioning. The AHV pulls in work wire A and therefore shortens the overall length of that mooring leg. According to Vryhof, the developer of the seabed tensioner, the tensioner can come up to 15 meters off the seabed during tensioning operations. When enough shackles pass through the tensioner and the mooring leg is at the required length, the activation wire is released, and the system locks the chain. The hauled-in chain is around 80-100 meters for this case. This chain can either be left on the seabed or disconnected by an ROV.

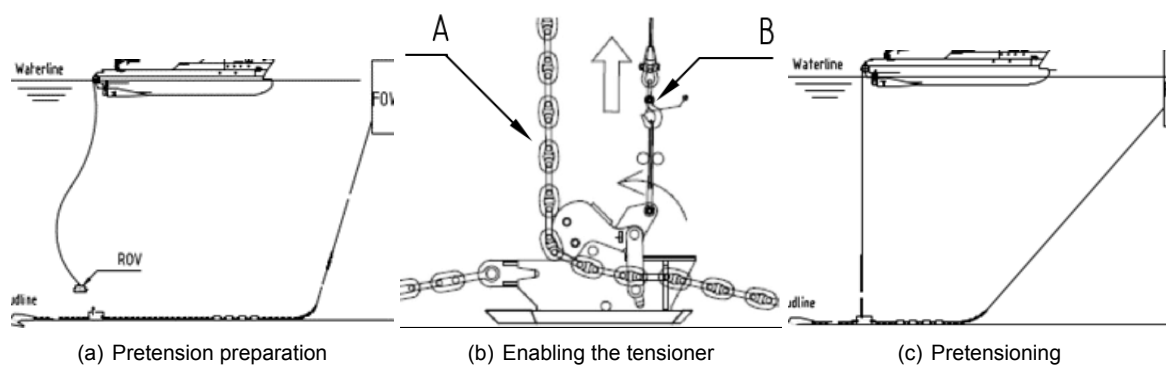


Figure 2.14: Pre-tensioning operation using a seabed tensioner

2.4. Variation in pre-tensioning

In the example above, a seabed tensioner was used. When one looks at other mooring systems of existing and future farms, one can find a variety of tensioning concepts. For floating wind turbines, three concepts are utilised: Seabed tensioning, inline tensioning and fairlead tensioning. The main

objectives when considering hook-up techniques are to minimise personnel risks, installation time and overall cost.

Seabed tensioner With a seabed tensioning system, tensioning of the mooring line is carried out using an AHV equipped with a winch. The inline tensioner is not an on-vessel device but a permanent component in the mooring line, as shown in figure 2.16(a). The mooring leg is shortened by applying a tension on the wire to the AHV from the tensioner. Shorting the chain at the seabed, thus controlling the tension in that line, is a new concept and has significant potential benefits: The tensions at the seabed are smaller than any suspended section due to weight in water. Furthermore, the tensioner is placed in a chain section that is not supposed to ever come off the seabed. The dynamic tensions are, therefore, relatively low. Depending on the exact configuration and depth, this method also allows the top section of the mooring line to be used as the towing element.

[27]

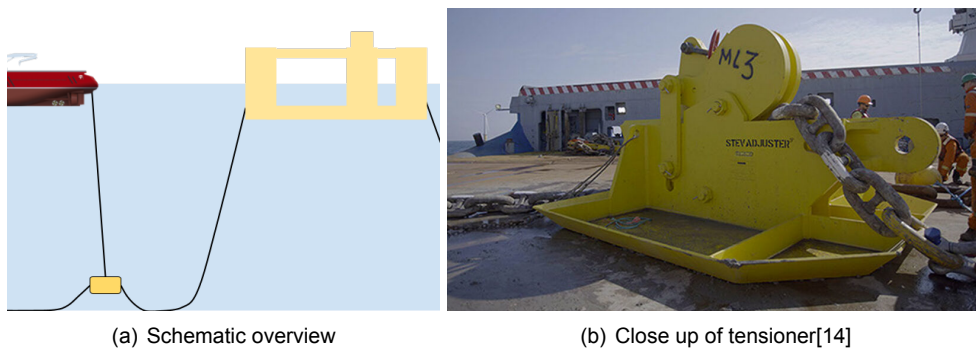


Figure 2.15: Seabed tensioning

Inline tensioner Similarly to the seabed tensioner, an AHV is required to tension the system, and the tensioner is a component in the mooring leg, not a piece of onboard equipment. The inline tensioner serves as a single pulley with the anchor as the fixed point, and the AHV can efficiently tension up the mooring line. Inline tensioning was first utilised in 2016 and was seen as an improvement on onboard tensioning systems on board the oil&gas rigs. The most apparent advantage of the inline tensioning system is eliminating the bulky tensioning equipment on the platform. Another significant advantage is that the mooring configuration with the inline tensioning system does not have any platform chain, which means the splash zone corrosion on platform chains is completely eliminated.[3]

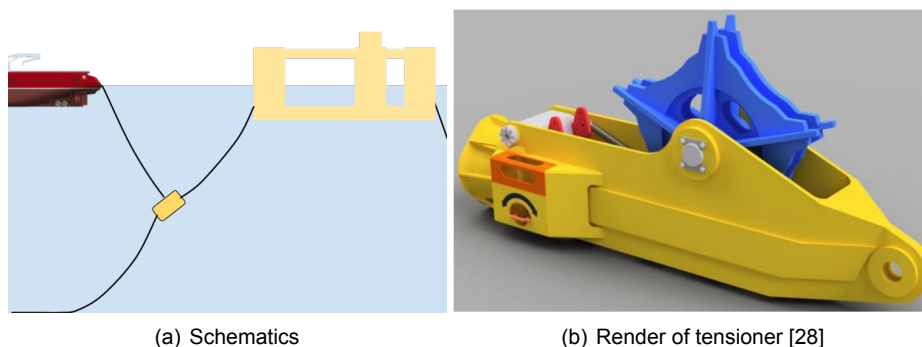


Figure 2.16: Inline tensioning

Fairlead tensioner Fairlead tensioning knows a couple of varieties. The main distinction should be made between systems where the tensioning equipment is on board the floater or those where the chain is pulled through the fairlead to an AHV that pulls the chain until the predetermined tension is

reached. For large oil&gas platforms that require regular repositioning, the first is standard. Onboard the rig, large winches or chain jacks are installed that haul in the chain under high tension. One FOWT concept exists with such a system: the Ideol barge[29].

More realistic for FOWTs is having a fairlead with a chain stopper and chain pulley that can guide the anchor chain to an AHV that pulls the chain through the fairlead. The Hywind Scotland wind turbines are an example of such a tensioning system.[30]

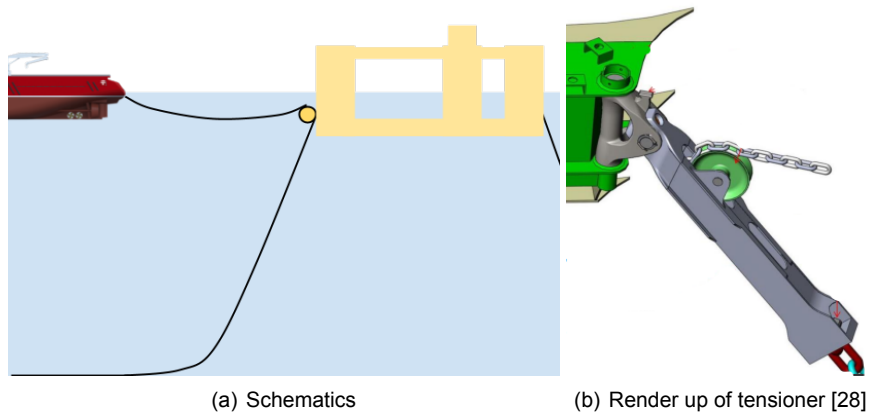


Figure 2.17: Fairlead tensioning

2.5. Simulation of catenary systems

Any chain or line has a 'hanging shape'. In this section, the theoretical background behind modelling a 3D catenary wire or chain is built up. For a static simulation of a mooring line, one starts with the catenary equation in a 2D scheme. Subsequently, the effect of elongation and seabed friction is included in the model.

The equations used to describe the shape of a suspended chain illustrated in figure 2.18 have been derived in numerous works [3][31][32]. For an inelastic wire or chain Wu describes the shape and tensions in the suspended chain accurately [3]. Irvine describes the catenary behaviour for uniform wire or chain, including elongation[31] and seabed interaction. In 2013, Jonkman further developed this theory into the Multi-Segmented, Quasi-Static(MSQS).[33]. The MSQS model allows finding the static equilibrium between mooring lines and floating bodies. The catenary line equations and the iterative model only use fixed lengths for each chain. While pre-tensioning, however, a sliding or rolling element is used and therefore should be included in the model. The process of finding an equilibrium between multiple mooring lines, floating bodies and unknown line lengths is described in the next chapter in section 3.4.

A catenary line with unstretched line length L is hanging between two points with a vertical and horizontal distance called h and l respectively. The line has an axial stiffness EA , the seabed friction coefficient of C_B and specific weight in water: W . These parameters can usually be found in data sheets of chain and wire manufacturers. Note that in the original documentation by Irvine, ω was used for the specific weight of the line in water. Because ω is later used for wave frequency, this is modified.

To denote a specific point in the mooring line, the inline distance s is denoted as seen from the lowest point. This point is referred to as the 'anchor point' while it is not necessary at a physical anchor. The lowest point of a catenary line could also be a connection point between an insert and a chain or be at a tensioner. The tensions at the two endpoints have a vertical component V and a horizontal component H . At the anchor point, the horizontal and vertical forces are identified by an 'a' subscript to indicate the anchor point.

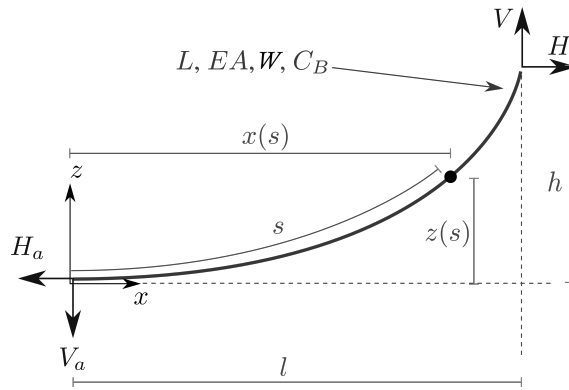


Figure 2.18: Single line definitions for a hanging catenary. Altered symbol for wet specific weight of mooring line. Original from Irvine[31]

The equations that relate the horizontal and vertical distances, the tensions at both points and the line shape are provided below. The x and y are coordinate axes in the local (line) frame and are a function of inline distance from the anchor s . The derivation of these analytical equations can be found in the book of Irvine[31].

$$x(s) = \frac{H}{W} \left\{ \ln \left[\frac{V_a + Ws}{H} + \sqrt{1 + \left(\frac{V_a + Ws}{H} \right)^2} \right] - \ln \left[\frac{V_a}{H} + \sqrt{1 + \left(\frac{V_a}{H} \right)^2} \right] \right\} + \frac{Hs}{EA} \quad (2.1)$$

$$z(s) = \frac{H}{W} \left[\sqrt{1 + \left(\frac{V_a + Ws}{H} \right)^2} - \sqrt{1 + \left(\frac{V_a}{H} \right)^2} \right] + \frac{1}{EA} \left(V_a s + \frac{Ws^2}{2} \right) \quad (2.2)$$

The following substitution can be made for horizontal and vertical component of the tension at the bottom point, (H_a and V_a), and those at the top point (H and V):

$$\begin{aligned} H_a &= H \\ V_a &= V - WL \end{aligned}$$

They state that the decrease in the vertical anchor force component is proportional to the mass of the suspended line. The equations for $x(s)$ and $z(s)$ both describe the catenary profile provided all entries on the right side of the equations are known. However, in practice, the force terms H and V are sought, and the known entity is the fairlead excursion dimensions, l and h . In this case, the forces H and V are found by simultaneously solving the following two equations:

$$l = \frac{H}{W} \left[\ln \left(\frac{V}{H} + \sqrt{1 + \left(\frac{V}{H} \right)^2} \right) - \ln \left(\frac{V - WL}{H} + \sqrt{1 + \left(\frac{V - WL}{H} \right)^2} \right) \right] + \frac{HL}{EA} \quad (2.3)$$

$$h = \frac{H}{W} \left[\sqrt{1 + \left(\frac{V}{H} \right)^2} - \sqrt{1 + \left(\frac{V - WL}{H} \right)^2} \right] + \frac{1}{EA} \left(VL - \frac{WL^2}{2} \right) \quad (2.4)$$

Line Touching the Bottom The solution for the line in contact with a bottom boundary is found by continuing $x(s)$ and $z(s)$ beyond the seabed touch-down point $s = L_B$. The horizontal tension at the touchdown point (B) is equal to that of the fair lead point. However, the tension decreases on the seabed due to drag force on the chain. It can be that the seabed drag entirely takes up the tension. The point where the line tension becomes zero $H(s) = 0$, is referred to as $s = \gamma$.

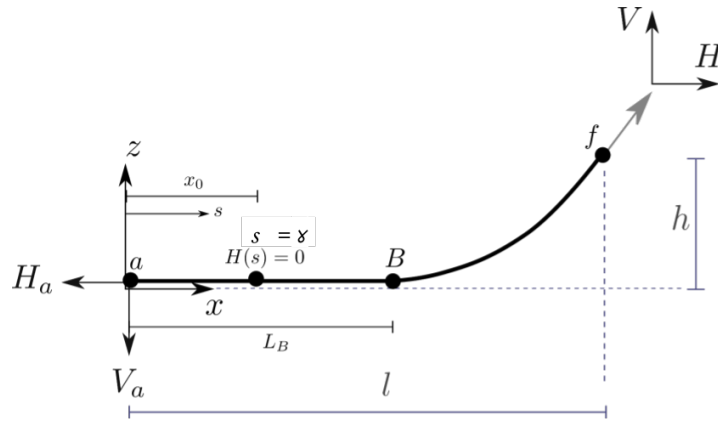


Figure 2.19: Single line definitions for a catenary touching a bottom boundary with friction. Symbol γ is added. Original from Irvine[31]

When a section of the catenary line touches the seabed, the equations 2.3 and 2.4 do not hold anymore. This is because of two reasons: Firstly, the seabed friction in the horizontal direction is not accounted for, and secondly, the vertical forces decrease due to the length of the cable lying on the seabed. This leads to modified equations 2.5 and 2.6 [33].

$$x(s) = \begin{cases} s & \text{if } 0 \leq s \leq \gamma \\ s + \frac{C_B W}{2EA} [s^2 - 2\gamma s + \gamma \lambda] & \text{if } \gamma < s \leq L_B \\ L_B + \frac{H}{W} \ln \left[\frac{W(s-L_B)}{H} + \sqrt{1 + \left(\frac{W(s-L_B)}{H} \right)^2} \right] + \frac{Hs}{EA} + \frac{C_B W}{2EA} [\gamma \lambda - L_B^2] & \text{if } L_B < s \leq L \end{cases} \quad (2.5)$$

where λ represents the theoretical length of line on the seabed where the tension is zero. It is calculated as such: $\gamma = L_B - \frac{H}{C_B W}$. Furthermore, λ is defined to avoid the use of a negative γ .

$$\lambda = \begin{cases} \gamma & \text{if } \gamma > 0 \\ 0 & \text{otherwise} \end{cases}$$

The three splits in equation 2.5, belong to three line section with different characterises: A section with no tension ($0 \leq s \leq \gamma$) and therefore no elongation. Note that is also possible that there is no section without horizontal tension ($\gamma = 0$). Secondly, a section on the seabed ($\gamma < s \leq L_B$) is under tension and on the seabed. Thirdly, the suspended section ($L_B < s \leq L$) is a modified version of the equation for the suspended chain, as found in 2.3.

Between the range $0 \leq s \leq L_B$, the vertical height is zero since the line is resting on the seabed, and forces can only occur parallel to the horizontal plane, regardless whether it is tensioned or not. This produces:

$$z(s) = \begin{cases} 0 & \text{if } 0 \leq s \leq L_B \\ \frac{H}{W} \left[\sqrt{1 + \left(\frac{W(s-L_B)}{H} \right)^2} - 1 \right] + \frac{W(s-L_B)^2}{2EA} & \text{if } L_B < s \leq L \end{cases} \quad (2.6)$$

The equations above produce the mooring line profile as a function of s . Ideally, a closed-form solution for l and h is sought to permit simultaneous solves for H and V , analogous to the freely-hanging chase

in the previous section. This is obtained by substituting $s = L$ to give:

$$l = L_B + \left(\frac{H}{W}\right) \ln \left[\frac{V}{H} + \sqrt{1 + \left(\frac{V}{H}\right)^2} \right] + \frac{HL}{EA} + \frac{C_B W}{2EA} [\gamma\lambda - L_B^2]$$

$$h = \frac{H}{W} \left[\sqrt{1 + \left(\frac{V}{H}\right)^2} - 1 \right] + \frac{V^2}{2EAW}$$

Finally, a useful quantity often evaluated is the tension as a function of s along the line. This is given using:

$$T_e(s) = \begin{cases} \text{MAX} [H + C_B W (s - L_B), 0] & \text{if } 0 \leq s \leq L_B \\ \sqrt{H^2 + [W (s - L_B)]^2} & \text{if } L_B < s \leq L \end{cases}$$

An iterative solver is used to find the line shape and forces at the ends, assuming that the endpoints are fixed. There are two unknowns: The forces at the points (H and V) and two equations to be solved are 2.3 and 2.4 or 2.32.3 in case the line is touching the seabed. The methodology to find the equilibrium between multiple catenary lines is explained in the next chapter. This is because the existing method does not allow for variable line lengths due to the wheels at the tensioners.

2.6. Conclusion literature analysis

In this chapter, a literature review of the floating wind area, mooring problems and available methods to quantify mooring loads has been performed. After this study, the variation in floater and mooring concepts is very well explainable. It can be explained by the fact that companies are still investigating what combination of features is the most cost-effective for large-scale wind farms. Zooming in on mooring installation, the decision on how to pre-tension is also not easily made. After analysing different floating farms, mooring components and installation methodologies, pre-tensioning was found to be a knowledge gap.

The following question is answered in this chapter: *What are the details for a typical FOWT pre-tension operation and what critical events must one account for, and how is this different from the oil and gas industry?*

The answer to the question is divided into three sub-items: characteristics, critical events and comparison with the oil and gas industry. Finally, a quick overview of the results is given in table .

Table 2.3: FOWT mooring installation characteristics, critical events and comparison with oil and gas.

Characteristics	Critical events	Comparison with oil and gas
Three main installation phases	AHV motion	More financial incentive to optimise
Variation exists of pre-tensioning operation	Floater motion	Scale advantage
Load quantification for offshore operations		More severe consequences in case of failure

Characteristics

The three main installation phases are anchor deployment, mooring line prelay and hook-up. The first two have more maturity from oil&gas, which makes hooking up floating wind turbines a more apparent research topic. The three concepts that exist have very little public research on their differences. Finally, the methods are discussed on the simulation techniques that can be used to prepare offshore operations.

Critical events

Each installation operation has its critical events. It heavily depends on the equipment that is decided to be used. However, from conversations with HES [26] five aspects regularly limit the continuity of offshore operations: Towing, human limits on the AHV deck, crew transfers to FOWT and accurate pre-tensioning.

comparison with oil and gas

Although offshore installation is not new and well researched in the last decades, the floating wind brings new challenges and requires a new approach. First, the financial margins on wind energy are lower. Therefore, the whole supply chain of the FOWT is looking for cost-effective installation. Secondly, if the FOWT industry will grow as expected, it is wise to spend resources on developing good installation techniques since they could be performed repetitively [13]. Finally, failure of a mooring line of manned oil and gas platforms may cause severe consequences.

3

Model description for a semi-submersible based FOWT

To understand the different pre-tension methods, the strategy is first to perform static analysis to find the static tensions in the wires and how the AHV and FOWT position relative to each other. The complete research approach can be found in the approach section 1.4 in the introduction.

This chapter describes how a good static comparison between the pre-tensioning methods can be obtained. In the literature review, the catenary line equations were introduced. The relation between catenary lines and floating bodies and how equilibrium is found will be presented in section 3.1. Subsequently, the physical properties of the model are discussed. A different base case is used than in the installation storyboard due to the available hydrodynamic data of this floater. Finally, an addition to the existing modelling technique is introduced to cope with rotating elements at the tensioning modules.

3.1. Model architecture

The code used for the static analysis finds its origin in 'Moorpy'[34]. Moorpy requires an input file with the *system* specification and then finds the equilibrium. A system is more than solely the mooring equipment; it also includes the water depth, the floater hydro-statics and the inclusion of any external forces. For this research, the Moorpy package has been used as an integral part of the model but has been heavily adjusted. In this section, the model architecture and modifications will be elaborated on.

On a high level, four codes form the basis of the model: The Main script, the system builder, the system class and the floating bodies class. All information of a mooring configuration is stored in a '**system**' object. Such an object is built up step by step by a '**system builder**'. For each pre-tensioning method, a separate system builder exists. The system builder finds the information about the AHV, FOWT and the tensioners in the '**floating bodies**' class. Finally, a '**main script**' is made from where all calculations are initiated and serves as a user interface. A schematic overview of the model is presented in figure 3.1:

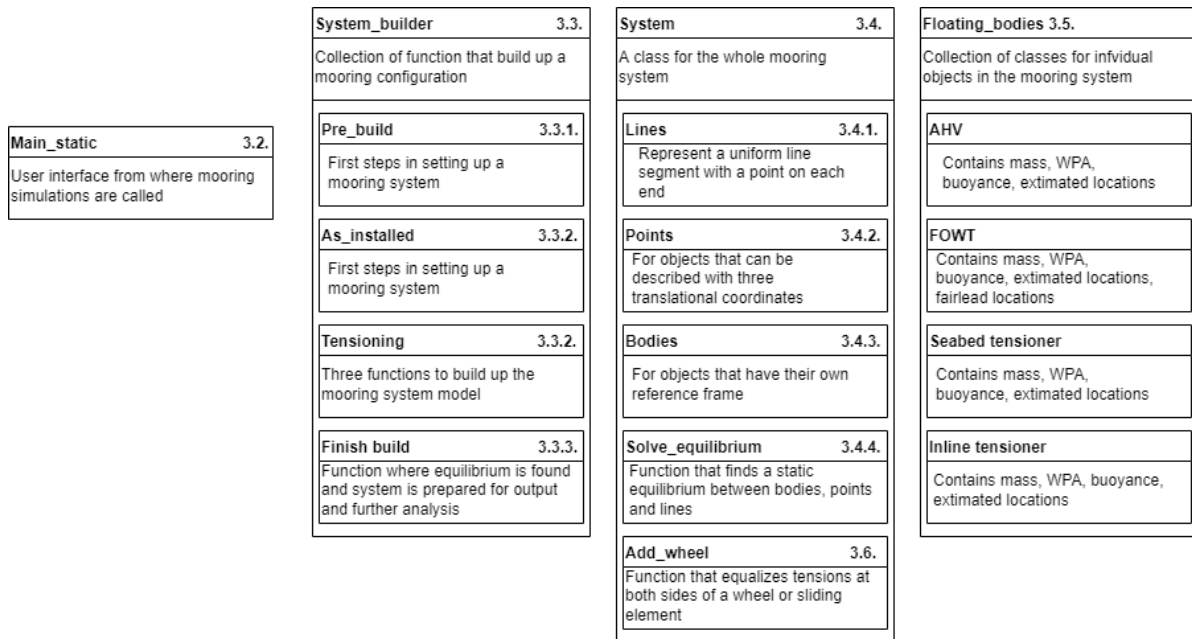


Figure 3.1: Architecture of the model code.

The four main components are each elaborated on in a dedicated section.

3.2. The main script: The user interface

The main script is the user interface with the rest of the code. It is designed for readability and has all the calculations in the underlying code. The main script is mainly used to call the four system builders (As installed, seabed-, inline- and fairlead tensioning). Therefore, only the parameters that usually vary are handled in the main script. The other values are stored as default values within the system builders. Model parameters that can be specified in the main script are defined below:

Table 3.1: Introduction of the parameters used to construct a mooring simulation

Parameter	Variable name	Description
External force on FOWT	$f_{ExtFOWT}$	To simulate static wind or back pulling by an extra tug
External force on AHV	f_{ExtAHV}	To simulate AHV bollard pull
length of payed out workwire	$l_{Workwire}$	Length of the AHV workwire in the configuration
Extra line length in the mooring line	l_{Slack}	To indicate whether the system is slack or fully pre-tensioned.

3.3. System builder: Structured configuring of mooring systems

Before any equilibrium is found and line tensions can be calculated, all aspects within the model must be adequately defined; this is referred to as 'building' the system. For any system that is build-up, there are three stages: The uniform pre-build, the specific build and the finishing of the building. The flowchart below summarises how they connect and provides an overview of what they do.

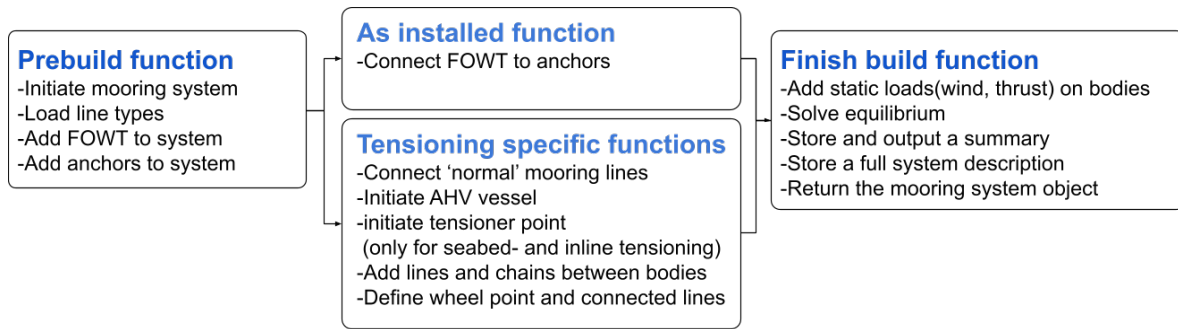


Figure 3.2: Flowchart of the building process of a complete system

At the end of the building process, the result is a complete system in equilibrium. The three stages are elaborated in more detail below:

3.3.1. Pre-build

The pre-build is mainly about initiating the system itself and the line types. The purpose of the uniform pre-build is to minimise the amount of duplicate code.

The steps within the pre-building sequence are listed below.

- The system object is initiated. It forms the 'container' in which all information is stored.
- The water depth and anchor radius are defined.
- Initiate the relevant line types: Chain, AHV wire, synthetic inserts or any line used in the system.
- Initiate anchor points.
- Load FOWT information and initiate the floating body within the system. When an external force on the FOWT is specified, it is added.
- Initiate the connection points for mooring lines on the FOWT by specifying their locations relative to the CoG of the FOWT.

3.3.2. Tensioner specific builds

It is now possible to build the model. As mentioned earlier, there are four specific building modules: One for solely the FOWT and the mooring lines and one for each pre-tensioning method.

The builder for solely the FOWT and the mooring lines initiated three mooring lines between the anchor and the fairlead and applies the defined force on the FOWT. The three other builders have more steps which are listed below:

- The AHV is initiated. For each pre-tension method, an estimate for its location is defined for the initial guess for equilibrium finding. Finally, when an AHV force is specified, it is added.
- The tensioner is initiated. In the case of fairlead tensioning, that point is already defined at the fairlead. The tensioners are simulated as a point mass.
- Add two standard lines with the fixed line length
- Depending on the pre-tension method, additional points are added to the system between two different line types.
- The uniform line segments of the adjustable mooring lines are added.
- Specify whether a point represents a wheel/sliding element. The specification requires the corresponding line numbers, line ends and range in which the equilibrium is expected. This is explained in more detail in section 3.6

3.3.3. Finish-build

All components of the system are now defined. The equilibrium is found in the last stage of the building process, and the results are stored. The three steps are listed below:

1. The system equilibrium is found: Fully explained in section 3.4.4.
2. Within the system, a compact summary dictionary is made for easy retrieval of the main outputs: Floater offset with respect to the original location, tension at the FOWT for the adjustable and the fixed mooring lines as the AHV position and AHV cable tension.

3.4. Systems class: Storing models of mooring configurations

In this section, the system itself is explained in more detail. The 'system' is the container of all information about the mooring system and the floaters. First, a system's three main building blocks are explained, and finally, the equilibrium finding is elaborated. The system class is originally a Moorpy class and adjusted to fit this research. The primary adjustment is the implementation of the 'wheel' module(section 3.6) and adjustments that allow for convenient information read-out.

A system consists of three elements: Lines, bodies and Points. Lines are uniform line segments within the mooring system. Bodies are defined by any object in the mooring system with its reference frame, and a point is anything that can be described by three translational coordinates [34]. Figure 3.3 connects the theory to the practical implementation of this model.

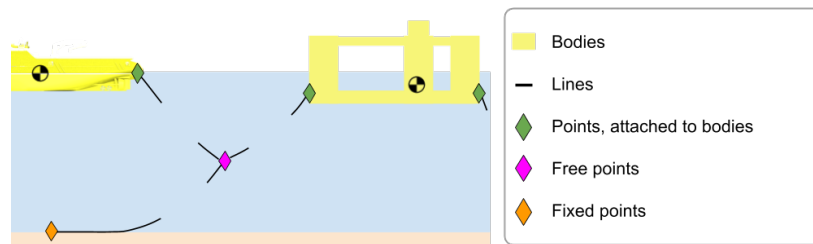


Figure 3.3: Illustration of the relation between bodies, lines and points in the static model

The relation between points, bodies and lines will be further elaborated on in dedicated subsections.

3.4.1. Lines

Line initialisation

Lines are homogeneous line segments and can be free hanging or (partially) on the seabed. Any given Line has constant/uniform properties of unstretched length, diameter, density, and Young's modulus. When a line is defined, the required inputs are only to what points it is connected, which of the pre-defined line types it is and its unstretched length. The line types are defined in the pre-build (see section 3.3.1).

Static solve function

The static solving function is where the equations as described in section 2.5 are called to calculate the horizontal and vertical forces in the two endpoints. Subsequently, the tension within the line is calculated. Note that this is just finding the line shape and tensions at the endpoints for a given geometric distance. The equilibrium finding of the complete system is described later.

3.4.2. Points

As seen in figure 3.3, points are found at both ends of each uniform line segment. Points can come in three variants: Firstly, they can be fixed in the overall reference frame, such as an anchor. Secondly, they can form an attachment point(fairlead) of a body. In that case, the relative location of the point with respect to the CoG must be defined. Examples of such points are the attachment point on the AHV stern roller or the FOWT fairleads. Finally, free points can be defined; they can be given a mass, buoyancy and water plane area. In the simulations for this research, the seabed tensioner and inline

tensioner are simulated as point masses. Their sizes are relatively small to the AHV and FOWT, and the rotations of the tensioners are not expected to give problems. That is assumed because the tensioner will align with the tensions.

3.4.3. Bodies

Bodies represent the AHV and FOWT in this research. They are given a mass, buoyancy and water plane area. Their main difference with points lies in the fact that bodies are rotational. The pitch of AHV and the FOWT result in translations of the fairlead points. Bodies can also have constant external forces and moments applied to them. In this way, a Body can represent a floating platform's complete linear hydrostatic behaviour, including a wind turbine's steady thrust force.

3.4.4. Finding the system equilibrium

The solution process begins by evaluating the catenary equations for each line based on connected point distances and line length. This process is described in section 2.5. Once the line's fairlead and anchor forces are known, the force contribution is added to the corresponding point it attaches to. The forces are transformed from the local $[x, z]$ frame into the global $[X, Y, Z]$ coordinate system. The complete solving procedure was first proposed in 1979 and described by A. Pevrot [35].

The force-balance equation is evaluated for each point, as follows:

$$\begin{aligned} \{\mathbf{F}\}_X^j &= \sum_{i=1}^{\text{line } i \text{ at point } j} [H_i \cos(\alpha_i)] - F_{X_j}^{ext} = 0 \\ \{\mathbf{F}\}_Y^j &= \sum_{i=1}^{\text{line } i \text{ at point } j} [H_i \sin(\alpha_i)] - F_{Y_j}^{ext} = 0 \\ \{\mathbf{F}\}_Z^j &= \sum_{i=1}^{\text{line } i \text{ at point } j} [V_i] - F_{Z_j}^{ext} + M_j g - \rho g B_j = 0 \end{aligned} \quad (3.1)$$

The essence of these three equations is that for each point, the external forces (F^{ext}) and the tensions from the lines should be in equilibrium. In the case of the X or Y axis, the horizontal component of the tension (H_i) is multiplied by the sine or cosine of the angle between the tension and the x -axis (α_i). The vertical component of the tension (V_i) is used for the vertical sum of forces. Furthermore, mass (M_j) and buoyancy ($\rho g B_j$) are also considered. Point forces are found based on the connectivity geometry between points and external forces applied at the boundary conditions. This process requires two sets of equations, one of which must be solved within the other routine, to find the static cable configuration. The first set of equations is the force balance relationships in three directions for each line as presented in section 2.5; the second set of equations are the equilibrium functions proportional to the number of bodies and points according to the set of equations 3.1. All equations and theory are in place for systems with fixed mooring line lengths to find the equilibrium. However, for this study, including tensioners require the current theory to be expanded. Before that new theory is presented, the code section where all floater information is stored is introduced.

3.5. Floating Bodies

The information on the components that are not lines, are stored in one place: The 'floating bodies' class. For the AHV, FOWT and tensioners, separate classes exist that allow for convenient data collection from anywhere in the model. The physical model properties will be presented in section 3.7.

3.6. The 'addWheel' module: Simulating the pre-tensioner

While using any of the three tensioning systems, one can observe a sliding in the system in the seabed tensioner or rotating gypsy wheels for the inline tensioner or fairlead tensioner. They will be referred to as sliding points for convenience. At any sliding point, the tension of the two lines at each side must

be approximately equal. A sliding element in a seabed tensioner probably has more friction than a gypsy wheel. Therefore a tension difference might be present. However, the tension difference will be minimal due to pulley behaviour regardless of whether it is a wheel or a sliding element. An optimisation function was made that minimises this tension difference.

In any pre-tensioning operation, one knows the total length of line in the system. The exact point where the chain goes through the fairlead is unknown but relevant for the static tensions. In figure 3.4, a Schematic overview of the situation is presented.

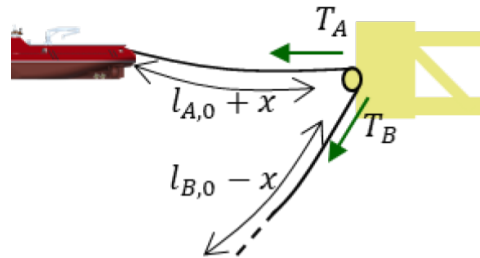


Figure 3.4: Schematic overview of the forces during a pre-tension operation using a fairlead tensioner.

T_A and T_B are the tensions at both sides of the sliding point. Line lengths $L_{0,A}$ and $L_{0,B}$ are estimated before the algorithms start to vary the location of the fairlead within the chain. Therefore, this variation x is the only input to calculate the tension difference $\Delta T = |T_A - T_B|$. The algorithm to find the optimum is described accordingly.

The lengths $L_{0,A}$ and $L_{0,B}$ are estimated before the algorithms start to vary the location of the fairlead within the chain. In an iterative process, x is sought after such that the tension difference ΔT is minimised. The wheel has been defined in the building process, and the corresponding line-end tensions are compared. If the tension difference is less than 3% of the line tension, the sliding point is considered in equilibrium. The 3% was chosen because smaller tolerances would not lead to different conclusions but would take a longer time to run.

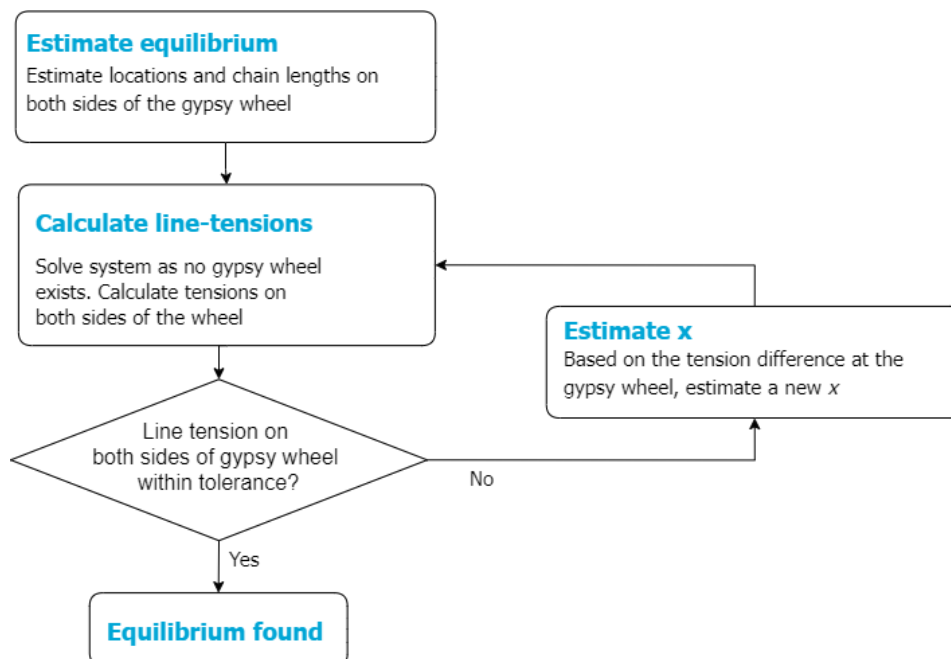


Figure 3.5: Methodology of including a sliding point in the mooring system

For the looping sequence, it was tried whether the sign and quantity of the tension difference could form

a gradient for an optimising algorithm. It was attempted to find a relation between tension difference and the gradient; $\frac{d\Delta T}{dx}$. However, it did not lead to improvements in terms of convergence speed or robustness of the algorithm. More time could be invested in the optimisation but is not the focus of this research. In the end, finding the optimal x can be done in two ways: By Simplicial Homology Global Optimisation (SHGO) or by brute force. SHGO is a solving method of the Scipy optimisation module and performs well for non-linear optimisation problems without gradients.[36]. It usually finds the global minimum of the tension difference functions. If the algorithm fails to find a solution, all options in a specified interval are tried, and the best option is considered optimum. If this 'brute' solution does not meet the 3% tension difference, the code returns an error because that usually indicates a mistake in the system definition.

Validation of functionality of the wheel module Throughout the building process and the equilibrium finding, information is added to a 'simulation summary'. That proved exceptionally useful for this module because the results can be manually checked very quickly.

This relation between x and the tension difference at the wheel can be visualised in a graph as seen in figure 3.6. This example comes from a fairlead tensioning simulation where line 2 is the line section between the FOWT fairlead and the AHV, and line 4 is the line section between the FOWT fairlead and the anchor.

From this graph, it can be seen whether a logical value of x is found. When the line tension difference has a distinct minimum and the two-line tensions are smooth, the model has found the correct value of x . At any time, the found value of x should never exceed the line length of one of the two connected lines.

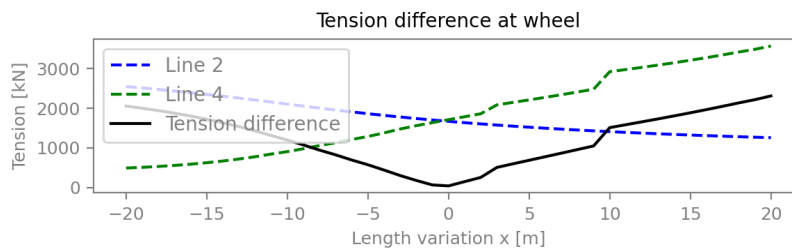


Figure 3.6: Tension differences at the wheel for a range of x .

Simulating the single line as two sections with equal tension at the connection point at the fairlead leads makes it possible to include the catenary effect in both sections. In reality, the mooring line rolls over the fairlead at the FOWT.

3.7. Description of modelled scenarios

It is required to define all geometrical aspects of the FOWT, AHV and mooring system to perform simulations of the pre-tensioning operations. Since this research focuses on pre-tensioning operations, an existing FOWT and AHV is selected based on its future potential and available information.

3.7.1. Floating turbine

Considering the strengths and weaknesses of the mentioned support structure concepts in 2.1, a decision is made on which concept to focus on for this project: TLP platforms have the potential to be relative light-weight structures while being very stable. However, TLPs are, by definition, do not have a catenary mooring system but a taut mooring system. Their hook-up procedure often involves more ballasting-related procedures instead of shortening one of the lines. Spars and semi-submersible (also referred to as *semi-subs*) form the majority of floating turbines already afloat or currently being developed[13]. Although the dynamic behaviour of spars and semi-subs are vastly different, they have similar catenary mooring systems[18][24]. Although some similarities, the semi-submersible has two advantages over a spar: Firstly, the depth range of a semi-submersible is favourable. Semi-submersibles can

be deployed in relatively shallow water compared to spars. For many of the planned FOWT farms, the depth is in a region where deep spar floaters would not be feasible[37]. Secondly, 'mating'(installing the turbine on the floater) of spar-type floaters has some draught-related constraints. The turbine and the semi-submersible can be mated at a quayside, which is very rare for spar types. Exceptions exist: The Hywind Tampen is built in a deep fjord with a custom quay. With the knowledge about the depth constraints, differences with taut mooring and the market predictions, it was chosen that a semi-submersible floater would be most logical to represent future projects.

Various semi-submersible configurations for FOWTs are being developed. Examples are WindFloat[20], OC4-DeepCWind[38] and the UMaine VoltturnUS[39]. A distinction can be made between types of floater designs based on the amount of floater columns and the presence and amount of braces in the waterline area.

The Stiesdal Tetraspar and its associated mooring system formed a sound basis for an installation storyboard in section 2.3. However, for load estimations for future pre-tensioning operations, the turbine's 3.6 MW rating is considered outdated for future projects. Of the mentioned semi-submersible configurations, the concept of the University of Maine stood out because its design and characteristics have been very well described in public literature[39]. A render of the turbine and floater is shown in figure 3.7:



Figure 3.7: The UMaine VoltturnUS-S reference platform[39]

The platform is designed to support the International Energy Agency (IEA) 15-megawatt (MW) reference wind turbine. The detail of the complete floating structure is presented in table 3.2. The floater consists of 4 four columns; The three outer columns have a diameter of 12.50 m and the centre column diameter of 10 m. That makes a waterplane area of 1786.8 m^3 . When installed, the platform has a draft of 20 m with a 15-m freeboard to the upper deck of the columns. The completely assembled installed unit displaces 20,206 cubic meters (m^3) of seawater (with an assumed density of 1,025 kilograms per cubic meter [kg/m^3]). The mass composition consists of a 2254 t (metric tonne) turbine, tower and interface mass, and a 17,839-t ballasted platform with 6,065 kilo-newtons (kN) of vertical mooring pretension. The mooring system is further elaborated on in the next section.

Parameter	Units	Value
Platform steel mass	Tn	3 914
Platform ballast mass(Fixed/Fluid)	Tn	2 540/11 300
Turbine,tower and interface mass	Tn	2 254
Total system mass	Tn	20 093
Hull displacement	m ³	20 206
Water plane area	m ²	1 786.8
Draft	m	20
Freeboard	m	15
Vertical Center of Gravity from SWL	m	-14.94
Vertical Center of Buoyancy from SWL	m	-13.63
Pitch Inertia about CoG	kg-m ²	1.25E + 10

Table 3.2: Information of UMaine 15 MW floater[39]

3.7.2. Mooring system

In the definition report of the Umaine VoltturnUS floater, a catenary mooring system is suggested. The system has an assumed deployment depth of 200 m and is held onto the station by a three-line chain catenary mooring system. The chain size and length are selected based on a desire to keep the system's peak surge-sway offset under 25 m during normal operating conditions to limit design constraints on a dynamic electrical umbilical. The mooring system consists of three uniform chain legs, and their geometry is shown in figure 3.8:

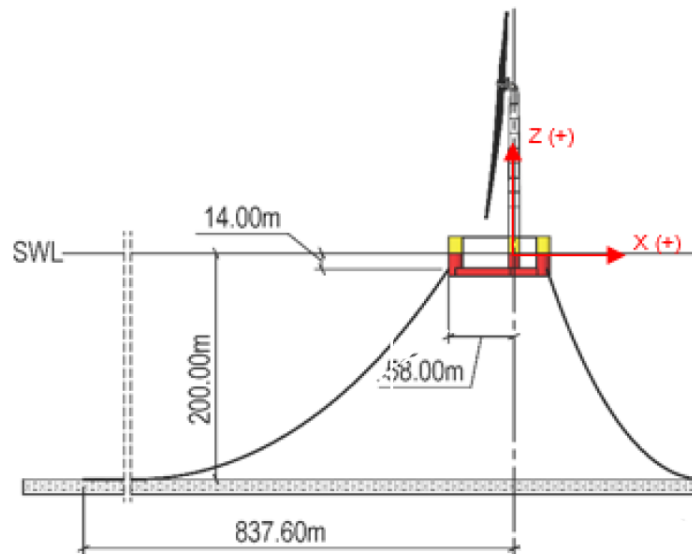


Figure 3.8: Mooring system

The chains have a diameter of 185 mm and are 850 m long each. Their weight is 685 kg/m, but when submerged, this reduces to 691 kg/m due to water displacement. One end of the line is attached to the anchor 200 meters on the seabed. The other end is found at the fairlead of the FOWT 14 meters below the water surface. This configuration leads to a pretension at the FOWT fairlead of 2,437 kN[39].

3.3:

Parameter	Units	Value
Line Type	-	R3 Studless Chain
Number of mooring lines	-	3
Anchor Depth	m	200
Fairlead depth	m	14
Anchor radial spacing	m	837.60
Unstretched line length(L)	m	850
Fairlead radial spacing	m	58
Dry line linear density	kg/m	685
Wet line linear density(W)	kg/m	591
Nominal Chain Diameter	mm	185
Fairlead pre-tension	kN	2 437
Chain axial stiffness (EA)	MN	3 270
Seabed drag coefficient(C_B)	-	0.92

Table 3.3: Information of Umaine mooring system

3.7.3. Vessel

A limited number of shipowners have the fleet to perform the offshore pretension operation. Boskalis, Van Oord, CBO, and Esvagt have large anchor handling vessels with high bollard pull capabilities and heavy winches. In practice, the vessel requirements could vary from one pre-tensioning concept to another. After the tension analysis, it could be concluded that the vessel requirements are reduced.

The main requirement for the vessel selection was that the bollard pull was sufficient to pretension using a fairlead tensioner. To obtain a wire tension at the fairlead of 2437 kN, it was assumed that the vessel should be able to perform a bollard pull in that order of magnitude. The tension analysis outcomes would validate this assumption. Another guide in the vessel selection was the vessels used in previous installations. Although companies are not eager to share installation details, YouTube videos reveal information on the mooring configurations and installation practices. The vessels used to install the Hywind projects, Windfloat Kincardine and Windfloat Atlantic, are all larger than 90 meters.

The CBO Iguacu is an Anchor Handling Tug Supply (AHTS) vessel with adequate bollard pull capabilities. The vessel houses four Huisman winches; therefore, thorough information and drawings are available for this vessel. A render of the vessel is shown in figure 3.9:



Figure 3.9: Anchor handling vessel 'CBO Iguacu'

The vessel is 81 m long and 19.5 m wide. Its maximum draught is 7 meters, with a gross tonnage of 3250 t. The vessel is certified to do up to 220 t bollard pull. The AHV has steel work wires on winches that can handle up to 400 t line tension. The vessel and line details are shown in table 3.4:

Parameter	Units	Value
Length overall	m	81
Vessel breadth	m	19.50
maximum draught	m	7
Gross tonnage	Tn	3 250
Rated Bullard pull	Tn	220
CoG location (from bow/from keel)	m	43.24/6.02
Work wire information	-	108 mm six strand wire rope
Work wire stiffness(EA)	MN	642.1
Work wire maximum breaking load (MBL)	kN	8 240
Work wire submerged weight	kg/m	43.9

Table 3.4: Information of CBO Iguacu

3.7.4. Tensioning equipment

In the mooring industry, one finds the three pre-tensioning concepts: Fairlead tensioning, inline tensioning and fairlead tensioning. They are introduced in section 2.4 and further evaluated in this section.

The pre-tensioners are simulated as a 'point' with a mass. The fact that the tensioners are sliding or rolling over the chain is covered by the 'addWheel' module. Each tensioner has another mass and manufacturer. The details of each are shown in table 3.5.

Parameter	Units	Seabed tensioner	Inline tensioner	Fairlead tensioner
Information	-	Vryhof StevAdjuster[19]	MacGregor ILMT[40]	Scana[28]
Mass	Tn	15	17	18
Size (L× B ×H)	m	4.2 × 3.5 × 2.3	5.3 × 1.8 × 1.0	6.0 × 1.1 × 3.0

Table 3.5: Information on the pre-tensioning cases

The tensioning concepts will be hanging in the following configurations. For each tensioner, it is visualised where to expect mooring chain(black) and AHV work wire(purple). The black circle forms the connection between the two. The chain in the model is the 185 mm mooring chain as specified in table 3.3. The AHV wire from the CBO Iguacu is modelled with the values as specified in table 3.4

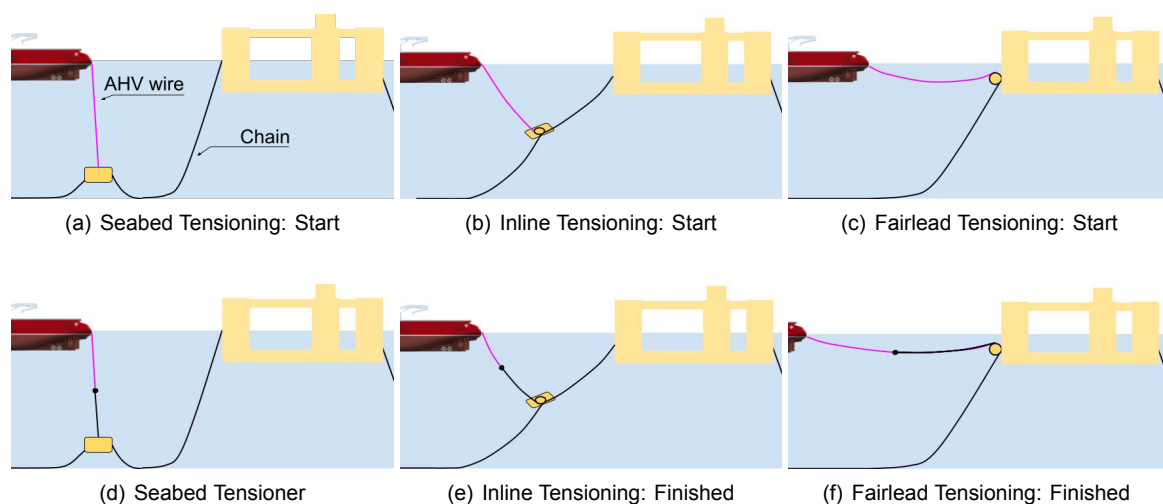


Figure 3.10: Tensioning configurations for three tensioners at the beginning and the end of the operation.

The exact lengths of the work wire are unknown at this point due to a lack of operational details. By

iterating vessel thrust, work wire length and hauled in chain length good understanding of the tensioners is obtained. The configurations details of the pre-tension operations and the static loads are presented in chapter 4

3.8. Conclusion

To conclude this chapter on the model definition. Each modelling element is briefly touched upon to summarise the characteristics and limitations of the simulations:

Mooring lines

- Mooring system for original simulation is three uniform 185 mm chains.
- Hanging shape according to equations as specified in section 2.5: This implies the line is at rest.
- The line modelling includes the effect of elongation and seabed friction.

Simulation of AHV and FOWT

- For the FOWT modelling, the complete turbine is included in the mass calculation.
- The AHV and FOWT's hydrostatic stiffness is included in the equilibrium as described in equation 3.1

Simulation tensioning equipment

- The seabed- and inline tensioner as modelled as point masses. Their rotation is not considered because it is designed such that it aligns with the tensions. The fairlead tensioner is considered to be at one of the fairleads on the FOWT.
- For each pre-tensioning case, a sliding element is present: At this element, the two corresponding line ends must have equal tensions.

Environmental forces Environmental forces are not included in the static analysis. The goal is to create a conceptual comparison of the pretensioning methods.

- Current cannot be interpreted with the catenary equations.
- Wind: Could be included as a static force on the AHV of the FOWT. However, Wind on the AHV would be compensated by the DP system of the AHV.
- Waves are not considered in the static analysis. From the results of the static analysis, the oscillating wave forcing is included in the dynamic modelled, specified in chapter 5.

Equilibrium finding

- Static equilibrium in three dimensions.
- Three 'layers' of iteration: 1) First layer is finding the shape of a single mooring line based on two equations with two unknowns, as specified in 2.5. 2)-The second layer is finding the model equilibrium based on fixed line lengths. 3) The third layer is an iteration of the static equilibrium such that the tensions at both sides of the 'wheel' are equal.

4

Static simulation results

The Umaine semi-submersible floater, CBO anchor handling vessel and mooring equipment are modelled. Firstly, the FOWT and associated mooring system are modelled as installed. From there, the model results are validated against the values in the FOWT description[39]. Subsequently, the AHV and pretension configurations are modelled.

4.1. Modelling of the installed floating turbine as validation

While modelling the system as specified in the previous chapter, the first step is to define the FOWT and its mooring system. Following the specifications, the first 'system builder' was developed to produce the standard mooring system. In figure 4.1, the mooring system is shown in equilibrium for two conditions: Without environmental loads('In rest') and while being subjected to the static rated thrust of $2.5MN$ ('At rated thrust').

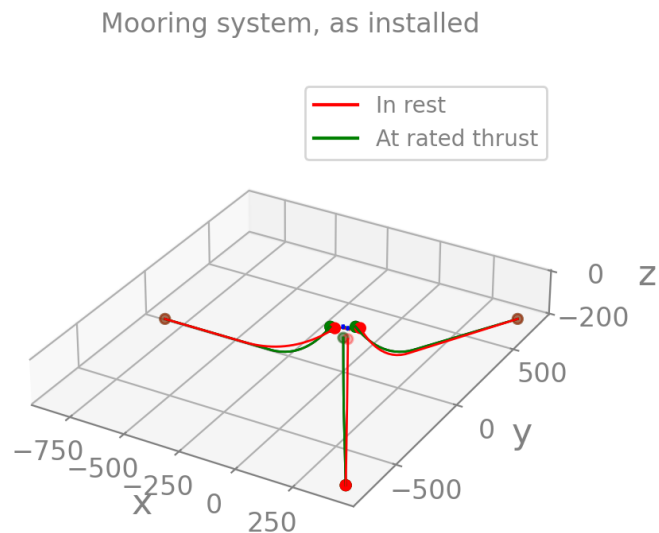


Figure 4.1: Simulation of the mooring system of the Umaine VoltturnUS-S.

To verify whether the model is accurate, the results are compared to the values from the performance assessment in the description of the Umaine floater. Two situations are compared: One in rest to see whether the pretensions from the model and the description match and one at a 25m surge. This is

chosen because it was possible to get the most accurate reading from the fairlead tension diagram from the description for the 25m surge offset. Furthermore, the mooring description included the angle between the sea water level(SWL) and the mooring line; hence, it could be compared.

Table 4.1: Validation of model results against Umaine platform description

	Model result	Description	Relative difference
Fairlead tension: In rest [kN]	2424	2437	0.54%
Fairlead angle from SWL: In rest [deg]	56.24	56.3	0.33%
Fairlead tension: 25m surge offset [kN]	4444	$\approx 4500 \pm 100$	N.A.

A second method for validating the model results is by checking the equilibrium between the floater mass, buoyancy and the vertical component of the line tension: In the model, the sum of the vertical components of the pre-tensioned lines at rest is $6,063kN$. This matches the force difference between the FOWT mass of $20,093t (= 197,045)$ and the buoyancy of $202,100m^3 = (203,107kN)$ within 1%. With a robust FOWT and standard mooring model, the system is expanded with tensioning devices and an AHV.

4.2. Results for the three pre-tensioning concepts

For each pre-tension concept, the tension development is examined at the start and the finish situations: During the pre-tensioning, all the loads gradually increase, and no load peaks are noticed. The beginning and finishing of the tensioning are defined as follows: After the FOWT is hooked up to its mooring legs, the AHV prepares the pretensioning: The three pre-tension systems all contain a kind of wheel or sliding element and a chain stopper. The 'start' scenario is defined where the AHV pulls sufficiently to unlock the chain stopper and have an equilibrium at the gypsy wheel. The 'end' scenario is defined such that the length in the mooring line(between the anchor and the FOWT) is 850 m and the wheel is in equilibrium. Then, the chain can be locked off, and the AHV can disconnect.

4.3. Line tensions

Until now, only the anchors, floater and mooring lines were simulated. For each pre-tensioning option, a model variation is created as specified in the previous chapter. The resulting catenary configurations are pictured below.

Seabed tensioning

In the case of seabed tensioning, the tensioning device is placed 300 meters from the anchor. This is based on the documentation of the Vryhof Stevadjuster[19]. It also specifies that a 15 t bollard pull is recommended during tensioning. After the equilibrium is found, the mooring configuration in the (x, z) plane is visualised in figure 4.2. The two fixed-length mooring lines overlap in the figure on the right of both figures. To understand the configuration better, the AHV and FOWT are illustrated in figure 4.2(a).

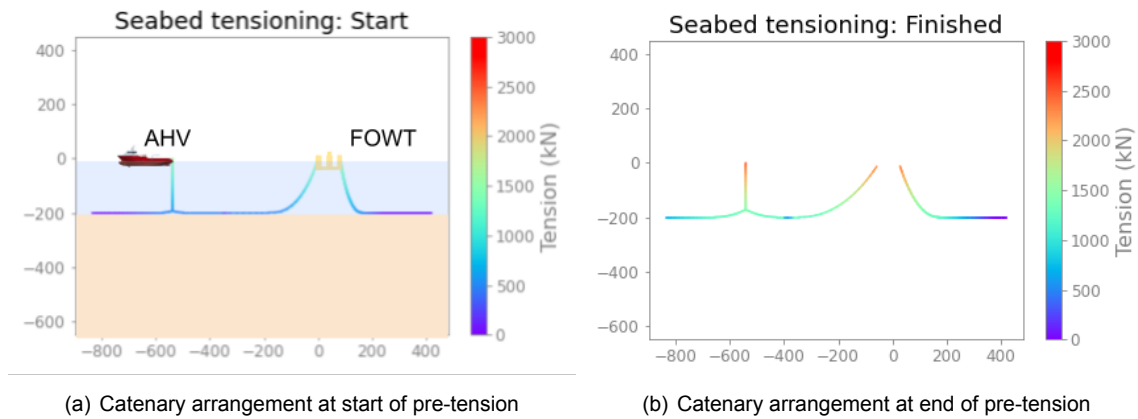


Figure 4.2: Static tensions while tensioning using a seabed tensioner

From the two figures, it is possible to see a chain segment on the seabed between the tensioner and the floater. This chain section needs to move over the seabed to pre-tension the system. To drag this segment over the seabed, the pulling force at the tensioner must be higher than the static drag force of the seabed chain.

Inline tensioning

The inline tensioner forms a more complex configuration than the seabed tensioner. This is because the location of the two floating bodies, the vessel and the FOWT, has become more dependent. After iterating for various line lengths between the tensioner and the left anchor and bollard pulls, it was found that 700 m of fixed chain length allows the tensioner to be off the seabed at every point in the operation.

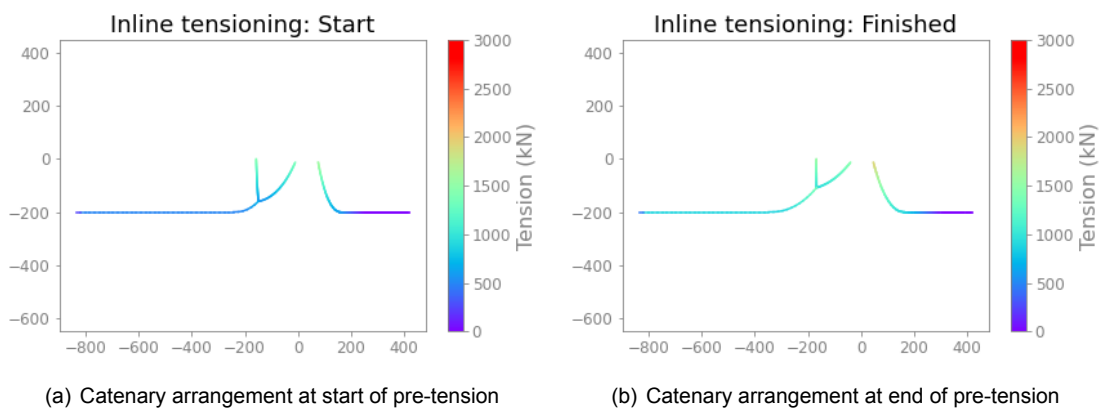


Figure 4.3: Static tensions while tensioning using an inline tensioner

Similarly to seabed tensioning, the tensioning device remains in relatively deep waters. With the all-chain set-up as proposed by the University of Maine, it can be seen that the tension changes within the suspended section by the changing colour. When two end-points of a chain have a significant height difference, the tension at the top of the chain will be higher since it has to hold the mass of the chain. When the chain is shortened, it thus requires less force to do so at the bottom than shortening at the top. The tension difference at the floater compared to the tensioner is shown in the comparison in section 4.4.

Fairlead tensioning

As explained above, the tension at the top end of the chain will be higher than at the bottom and hence, one expected higher required tensions from the AHV to pre-tension the mooring system. Furthermore,

the wire leaves the AHV almost horizontally. That means the AHV has to use its propulsion system to maintain this tension in the wire between the vessel and the floater. In the other concepts, an onboard winch could apply and retain the tension wire.

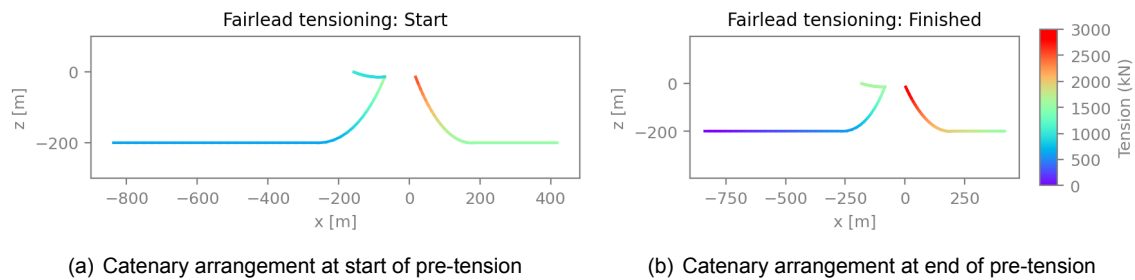


Figure 4.4: Static tensions while tensioning using a fairlead tensioner

In the catenary arrangement at the end of pre-tensioning, it can be seen that the two fixed-length mooring lines on the right of FOWT are under higher tension than the other two pre-tensioning concepts. This is because the AHV exerts a force of 1557 kN on the FOWT. Therefore, the two right mooring lines must compensate for this to remain in equilibrium.

4.4. Load development

This research aims to contribute to decision-making in the pre-tension phase planning. The first load comparison can now be performed. A total of nine features contributed to understanding the pre-tensioning: The lengths of the lines within the system, the vessel bollard pull and the line tensions at the AHV, tensioner and FOWT.

Table 4.2: Results of pre-tensioning operation static simulation with original mooring system

	Unit	Seabed tensioning		Inline tensioning		Fairlead tensioning	
		Start	Finished	Start	Finished	Start	Finished
AHV workwire length	m	180	80	180	0	47	47
Chain length between AHV and tensioner	m	0	100	0	100	0	103
Total line length between AHV and tensioner	m	180	180	180	100	47	150
Chain length between FOWT and tensioner	m	650	550	300	200	N.A.	N.A.
Vessel bollard pull	Tn	15	15	1	1	139	167
Line tension at AHV	kN	857	1707	588	1304	1 392	1645
Line tension at FOWT fairlead	kN	1 580	2 485	1 380	1707	1 388	1 671
Line tension at fairlead wheel	kN	780	1 166	425	1 085	1 388	1 671
Line tension in fixed lines	kN	1 580	2 585	593	1 313	2 235	3 321

The wire tensions of the AHV are considered an essential criterion of which method is favourable. Table 4.2 clearly shows that the AHV line tensions remain at the lowest during inline-tensioning. This can be explained by the fact that the inline tensioner combines the advantages of the other two mechanisms: During the tensioning, no chain has to be dragged over the seabed while also having a 'low' point within the suspended chain where it is shortened. The line tensions at the FOWT are all significantly lower than what can be expected during extreme weather. However, the tensions on the fixed-length lines during fairlead tensioning are considerably higher than the other concepts. Although the bollard pull during seabed tensioning is adopted from the Vryhof manual, the bollard pull for inline-tensioning is arbitrary. The required bollard pull during fairlead tensioning is the largest as expected. In the very

primarily estimates during the vessel selections, a higher bollard pull was assumed because it was not known that the gypsy wheel acts as a 2:1 pulley system during tensioning.

Besides the conclusions drawn from table 4.2, the figures of the previous section also reveal information about the systems. The colours change within most of the mooring lines. These tensions can have two different explanations: The seabed friction gradually decreases the tension in the mooring line on the seabed. This effect is quantified with the equations from the literature review but is more apparent in the figures above. Secondly, it is surprising to see how much tension is introduced in the suspended section. The sections of chain suspended in all sea states do not contribute much to the overall mooring stiffness[41]. Synthetic or steel inserts are usually used to maintain a specific mooring stiffness with less weight per mooring line.

As for the Umaine floater case, the all-chain mooring configuration has been used for the hydrodynamic simulations. However, it is stated that the mooring system is dependent on local conditions and is not certainly fixed. Although the mooring composition becomes more complex, the load reduction brings more benefits than disadvantages. This research should be helpful in the future and apply to future concepts. Therefore the relation between mooring configuration and loads during pre-tensioning is analysed.

4.5. Sensitivity study: Advanced mooring system with inserts

An alternative mooring system is designed to perform the pre-tensioning operations on. Eventually, the tensions while pre-tensioning for the alternative mooring system should give insight into the relation between mooring configuration and pre-tension characteristics.

The mooring system proposed in this section is only designed to have a horizontal restoring force behaviour. This is a usual first step for mooring system design, but it does not ensure that a mooring system with an insert is fully compliant. That would require more research.

4.5.1. Setting up the mooring system

While designing the alternative mooring system, it was ensured that as many elements of the mooring system remained equal, the difference would solely come from the insert. An insert material was selected, and then the chain length was tuned to have an equal restoring force.

The common materials for inserts are synthetic inserts or steel wires. To get the most out of this research, large differences with respect to the original mooring system are favourable. Steel wires are relatively heavy compared to synthetic, so a synthetic insert is selected. Furthermore, most of the current mooring systems with semi-taut configurations use synthetic inserts. According to the documentation of the Umaine Floater, the highest fairlead tension that can be expected in an all-chain set-up is 6.4MN. API RP 2SK recommends a safety margin of 2. According to Vryhof Mooring Manual[14], a 137 mm rope is sufficient. The length of the synthetic insert must be such that the inserts would never touch the seabed during regular operation. It is possible to pre-lay the synthetic fibre on the seabed before pre-tensioning.

The chain length is then altered to match the mooring stiffness of the original mooring system. It led to a mooring system with a 200 m insert and a slightly shorter overall line length of 846 m, compared to 850m for the original mooring system. The anchor locations are not changed. This new mooring configuration with the required line weight only requires 1313.2 kN of pre-tension. Table 4.3 fully specifies the alternative mooring system with inserts:

Parameter	Units	Value
Total line length	m	846
Chain length	m	646
Insert length	m	200
Insert type	-	Dyneema
Nominal line diameter	mm	137
Dry line density	kg/m	12.9
Submerged line density	kg/m	3.08
Pre-tension at FOWT fairlead	kN	1 313.2
Fairlead angle from SWL [deg]	deg	45.6

Table 4.3: Information of the alternative mooring configuration for the Umaine floater with Dyneema inserts

The mooring system as specified above is simulated. The resulting configuration is shown in figure 4.5(a) and the restoring force behaviour is compared to the original system:

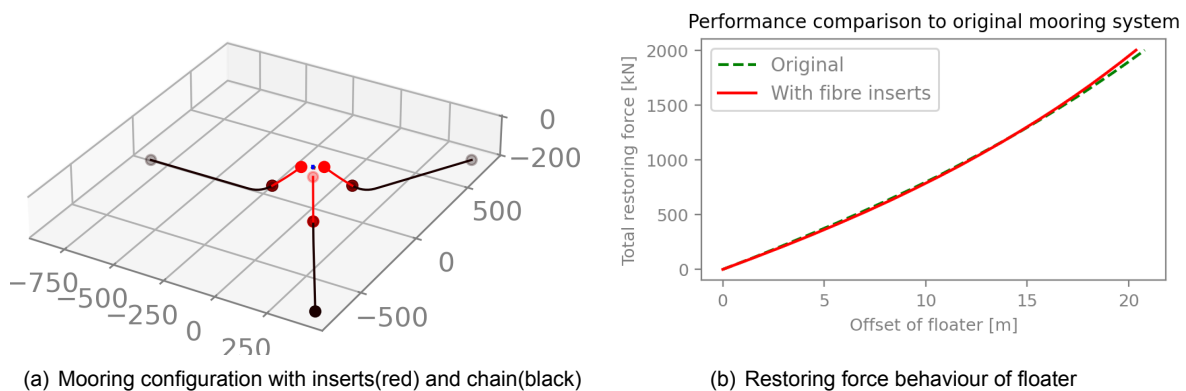


Figure 4.5: Mooring configuration with inserts visualisation and restoring force comparison

The restoring force comparison shows that the alternative mooring system matches the restoring force behaviour of the original mooring system. The total dry mooring line weight for the new mooring line is 444.1 Tn, which is only 76% of the original 850 m line with 185 mm chain shackles. Furthermore, the pre-tension of 1 313.2 kN is a 46% reduction. The practical implications include that the floater does not have to support 6 063 kN of vertical pre-tension anymore, but just 2 816 kN. This difference of 3,184 kN could be compensated by additional ballast or potentially a smaller floater. This effect is not further studied.

4.5.2. Pre-tension load development results

The definitions of points and lines is adjusted to include the inserts and for each pre-tensioning mechanism, the operation is simulated at the beginning and the finish.

Seabed tensioning

For the images with synthetic inserts, the mooring configurations are shown where the colour represents the line material: Black lines represent the 185 mm chain, red represents the synthetic insert and blue represent the AHV work wire.

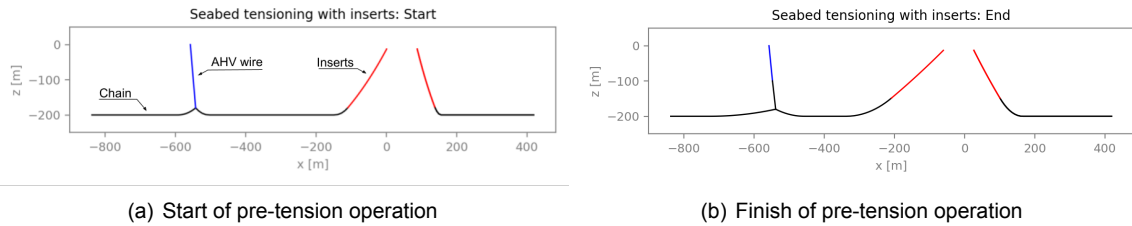


Figure 4.6: Configurations during the start and finish of the seabed pre-tensioning with inserts

What is interesting to see is that the suspended section is completely straight because it doesn't sag under its own weight. The result is that the section on the seabed is longer, hence a higher required drag force to pull the chain through the seabed tensioner.

Inline tensioning

In both the beginning and the finish of the tensioning, it can be observed that the catenary shapes are mostly found within the chain segments. Without the inserts, these hanging segments were more uniform within one line. Now with the inserts, one can see that the lightweight inserts almost remain straight since they barely hang under their weight.

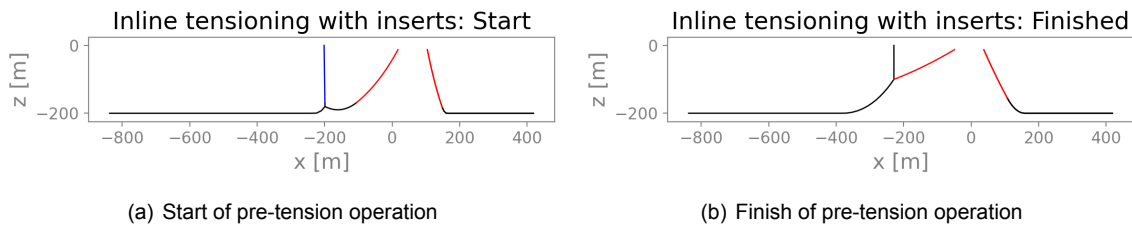


Figure 4.7: Configurations during the start and finish of the inline pre-tensioning with inserts

The exact tensions are described in table 4.4.

Fairlead tensioner

The fairlead tensioning is expected to show the most significant difference between the mooring confirmation with and without inserts. The AHV fully takes on the weight of the suspended mooring line section. Exactly the suspended section is much lighter with the inserts.

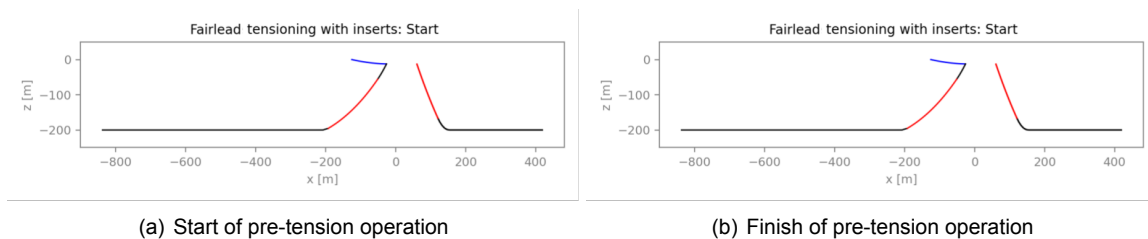


Figure 4.8: Configurations during the start and finish of the fairlead pre-tensioning with inserts

Result comparison The results are compared to each other and the mooring configuration without inserts and tabulated below:

Table 4.4: Results of pre-tensioning operation static simulation with mooring system with inserts

	Unit		Seabed		Inline		Fairlead	
			Value	Difference	Value	Difference	Value	Difference
Bollard pull	T	Start	15	0%	1	0%	39	-65%
		Finish	15	0%	1	0%	103	-39%
Tension at AHV	kN	Start	646	-25%	585	-1%	395	-75%
		Finish	1 525	-11%	1 142	-12%	1 034	-37%
Tension at FOWT	kN	Start	479	-70%	308	-78%	390	-66%
		Finish	1 389	-44%	853	-50%	1 082	-35%

Implementing inserts has led to lower pre-tensioning requirements in all aspects. Three particularly interesting outcomes: Firstly, the tension at the fairlead of the FOWT is consistently lower: This can be explained that regardless of the tensioning method, this heavy 200 m of the chain had to be hung from the floater. Secondly, while tensioning using a seabed tensioner, the inserts have not led to decreased tension at the AHV. This can be explained that most of the tension gains are found between the FOWT fairlead and the touchdown point of the chain. Thirdly, fairlead tensioning shows the most significant dependency on the mooring components and required pre-tension load. As mentioned, the suspended line weight largely influences the tensioning at the top. By pre-tensioning at the lower location, the floater takes some of the weight of the mooring system.

4.6. Conclusions on static modelling

The current model gives insight into the static configuration while pre-tensioning. At sea, waves, wind and current can excite the floater, the AHV or the mooring lines.

It can be concluded from the static research that inline tensioning yields the lowest maximum static tensions while pretensioning on the AHV for the original mooring system. Including inserts resulted in lower tension at the AHV when using a fairlead tensioning. However, this must be maintained by fuel-intensive bollard pull instead of having it on a winch.

To gain more confidence in the comparison, it is helpful to understand how the environment and floater motions influence the wire tensions. More specifically, the wire tensions at the AHV. The mooring system, including the tensioner itself, is built to withstand storms that will yield higher forces at the anchor, tensioner and floater. The AHV, however, is the temporary component during installation and involves human activity on deck.

Additionally, the possibility of resonance occurrence could be a limiting factor in operations planning for this complex mooring configuration. Mooring configurations for floating wind turbines usually have eigen frequencies of around 120 seconds. [3]. Possibly, due to the introduction of new floaters and mooring lines, this resonance issue might become more critical.

To conclude, the dynamic model should answer the following two questions:

- Can resonance occur with such mooring setups?
- Do the motions of the bodies strongly influence the tensions such that one becomes more preferable over the other?

This analysis is only performed for the inline and fairlead tensioners. A characteristic of the seabed tensioner is that it has a chain on the seabed between the tensioner and the floater. From the models above, it is deduced that there are between 95 and 332 m of chain (without inserts). The static drag required to move this chain is so high that no dynamics will happen between the floater and the vessel. Therefore seabed tensioners are not considered in the dynamic simulation.

5

Model extension for dynamic simulation

The dynamic model builds on the results of the static simulation. In this chapter, the model and its assumptions are discussed. First, the modelling approach is introduced as well as extra inputs that are required for dynamic modelling.

Two configurations are run: The inline tensioner and fairlead tensioner. They have common elements, but the differences become evident throughout the description of the model inputs and simulation method.

5.1. Dynamic simulation methodology

Mooring dynamics can be simulated in a variety of methods. However, the difference between the results is a well-studied area, and the limitations are known.[42]. This research aims to identify differences in floating body dynamics and tensions between pre-tensioning concepts. More specifically, two main questions were raised from the static analysis: Firstly, the dynamic model should indicate potential resonance issues. Secondly, the model should show which of the pre-tensioning concepts results in the highest loads. In this section, the modelling methodology is selected.

Discretised cases or full operation simulation Pre-tensioning is a process where the system changes over time. Changes in the chain lengths, tensions and locations of the AHV and FOWT are all due to hauling in the slack chain, as seen in the previous chapter. Two strategies were considered to handle the changing line length: The first option is discretisation into several 'cases' from the beginning to the end of the operation. This way, the dynamics would be simulated as if the chain length is constant during the duration of the simulation. Alternatively, a time simulation for the entire length of the operation was considered. However, A pre-tension procedure takes between 2 and 8 hours[26] and performing a simulation for such a long period was considered not practical. It was decided that the two initial cases(the beginning and the final configuration) had large differences, and analysis in the middle could contribute to understanding the pre-tensioning. Hence, a dynamic simulation will be done at the beginning, halfway and at the end of the pre-tensioning operation. If two simulations show significant unexpected differences, more intermediate simulations can be performed.

Time domain or frequency domain Simulations in the time-domain as frequency domain are considered. In the time domain, nonlinear behaviour can be included, but it is a more complex simulation to set up, especially if the model is developed from scratch. Frequency domain simulations benefit because they are computationally simpler than their nonlinear counterparts. Therefore, it is often desirable to linearise the governing dynamics to simplify the analysis and reduce the computational requirements of the model. For example, In a study by Cerveira et al.[43], the power production of a Wave Energy Converter (WEC) is analysed. During operation, the WEC motions are of relatively small amplitude; therefore, it is assumed possible to approximate the nonlinear mooring characteristics as a linear system. The basis of the model is linear equations of motion for the WEC, which are then solved in the frequency domain. This computational advantage, unfortunately, comes at the price of

model accuracy; Complex nonlinear responses can be found in mooring systems. They are introduced into the system by geometric non-linearity or quadratic drag and can not be predicted by an equivalent linearisation method.[42]

Since this research aims to compare the dynamic models between pre-tensioning concepts, it was ought that differences between concepts could already become evident using a linear model. Furthermore, pre-tensioning is limited anyway by AHV workability; thus, similarly to the research of Cerveira, such operations will occur in small-amplitude waves.

Environmental conditions In reality, the complete system of AHV, FOWT and mooring system can be excited by various external factors. In this model, first-order wave excitation is considered. Therefore, wind and current are not treated but are elaborated on shortly.

Pre-tensioning is a subsea operation, and as a result, the wind has no to little impact on the loads within the mooring system or floating responses. During installation, the wind turbine is not operational, and the blades are rotated such that the turbine generates as little drag as possible. In the static analysis, the influence of wind was observed. It was observed that the static wind had a negligible impact on the position of the FOWT and the that the AHV would correct for the wind by holding its position with the DP system.

Currents generate loads not only on the mooring system but also on the floater and generate vortex-induced motions(VIMs)[3]. This study aims to compare the differences in static and dynamic loads and behaviour. Since the simulations of the concepts have a considerable overlap in terms of FOWT, AHV and most subsea configurations, the current is not expected to contribute significantly to insights into pre-tension concept differences. However, when more accurate simulations are required, currents must be evaluated and included in the modelling.

The relation between waves and floating structures is an extensive field of research and is relevant for this study. Transfer functions for both the AHV CBO Iguacu and the Umaine floater allow quantifying the forces or motions associated with waves of a particular frequency. The transfer functions are described in the next section and account for linear first-order waves. However, the influence of second-order waves is neglected in this comparative study. In other simulations, ignoring wave drift has contributed to more damping, hence, smaller FOWT responses[44].

5.2. Dynamic modelling components

For this research, the pre-tensioning configurations will be modelled as 2D systems as visualised in figure 5.1.

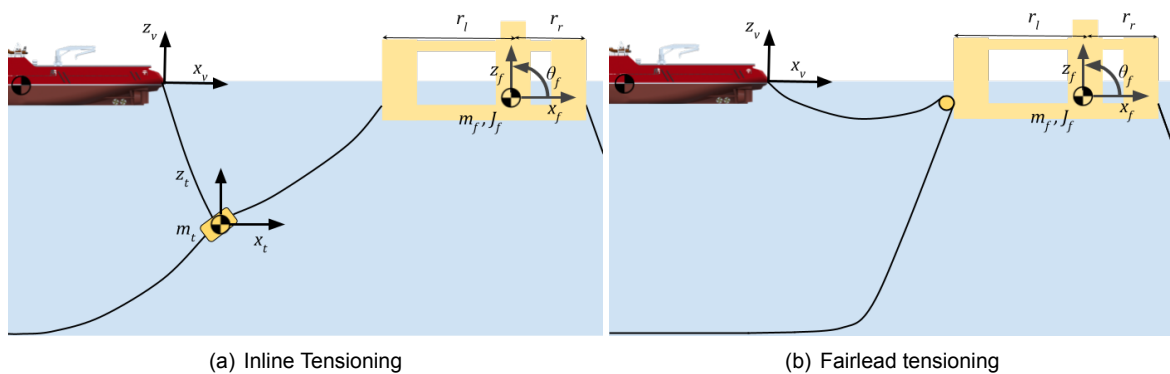


Figure 5.1: Kinetic diagrams for dynamic simulation

The above elements will be elaborated on in more detail in the coming subsections. Depending on the pre-tension configuration, the system is assumed to consist of two or three rigid bodies. The inline tensioning has three bodies, and in the fairlead tensioning, two and all only move within the xz -plane. The movement of the FOWT(X_f) is described by surge(x_f), heave(y_f) and pitch(θ_f) as shown in equation

5.1:

$$X_f = \begin{bmatrix} x_f \\ z_f \\ \theta_f \end{bmatrix} \quad (5.1)$$

The motion of the tensioner is described slightly differently. Due to the small size of the tensioner, the tensioner is simulated as a point mass that has no pitch. The motion of the floater (X_t) is thus only described by its surge (x_t) and heave (z_t) as shown below.

$$X_t = \begin{bmatrix} x_t \\ z_t \end{bmatrix} \quad (5.2)$$

The AHV motions around the CoG ($X_{v,CoG}$) are defined as follows:

$$X_{v,CoG} = \begin{bmatrix} x_{v,CoG} \\ z_{v,CoG} \\ \theta_{v,CoG} \end{bmatrix} \quad (5.3)$$

However, the main point of interest for this simulation is where the chain or work wire attach to the AHV. This is the stern roller at the aft of the vessel. The distance between the vessel stern roller is deduced from table 3.4: 37.8 m. Hence, the surge (x_v) and heave (z_v) motion of the stern roller is defined as:

$$\begin{bmatrix} x_v \\ z_v \end{bmatrix} = \begin{bmatrix} x_{v,CoG} \\ z_{v,CoG} + 37.8\theta_v \end{bmatrix} \quad (5.4)$$

The motions, as mentioned above, are relative to their position in rest. The positions in rest are found in the static analysis.

5.2.1. Floating turbine

The FOWT is modelled as a rigid body subjected to added mass, hydrodynamic damping, hydrostatic restoring forces and external forces from waves and the mooring system. Equation 5.5 forms the equation of motion for the floating body. As mentioned above, the motion of the FOWT is described by the surge, heave and pitch.

$$\left(\begin{bmatrix} [M] \\ \text{Mass} \end{bmatrix} + \begin{bmatrix} [A(\omega)] \\ \text{Added mass} \end{bmatrix} \right) \begin{bmatrix} \ddot{x}_f \\ \ddot{z}_f \\ \ddot{\theta}_f \end{bmatrix} + \left(\begin{bmatrix} [B_{visc}] \\ \text{Damping} \end{bmatrix} + \begin{bmatrix} [B_{rad}(\omega)] \end{bmatrix} \right) \begin{bmatrix} \dot{x}_f \\ \dot{z}_f \\ \dot{\theta}_f \end{bmatrix} + \begin{bmatrix} [K] \\ \text{Restoring} \end{bmatrix} \begin{bmatrix} x_f \\ z_f \\ \theta_f \end{bmatrix} = \underbrace{\begin{bmatrix} F_{Hyd,x}(\omega) + F_{Moor,f,x} \\ F_{Hyd,z}(\omega) + F_{Moor,f,z} \\ \tau_{Hyd}(\omega) + \tau_{Moor,f} \end{bmatrix}}_{\text{Loads}} \quad (5.5)$$

Each individual variable in the equation will be elaborated on and quantified in the sections below. The University of Maine made many of the floater hydrodynamic coefficients publicly available through the documentation of the floater[39] as well as an online Github repository[45] where the coefficient could be found.

Mass and added mass

The mass matrix without added mass is shown below on the left: For the translation motions (surge and heave), the total system mass of 20.09E6 kg is used. For the rotational motion (pitch), the total pitch inertia about the CoG of 1.25E10 is used.

$$[M] = \begin{bmatrix} m & 0 & 0 \\ 0 & m & 0 \\ 0 & 0 & I_\theta \end{bmatrix} \quad (5.6) \quad [A(\omega)] = \begin{bmatrix} A11 & 0 & A15 \\ 0 & A33 & 0 \\ A15 & 0 & A55 \end{bmatrix} \quad (5.7)$$

When the floater moves through the water, it accelerates the surrounding water to a certain extent. This phenomenon is modelled as added mass. The quantity of the added mass is calculated by the boundary element method in WAMIT for the definition of the Umaine floater[39]. This added mass is dependent on the excitation wave frequency (ω). Hence, all the entries in the added mass matrix A are

dependent on wave frequency. The diagonal entries are shown in figure 5.2; the remaining entries can be found in the appendix.

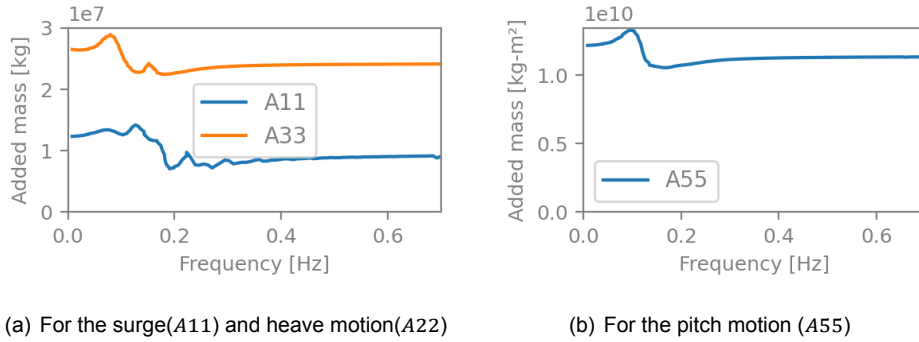


Figure 5.2: Added mass entries for the Umaine semi-submersible floater

The constant mass matrix M is summed with the added mass per wave frequency $A(\omega)$ in the equation of motion as shown earlier in 5.5.

Hydrodynamic damping

The floating turbine undergoes two forms of damping: Viscous damping and radiation damping. The viscous damping is frequency independent and calculated for the development of the floater. The viscous damping values are provided below.

$$[B_{visc}] = \begin{bmatrix} 9.225E5 & 0 & -8.918E6 \\ 0 & 2.296E6 & 0 \\ -8.918E6 & 0 & 1.676E10 \end{bmatrix} \quad (5.8) \quad [B_{rad}(\omega)] = \begin{bmatrix} B11 & 0 & B15 \\ 0 & B33 & 0 \\ B15 & 0 & B55 \end{bmatrix} \quad (5.9)$$

In addition to the viscous damping, radiation damping also applies to the structure. Radiation damping is the phenomenon of energy propagation away from the structure by motion-induced waves. As with added mass, this damping influence depends much on the frequency of the excitation wave. The damping matrix for surge, heave and pitch is shown in equation 5.9. The diagonal entries are shown in figure 5.3.

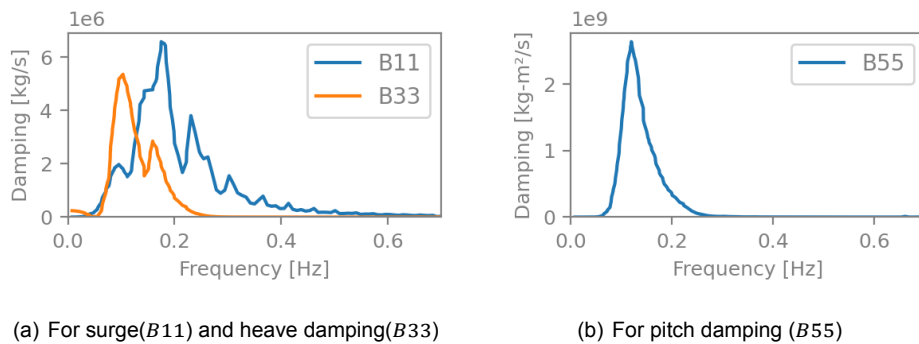


Figure 5.3: Radiation damping for the Umaine semi-submersible floater

The constant viscous damping matrix B_{visc} is summed with the radiation damping B_{rad} , which is a function of the wave frequency ω .

Restoring stiffness

The hydrostatic stiffness matrix defines how the net weight/buoyancy load varies with changes in position from the CoG position. Within the three DOFs that are considered, there only exists a hydrostatic

stiffness for heave and pitch. When the floater is moved in the surge(x) direction, no fluid-related force will force it back to its original position. This is the primary function of the mooring system and will be handled separately. The hydrostatic stiffness for heave and pitch is calculated based on the geometry of the floater within the study for the definition of the Umaine floater[39].

$$[K] = \begin{bmatrix} 0 & 0 & 0 \\ 0 & 4.47E6 & 0 \\ 0 & 0 & 2.19E9 \end{bmatrix} \quad (5.10)$$

Hydrodynamic loads

For this frequency domain analysis, regular waves excite the structure and vessel in a sinusoidal way. The wave-induced forces on the structure are included in the equation of motion for the floater as $F_{hyd,x}$, $F_{hyd,z}$ and τ_{hyd} . The wave forcing has an amplitude that scales linearly with the wave height(ζ). The wave excitation coefficients are shown in figure 5.4(b). The phase shifts per wave frequency can be found in appendix A.1. The wave excitation coefficients and phase differences are taken from the description of the Umaine floater[39].

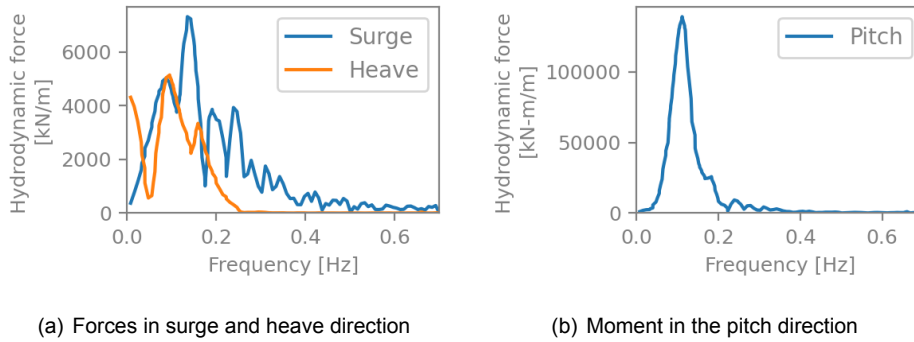


Figure 5.4: Wave induced force coefficients

The methodology for solving the equations of motions will be discussed in section 5.3

5.2.2. Tensioning equipment

The tensioning equipment requires two different approaches for the two pre-tensioning concepts. In case of the inline tensioning, the tensioner is modelled as a rigid body that is subjected to tensions from the mooring line. Damping is not considered due to the small size of the tensioner. The equation of motion for the tensioner then forms to be:

$$\left(\begin{matrix} \underline{M} \\ \text{Mass} \end{matrix} + \begin{matrix} \underline{A} \\ \text{Added mass} \end{matrix} \right) \begin{bmatrix} \ddot{x}_t \\ \ddot{z}_t \end{bmatrix} = \underbrace{\begin{bmatrix} F_{Moor,t,x} \\ F_{Moor,t,z} \end{bmatrix}}_{\text{Loads}} \quad (5.11)$$

It was mentioned earlier that the motion of the tensioner would solely be described by its translations in the x and z direction. However, due to its small size, the tensioner is simplified to a point mass.

Mass and added mass and damping

Although it's small in size, the tensioner will have added mass due to its movement in the water. For preliminary calculations, Den Norske Veritas(DNV) provides guidance in their recommended practices(RP) RP-C205: Environmental Conditions and Environmental Loads. It states that 51% of the mass can be assumed as added mass for rectangular-shaped objects in the water. Hence, the mass term of the equation of motion for the tensioner can be rewritten as:

$$[M + A] = \begin{bmatrix} 1.51m_t & 0 \\ 0 & 1.51m_t \end{bmatrix} \quad (5.12)$$

Hydrodynamic damping and hydrodynamic forces are not considered on the tensioners due to their small relative size. The hydrodynamic damping is a function of the area, and both tensioners are small. Restoring forces do not apply to the floater since it's fully submerged.

Restoring stiffness The tensioner is solely influenced by the mooring lines. Unlike the floater, no fluid-related force will force the tensioner into its original position. In contrast to the floater, the tensioner doesn't have a restoring force for heave motion either. It is solely the tensions from the mooring lines that will influence the position of the tensioner.

Fairlead tensioning

Simulation of the fairlead tensioning does not require the implementation of an extra rigid body. The tension module is directly attached to the FOWT. The mass of the fairlead tensioner is 18 t and the mass matrix is corrected for the presence of the tensioner: The 18 t is added to the mass entries and the tensioner is considered as a Steiner term and added to the mass moment of inertia J_θ . For the Steiner term, an arm of 58 m is used between the CoG and the fairlead. Below, the two altered values for the mass matrix (equation 5.6) are provided. The influence on the totals is minimal.

$$m = 20,093 + 18 = 20,111 \text{ [Tn]} \quad J_\theta = 1.25E10 + 1/2 \cdot 18,000 \cdot 58^2 = 1.256E10 \text{ [kg-m]}$$

5.2.3. Vessel

The CBO Iguacu is subjected to waves and the tension from the work wire at the stern roller. Preferable, the AHV would be simulated with a similar approach to how the FOWT was modelled. The modelling of FOWT allows for external forcing: Waves and mooring tensions for this simulation. For the AHV, Huisman has the transfer functions for the vessel motion caused by first-order wave excitation. The damping added mass, and hydro-statics information is not available. The AHV is therefore modelled with imposed motions, solely based on the wave-excitation. Contrary to the FOWT and the tensioner, there is no influence on the AHV motion based on the line tension. It is unknown how much impact this will have on the final result but will be evaluated later. The motion information of the AHV is provided as a motion response amplitude operator (RAO) and the phase difference ($\phi(\omega)$) relative to the incoming wave. The RAO of the AHV is shown in figure 5.5; the phase characteristics are in the appendix.

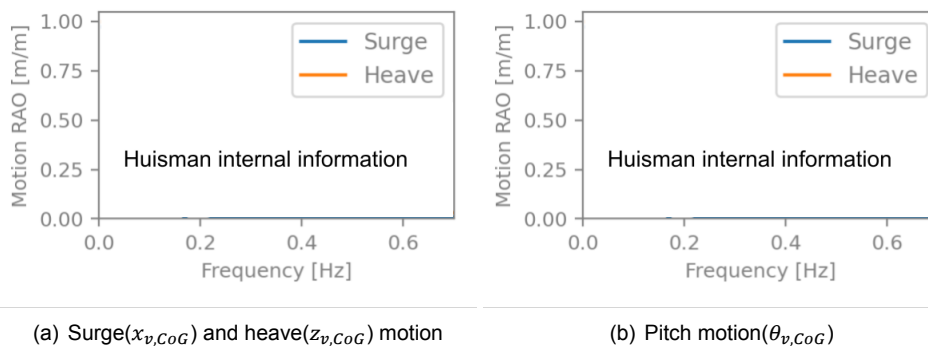


Figure 5.5: Surge, heave and pitch motion for the CBO Iguacu

As shown in the RAO above, the AHV is mainly influenced by waves with a frequency of 0.2 or lower. It will be interesting to see the relationship between the AHV excitation and the dynamic tensions.

5.2.4. Combined equation of motion

The FOWT, AHV and tensioner (in the case of inline tensioning) are still separate elements. For inline- and fairlead tensioning, a different equation of motion is valid, and it starts with the fact that the degrees of freedom for both simulations are different. In the case of inline tensioning: five degrees of freedom apply: The surge, heave and pitch for the floater and the surge and heave of the tensioner. The AHV is not considered 'free' since the RAO imposes the motions. For fairlead tensioning, only the motions of the FOWT are regarded as degrees of freedom.

In both cases, the equation of motion can be written as:

$$[M + A]\ddot{X} + [B]\dot{X} + [K]X = \vec{F} \quad (5.13)$$

Where:

$$X = \begin{cases} [x_t, z_t, \theta_t, x_t, z_t]^T & \text{For inline tensioning} \\ [x_f, z_f, \theta_f]^T & \text{For fairlead tensioning} \end{cases}$$

And \dot{X} and \ddot{X} are the vectors containing the first and second time derivatives, respectively.

5.2.5. Mooring system

The static equilibrium of a mooring configuration, including steady loads and hydrostatics, has been described in the previous section. The bodies and mooring lines move when waves or other factors excite the system. The influence of mooring systems can be simulated in various ways and is related to how the different elements (vessels, weather) are simulated.

The difference between time-domain and frequency-domain has been elaborated on in section 5.1. The mooring system is simulated within a frequency domain simulation as a set of springs with linear stiffness. The advantage is a fast simulation, and as Cerveira suggested in their study, the linear approximation yields reliable results for operational conditions [43].

First, the concept of a catenary mooring line as a linear spring is introduced. From there, the methodology for obtaining the linear stiffnesses is explained. Finally, the mass-spring systems and associated stiffness matrices are shared.

Linear equivalent spring

Changes in the vertical and horizontal distance between two points cause a changing horizontal and vertical force at both ends of the mooring line. The relation between the forces at the nodes (H and V) and a change in horizontal distance (dx) or vertical distance (dz) can be caught in a 2-dimensional stiffness matrix.

$$[K^{2D}] = \begin{bmatrix} K_{11}^{2D} & K_{12}^{2D} \\ K_{21}^{2D} & K_{22}^{2D} \end{bmatrix} = \begin{bmatrix} \frac{\partial H}{\partial x} & \frac{\partial V}{\partial x} \\ \frac{\partial H}{\partial z} & \frac{\partial V}{\partial z} \end{bmatrix} \quad (5.14)$$

Catenary stiffness is usually not linear; however, the restoring force acts relatively linear when the motions remain relatively small. For example, the restoring force for one of the two fixed length mooring lines is shown below. It can be observed that the curve is not linear. However, when one performs a dynamic analysis where the motions are limited, the restoring force around that point shows linear. After the dynamic model, it must be checked that the motions remain in the area where the linear approximation holds.

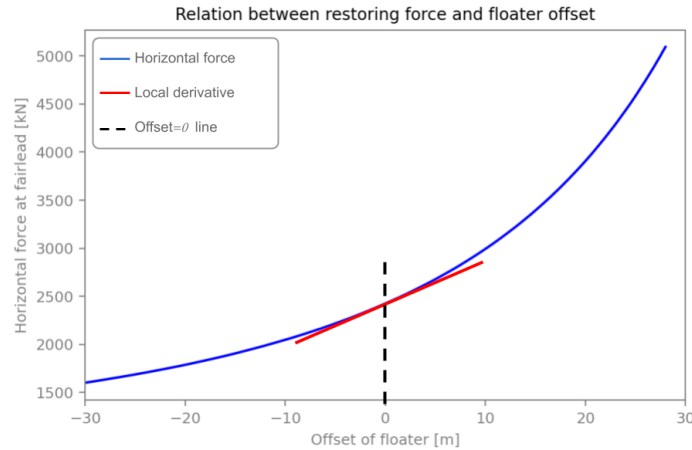


Figure 5.6: Non-linear relation between FOWT surge and restoring force of a mooring line. However, for small oscillation movement, the curve is more linear.

For this mooring line, it can be seen that around the point where there is no surge offset from its natural position, a linear derivation is taken. As long as the oscillatory motion remains limited, the linear approximation is valid. For large motion(10 m and over), it can be seen that the linear approximation is no longer accurate.

The gypsy wheel at the tensioner doesn't rotate with the wave frequency. It turns slowly during pretension when the load on one end builds up.[18]. Unfortunately, the minimum tension difference before an inline or fairlead tensioner started to rotate was not shared. For the modelling, it is thus assumed that the line lengths remain constant within a wave oscillation.

Added mass of chain onto floating bodies and hydrodynamic damping

In the proposed linear mass-spring approach with rigid bodies, the dynamics of the line mass are currently ignored. It has been considered to add a fraction of mooring lines mass to the rigid body masses. This way, the mass inertia of the mooring legs would be better represented by the model. However, no suggestion could be thought of approximating this 'added mass' to the rigid bodies.

When the mooring line moves and oscillates through the water, energy is dissipated through hydrodynamic drag. This drag is not quantified and included in this model. Time-domain simulations are often used to estimate the damping coefficients that are subsequently inserted in a frequency domain. [46]. Neglecting a damping force will cause overestimated motions.

Inline tensioning

With the knowledge of how catenary lines can be modelled as springs for vertical and horizontal distance, one can expand the stiffness matrix with the influences of the mooring line. An overview of the equivalent springs of the mooring lines while inline-tensioning is shown in figure 5.7:

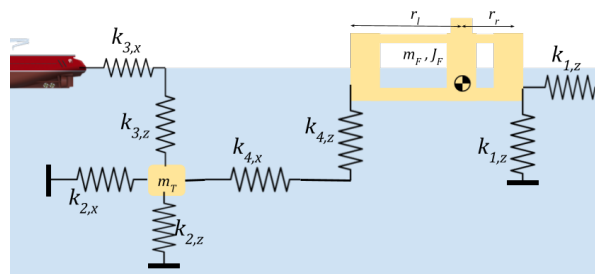


Figure 5.7: Spring configuration of inline tensioning

The equivalent stiffness $k_{1,x}$ and $k_{1,z}$ are the combined stiffness from both mooring lines with the fixed line length. All the other elements represent one sole line. Each spring's elongation is expressed as

a function of the degree of freedom terms in Maple, which is software for mathematics. Subsequently, the relations between degrees of freedom and the restoring forces caused by the lines are expressed in a matrix:

$$\begin{bmatrix} F_{\text{Moor},f,x} \\ F_{\text{Moor},f,z} \\ \tau_{\text{Moor},f} \\ F_{\text{Moor},t,x} \\ F_{\text{Moor},t,z} \end{bmatrix} = \begin{bmatrix} k_{1,x} + k_{4,x} & 0 & 0 & -k_{4,x} & 0 \\ 0 & k_{1,z} + k_{4,z} & k_{1,z}r_r - k_{4,z}r_l & -k_{4,z} & 0 \\ 0 & k_{1,z}r_r - k_{4,z}r_l & k_{1,z}r_r^2 + k_{4,z}r_l^2 & k_{4,z}r_l & 0 \\ k_{2,x} - k_{4,x} & 0 & 0 & k_{3,x} + k_{4,x} & 0 \\ 0 & -k_{4,z} & k_{4,z}r_l & k_{4,z} & k_{2,z} + k_{3,z} \end{bmatrix} \begin{bmatrix} x_f \\ z_f \\ \theta_f \\ x_t \\ z_t \end{bmatrix} + \begin{bmatrix} 0 \\ 0 \\ 0 \\ k_{3,x}x_v \\ k_{3,z}z_v \end{bmatrix} \quad (5.15)$$

The values for r_l and r_r reflect the distance in the x direction between the CoG and the left and right fairlead, respectively. $r_l = 58\text{m}$, which is the fairlead radius, for $r_r = 58\text{m} \cdot \cos(60^\circ) = 29\text{m}$. Furthermore, as can be seen, the AHV motion is modelled as an external force and not one of the degrees of freedom.

Fairlead tensioning

For fairlead tensioning, the only degrees of freedom are the FOWT motions as described earlier. The mooring line configuration has fewer components than used inline-tensioning. The spring definition and relation is shown in figure 5.8:

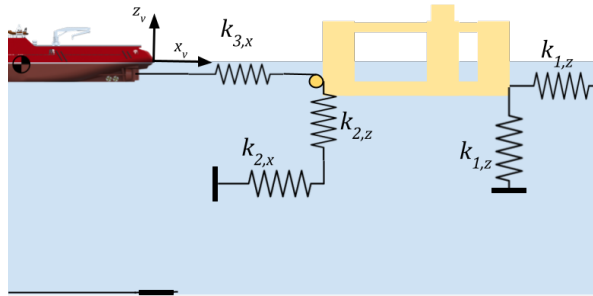


Figure 5.8: Spring configuration of fairlead tensioning

With one line segment and two degrees of freedom less, the equation of motion reduces down to:

$$\begin{bmatrix} F_{\text{Moor},f,x} \\ F_{\text{Moor},f,z} \\ \tau_{\text{Moor},f} \end{bmatrix} = \begin{bmatrix} k_{1,x} + k_{2,x} + k_{3,x} & 0 & 0 \\ 0 & k_{1,z} + k_{2,z} & k_{1,z}r_r - k_{2,z}r_l \\ 0 & k_{1,z}r_r - k_{2,z}r_l & k_{1,z}r_r^2 + k_{2,z}r_l^2 \end{bmatrix} \begin{bmatrix} x_f \\ z_f \\ \theta_f \end{bmatrix} + \begin{bmatrix} k_{3,x}x_v \\ 0 \\ 0 \end{bmatrix} \quad (5.16)$$

Not that line 3, between the AHV and the FOWT, has no vertical equivalent stiffness. From the stiffness calculations, it was seen that for a line where the endpoints were at a similar height, the stiffness in the z -direction was less than 1% of the horizontal stiffness and therefore deduced.

5.3. Solving the equation of motions

All components of the model are now quantified and linearized where necessary. The degrees of freedom and equation of matrix were introduced in 5.2.4. The values for mass, added mass, damping, stiffness and external forcing have been elaborated on and are ultimately combined in 3×3 or $5 \times$ matrices, depending on the pre-tension configuration. The full matrices are shown in appendix B because all entries have been introduced already.

Each degree of freedom is assumed to have a sinusoidal shape with an amplitude, the same radial frequency as its excitation wave(ω) and phase shift relative to the incoming wave on the AHV. For a system with 3 or 5 DOFS, the motion response(X) can be described by a vector of amplitudes(a) and

a vector of phase differences (ϕ). The first and second time derivatives (velocity and acceleration) are also derived:

$$X = a \cos(\omega t + \phi) \quad (5.17)$$

$$\dot{X} = -a\omega \sin(\omega t + \phi) \quad (5.18)$$

$$\ddot{X} = -a\omega^2 \cos(\omega t + \phi) \quad (5.19)$$

For more convenient solving within *Python*, the motion is described as a complex exponential:

$$X = \hat{X} e^{-i\omega t} \quad (5.20)$$

$$\dot{X} = -i\omega \hat{X} e^{-i\omega t} \quad (5.21)$$

$$\ddot{X} = -\omega^2 \hat{X} e^{-i\omega t} \quad (5.22)$$

Where \hat{X} is a complex number. By doing so, phase differences are handled accordingly. Substituting this in the equation of motion:

$$[M + A]\ddot{X} + [B]\dot{X} + [K]X = F \quad (5.23)$$

The time dependant exponent is deduced and \hat{X} is isolated:

$$\hat{X} = F (\omega^2 [M + A] + i\omega [B] - [K])^{-1} \quad (5.24)$$

In its current form, \hat{X} is dependent on wave height since the external force vector F is dependent on wave height. When the wave height (ζ) is isolated, one can use the results of solving equation 5.24 as linear motion coefficients. Both the implied motions on the AHV (X_v) as the wave forcing on the FOWT (F_{hyd}) are described by a coefficient for the amplitude and a phase difference. The AHV motion or wave forces could also be described as the product of a complex transfer function and the wave height, as shown below. The transfer function for the AHV (H_{AHV}) is calculated with the RAO amplitude vector ($|X_v|$) and phase vector (ϕ_v). They are found in appendix A.2.

$$\hat{X}_v = H_{AHV} \cdot \zeta \quad (5.25) \quad H_{AHV} = |X_v| \cdot \exp(i\phi_v) \quad (5.26)$$

Similarly, for the hydrodynamic forcing on the FOWT, one uses the RAO amplitude vector ($|F_{FOWT}|$) and a phase vector ($\phi_{F,FOWT}$):

$$\hat{F}_{FOWT} = H_{FOWT} \cdot \zeta \quad (5.27) \quad H_{FOWT} = |F_{FOWT}| \cdot \exp(i\phi_{F,FOWT}) \quad (5.28)$$

The pragmatic method of solving this, is using a wave amplitude of 1 meter, solve for \hat{X} and calculate the amplitude $|\hat{X}|$ and phases using equations 5.29 and 5.30. This is done because amplitudes and phases are generally easier to interpret than complex values.

$$A = \sqrt{\text{Re}(\hat{X})^2 + \text{Im}(\hat{X})^2} \quad (5.29) \quad \phi = \tan^{-1} \left(\frac{\text{Im}(\hat{X})}{\text{Re}(\hat{X})} \right) \quad (5.30)$$

Maximum tensions From the motion responses, it is possible to calculate the dynamic line tension. From a practical point of view, the line tensions at the FOWT fairlead and the AHV stern roller are most interesting, similar to the static analysis. Although two different pre-tension concepts are considered, and two points of interest are present for each concept, the method to calculate the maximum line tension is the same. For any mooring line, indicated by i , four steps are required to find the maximum tension at a line-end:

- The mooring line tension at an endpoint has a horizontal component (H) and a vertical component (V). For the static case, they are found by finding the catenary equilibrium. In section 5.2.5, the linear relation between the horizontal and vertical components and changes in vertical and horizontal distance between the line ends is elaborated on. The stiffness matrix line (K_i^{2D}) is calculated for the mooring line of interest.

- The horizontal($\hat{\Delta x}$) and vertical($\hat{\Delta z}$) distance between the two endpoints are described as complex values. Depending on the line, this might be the distance between two moving points or a moving point and a fixed point (an anchor). By using complex numbers, the phase difference is accounted for.
- When the horizontal and vertical distance is calculated, they are multiplied by the stiffness matrix of that mooring line(K_i^{2D}) to quantify the dynamic vertical and horizontal component of the line tension:

$$\begin{bmatrix} H_{d,i} \\ V_{d,i} \end{bmatrix} = K_i^{2D} \begin{bmatrix} \Delta x \\ \Delta z \end{bmatrix} \quad (5.31)$$

- The maximum dynamic line tension can be calculated by combining the vertical and the horizontal component:

$$T_d = \sqrt{H_i^2 + V_i^2} \quad (5.32)$$

- At this point, T_d is still a complex number. The final step is to calculate the amplitude $|T_d|$ with the same function as described in equation 5.29.
- If required, the dynamic tension can be summed with the static tension to find the maximum tension.

5.4. Natural frequencies

Resonance issues may lead to the failure of mooring equipment. Hence analysis of natural frequencies(ω_n) is essential. A floating structure and its mooring system are designed so that the natural frequencies are not in the range of external excitements such as wave frequency or rational frequency of the wind turbine rotors.

This eigenvalue problem is now defined and solved in *Python*. To find these frequencies, the undamped system without external influences is considered. This method is adopted from the TU Delft course 'Floating Structures and Offshore Moorings'[47] Hence, the system that needs to be solved reduces to:

$$[K - \omega_n^2 \cdot M] \cdot \hat{X} = 0 \quad (5.33)$$

The determinant of this matrix needs to be zero if the equation shall have more than one trivial solution. Hence, the natural frequencies are found by finding the determinant

$$\det[K - \omega_n^2 \cdot M] = 0 \quad (5.34)$$

Depending on the pre-tensioning situation, five or three degrees of freedom apply. Solving the above equation will leave double the number of degrees of freedom as solutions for ω_n . Due to the square, the roots come in pairs of positive and negative numbers of the same magnitude. We select the positive roots as our natural frequencies. The angular frequencies are divided by 2π as indicated in 5.35 to find the natural frequencies.

$$f_n = \frac{\omega_n}{2\pi} \quad (5.35)$$

For solving the equation, an arbitrary frequency of 0.4 Hz is assumed. The related added mass is used to find the eigenfrequencies. However, the matrices for added mass (A) as found in 5.2.1 result in slightly different eigenfrequencies for each wavelength due to the dependency of wave frequency on added mass. An iteration resolves this: For each natural frequency, the eigenfrequency is found again with the associated added mass. By doing so, the natural frequency matches better with the related added mass.

5.5. Code structure

The existing code structure is expanded to implement the new data and calculations. A new **main script** is used for initiating dynamic simulations. A new class **system dynamics** is built that contains all dynamics-related functions. The **Floating bodies** class is expanded with the hydrodynamic information on the AHV, FOWT and inline tensioner. Finally, the **System** class is modified to calculate the mooring stiffness matrix as specified in equation 5.15 and 5.16. The overview of implementations in figure 5.9 :

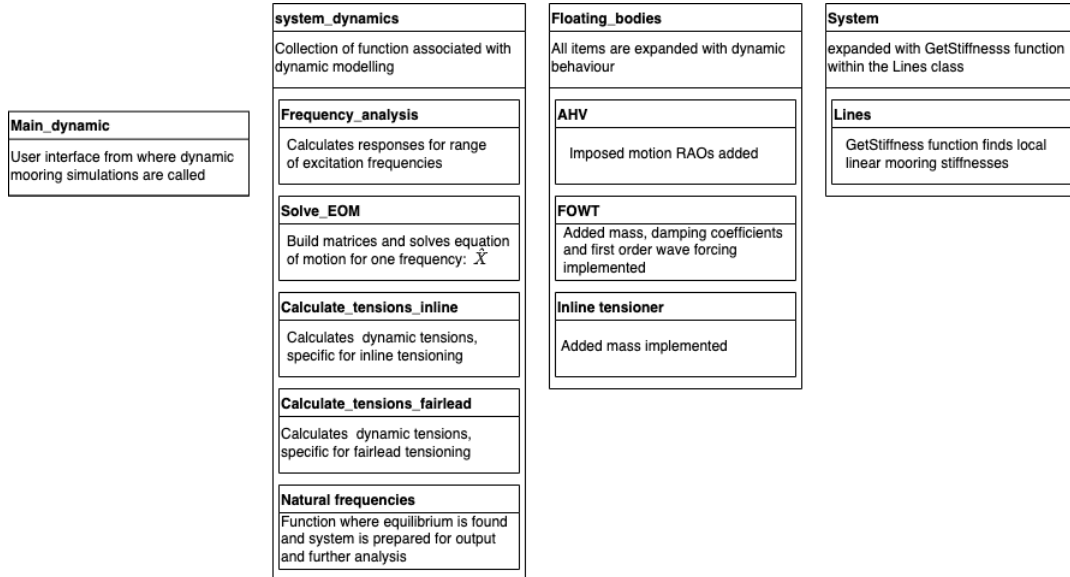


Figure 5.9: Code structure for dynamic simulations and tension quantification

The code segments that are new or heavily adjusted are further elaborated on:

Frequency analysis

This is the function that is called from the main script. It requires a static mooring system as an input. From there, it starts by calling the function to calculate the mooring stiffness since this is constant for each wave frequency in this study. Subsequently, a loop that calls the EOM solver for each frequency. After all frequencies have been evaluated, the tensions are calculated for each line based on the responses and the stiffness matrix. Finally, the natural frequencies are calculated.

SolveEOM

This function requires the wave frequency as input and collects the associated added mass, damping, forcing and AHV motion. The matrices are built up and solved with that information as described in the previous section. It returns the motion responses.

GetStiffness

The restoring stiffness per line is found as described in section 5.2.5. Per The values per line are then inserted in the mooring stiffness matrix as specified in matrix 5.15 or 5.16.

Calculate tensions

For both pre-tensioning methods, the steps in calculating the dynamic tensions are similar but should be performed for different lines. The steps required to come to the dynamic line tensions and the maximum line tension at the AHV and the FOWT are described in section 5.3

Natural frequency

For the quantification of natural frequencies according to section 5.4.

6

Results and validation

The dynamic calculations are performed using the techniques discussed in the previous chapter. Before any results are trusted, two validation studies are performed. The results of the mooring simulation are then compared to the Umaine floater description. This is discussed in the first section. The results of the pre-tension simulation are elaborated on in section 6.2 and 6.3. Finally, the results of the simulations are compared with a third-party simulation, and a closer look into the sliding element is taken.

6.1. Validation of dynamic model

The description of the Umaine floater contains motion RAOs and natural frequencies. First, the calculation of equivalent spring stiffness and natural frequencies is validated by setting up a dynamic simulation for solely the floating body. Secondly, to validate the rest of the FOWT behaviour, the FOWT motion responses are calculated and compared with those from the description.

6.1.1. Generation of equivalent mooring stiffness and natural frequency

To calculate the natural frequency of solely the FOWT, the line stiffness of the three mooring lines is calculated. The stiffness matrix in [kN/m] for the mooring line that is in line with the (x, z) plane is:

$$K^{2D} = \begin{bmatrix} \frac{\partial H}{\partial x} & \frac{\partial V}{\partial x} \\ \frac{\partial H}{\partial z} & \frac{\partial V}{\partial z} \end{bmatrix} = \begin{bmatrix} 45\,990 & 24\,560 \\ 24\,560 & 20\,103 \end{bmatrix} \quad (6.1)$$

The $\frac{\partial H}{\partial x}$ entry thus represents the change in restoring horizontal force for a surge motion of the FOWT. This value can be compared to the derivative of the restoring force as shown in figure 5.6. That figure results from repetitive static simulations and visualising the horizontal component of the line tension for various FOWT surge offsets. The local derivative around the point in rest has a gradient of 45 732 kN/m and matches with 0.4% accuracy.

The total restoring stiffness matrix of the three mooring lines is calculated and summed with the hydrostatic stiffness:

$$[K] = \begin{bmatrix} 71\,639 & 0 & 1.24\text{E}6 \\ 0 & 60\,324 & 0 \\ 1.137\text{E}6 & 0 & 2.63\text{E}8 \end{bmatrix} + \begin{bmatrix} 0 & 0 & 0 \\ 0 & 4.47\text{E}6 & 0 \\ 0 & 0 & 2.19\text{E}9 \end{bmatrix} = \begin{bmatrix} 71\,639 & 0 & 1.24\text{E}6 \\ 0 & 4.53\text{E}6 & 0 \\ 1.137\text{E}6 & 0 & 2.453\text{E}9 \end{bmatrix} \quad (6.2)$$

An arbitrary frequency of 0.4 Hz is assumed to calculate the added mass. This yields the total of the mass and added mass matrix:

$$[M + A](\omega = 0.4) = \begin{bmatrix} 3.25\text{E}7 & 0 & -1.18\text{E}8 \\ 0 & 4.65\text{E}7 & 0 \\ -1.18\text{E}8 & 0 & 2.47\text{E}10 \end{bmatrix} \quad (6.3)$$

The natural frequencies are calculated and iterated once to correct the added mass, depending on wave frequency. Finally, the values are compared to those from the Umaine floater description below.

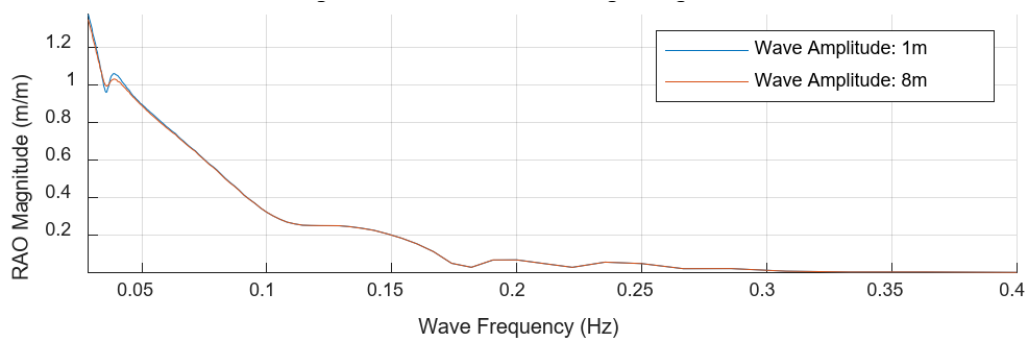
Table 6.1: Model validation by comparing the natural frequencies, calculated by the model, with the specified natural frequencies in the Umaine description

Motion	Estimate	Iterated natural frequency	From description	Relative difference
Surge [Hz]	0.0074	0.0069	0.007	0.59 %
Heave [Hz]	0.0491	0.0483	0.049	1.42 %
Pitch [Hz]	0.0371	0.0363	0.036	1.40 %

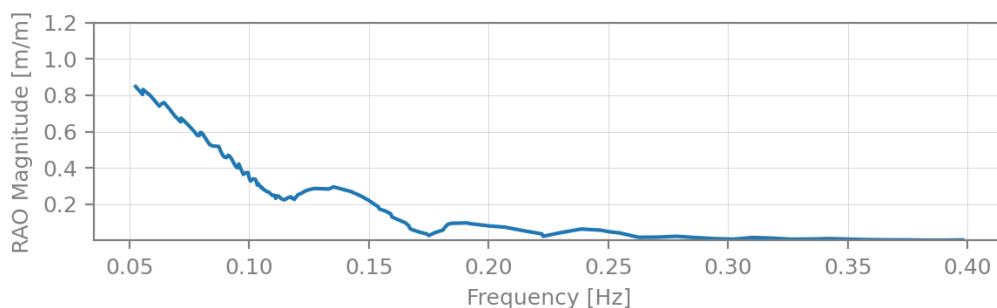
As can be seen, the calculated values match well with the reference values in the specification by the University of Maine. This gives confidence that the mooring stiffness matrix and added mass are calculated correctly. In the next section, the implementation of hydrodynamic forcing and damping are validated.

6.1.2. Motion comparison for the installed case without pre-tensioner

Implementing the hydrodynamic database in a *Python* model is vulnerable to typos or errors. This section presents the validation for the floating offshore wind turbine's rigid-body wave-induced responses. The reference RAO from the description is calculated in an OpenFAST regular wave simulation in the time domain and is shown in 6.1(a). The effects of aerodynamic loading were not considered in either the model for this study, either the reference RAOs from the description. In the reference RAOs, both wave amplitudes of 2 m and 8 m were analysed better to understand the nonlinear damping effect. This is not included in the model for the pre-tensioning study. The motion RAO of the FOWT is obtained by solving the equation of motion for the FOWT as specified in section 5.2.1. The resulting motion responses are shown in figure 6.1(b).



(a) Motion response taken from the Umaine floater description[39]



(b) Motion response from frequency domain modelling

Figure 6.1: Validation of motion responses for the FOWT

Comparing the two motion responses shows that the frequency and time domain models produce very similar results. Furthermore, the handling of imported data does not cause any unexpected effects. However, this validation does not prove that the theoretical modelling represents the real full-scale hydrodynamics. That is, however, outside of the scope of this research.

6.2. Dynamic responses while inline tensioning

When simulating the inline-tensioning operation, the five degrees of freedoms are displayed in one figure: The floater motion (x_f, z_f, θ_f) and tensioner motion (x_t, z_f). Next to the motion responses, the dynamic tensions are calculated in lines 3 and 4. Line 3 is the line between the AHV and the tensioner; line 4 is between the tensioner and the FOWT. The static model results described in chapter 4 form the basis for dynamic simulations. In addition to the two static simulations performed then, the configuration halfway during the tensioning is also considered. Halfway is there where half of the 'slack' chain is already hauled in during the pretension operation. The model results are shown below:

Start

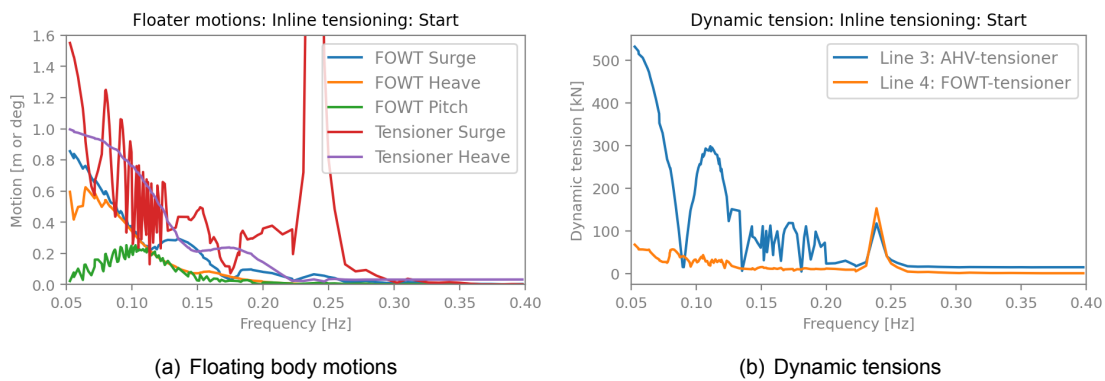


Figure 6.2: Dynamic behaviour while begin of inline tensioning

To understand the fluctuations in the low-frequency region for the surge motion of the tensioner, it is necessary to recognise the phase difference between the AHV and the FOWT. This is because the FOWT has a very inconsistent phase delay compared to the incoming wave (appendix A.1). This means that when the frequency changes slightly, the phase difference between the AHV and the FOWT can completely change from 'in phase' motion to opposite motion. However, their distance difference remains smaller when the floaters move in phase than when the movement is in the opposite direction. Hence, the larger distance differences yield higher simulated tensions.

A distinct peak in the surge motion of the tensioner can be identified at around 0.24 Hz. This complies fully with one of the natural frequencies of the system. With this, it can be observed that the inline tensioner is vulnerable for resonance. However, the hydrodynamic damping effect on the chain and tensioner body might reduce the severity of this resonance. This would require further damping modelling.

Halfway

When halfway the pre-tensioning operation, one expects to see higher restoring stiffnesses for the equivalent springs and hence, smaller motions. Furthermore, changing the mooring configuration might influence the extreme tensioner surge as was seen around 0.25 Hz in figure 6.2(b).

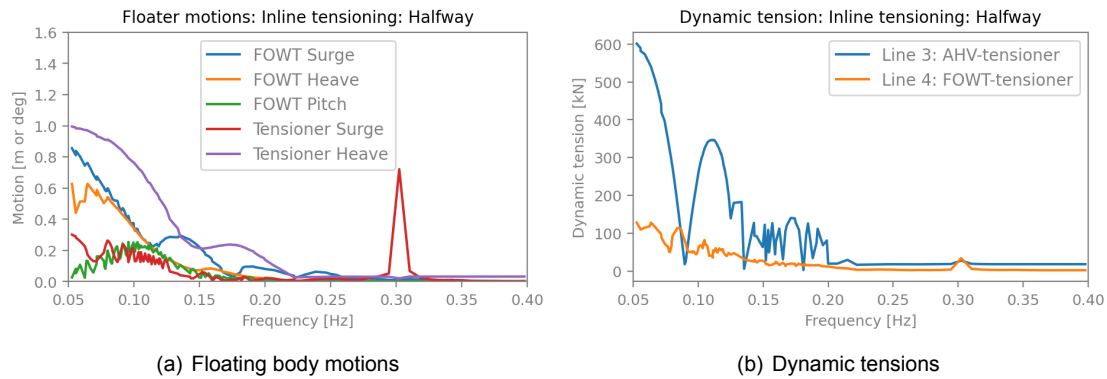


Figure 6.3: Dynamic behaviour while halfway of inline tensioning

The fluctuation in the low frequencies has reduced. The stiffness matrix is the only difference between simulating the beginning or halfway operation. Hence the increased stiffness has to lead to reduced motion. Furthermore, the peak shifted to a higher frequency: A higher stiffness implies a higher natural frequency and the natural frequency calculation according to section 5.4 again aligns with the peak at 0.30 Hz.

Finish

When the pretension operation is continued, the mooring line reaches its prescribed length. At that point, 100 meters have been hauled in, which stiffens the mooring systems. The dynamic responses and related tensions in this situations are considered below:

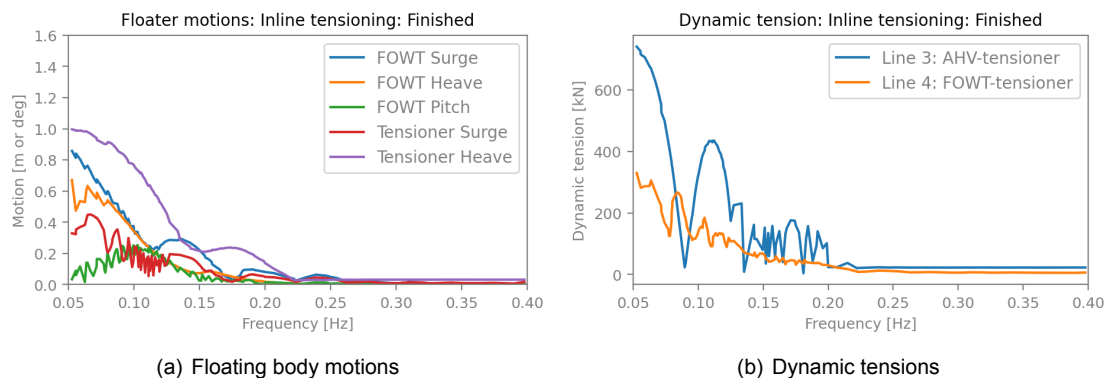


Figure 6.4: Dynamic behaviour while end of inline tensioning

The surge motion of the tensioner has been reduced to a minimum: 0.32 m is the maximum surge motion for long waves ($\omega = 0.05$ Hz). The heave motion of the tensioner seem to continue to follow the AHV motion.

6.3. Dynamic responses while fairlead tensioning

The fairlead tensioning is simulated and discussed similarly to inline tensioning. A difference is that the tensioner is now at the floater; hence, the system reduces to 3 DOFs.

Start

At the beginning of the operation, the wire between the AHV has slight sag and hence, a high geometric stiffness.

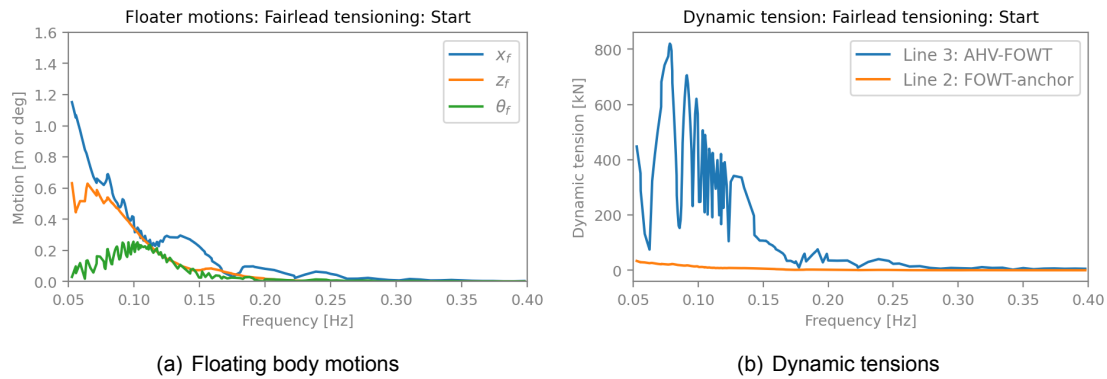


Figure 6.5: Dynamic behaviour while begin of fairlead tensioning

The dynamic responses of the floater seem to be hardly changed due to the connection with the AHV. The tensions, however, go up to 821 kN while the static line tension at the beginning of the operation is 1 388 kN. It seems that the 'locking' of the wheel causes an overestimation of the equivalent spring stiffness between the AHV and the FOWT. This again does not seem large enough to generate increased motion of the FOWT.

Halfway

While simulating the next phases in operation, it must be considered that the tension in the AHV work wire is higher than at the beginning of the operation. This increased tension will result in less sag in the line and, therefore, even more stiffness. This increased stiffness might lead to even higher dynamic tensions.

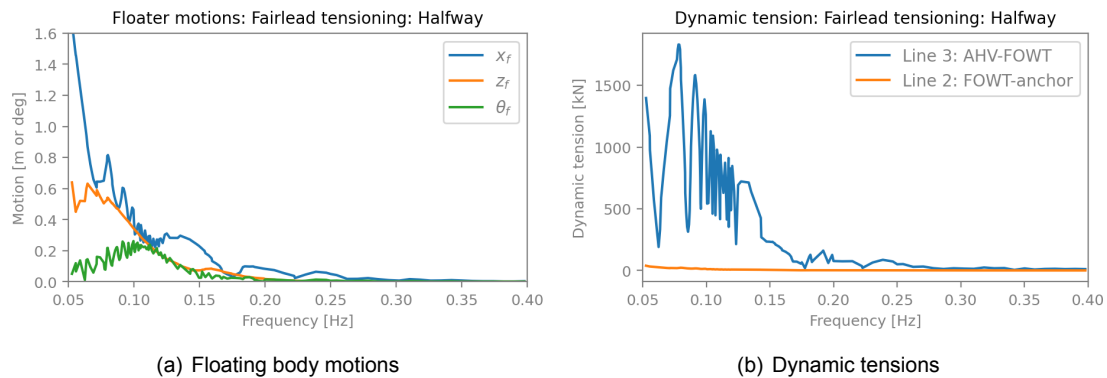


Figure 6.6: Dynamic behaviour while halfway of fairlead tensioning

As expected, the dynamic tensions have further increased, but again, they are expected to be overestimated by assuming a fixed line length between the AHV and the FOWT. However, What can be seen now, too, is that the FOWT surge motion has increased for relative low wave frequencies (<0.10 Hz). This is because high-frequency tension oscillation does not have enough time to give the FOWT substantial inertia.

End

In the final phase of the installation, the line tension at the FOWT fairlead is 1;671 kN. It is expected that the dynamic tension will further increase.

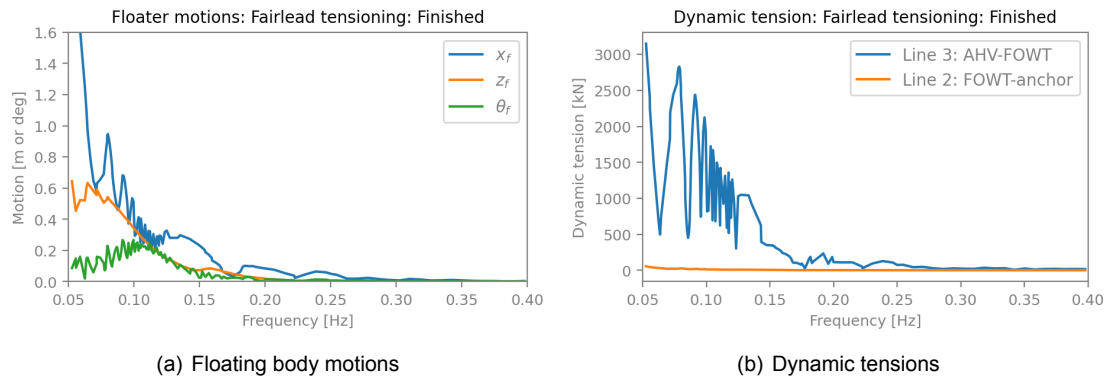


Figure 6.7: Dynamic behaviour while end of fairlead tensioning

The combination of uncoupled AHV motions, a large mass FOWT and overestimated equivalent stiffness leads to simulated tensions of 3; 120 kN. In the case of 1; 671 kN static load and such a dynamic load amplitude, one can expect significant non-linear effects such as line-snapping [35].

In conclusion, the FOWT motions seem hardly influenced by the changing mooring configuration during tensioning. Both inline- as fairlead tensioning hardly affect the FOWT responses to first-order waves. Furthermore, the motion of the inline tensioner in the heave direction is governed by the AHV motion, while the surge motion is excited by the surge motion of both the FOWT and the AHV.

Based on the simulation results, the linear equivalent spring stiffness assumption is reviewed in the next section.

6.4. Assessment of spring linearity

The results rely on the assumption that all line segments can be simulated by linear equivalent springs. In section 5.2.5, it was shown that this assumption holds for catenary lines and limited offsets. However, the lines with little sag thus have a higher stiffness that can go up to the axial stiffness(EA). In the case of inline-tensioned, the tensioner heave was mostly based on the heave motion of the stern roller of the AHV. For fairlead tensioning, this assumption, combined with the imposed AHV motion and no rotation at the fairlead, led to tensions that are not realistic.

The results are compared with alternative calculation methods in the two subsections below. Firstly, the including of the fairlead wheel is considered, and secondly, validation by a third party related to Huisman is performed.

6.4.1. Unexpected high stiffness during the finish of fairlead tensioning

The dynamic tensions during the final phase of the fairlead tensioning are significantly higher than realistic. For low wave excitation frequencies, the dynamic tensioning outnumbers the static tension, which is unrealistic.

When the modelling approach was developed, it was not expected that the chain would oscillate over the fairlead gypsy wheel within the wave frequencies. However, in this case, the tension differences on both sides of the wheel go up to 3000 kN which is very unrealistic. As a result, a static simulation is performed to quantify the relationship between the distance between the AHV and the FOWT, including a rotating fairlead gypsy wheel. As illustrated below:

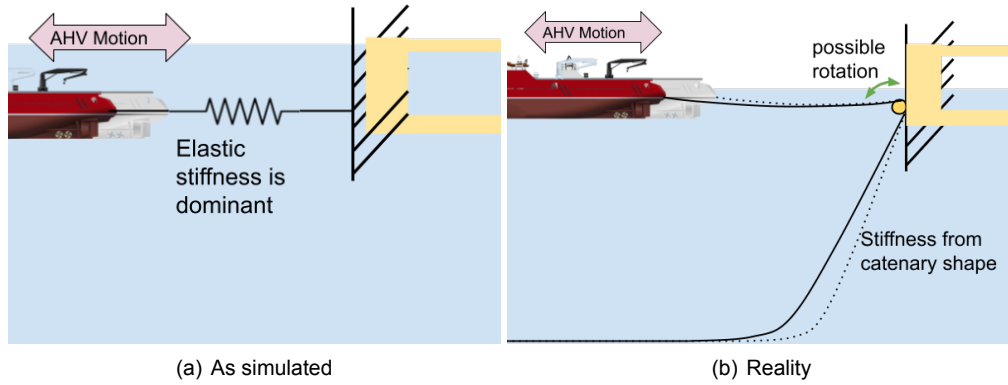


Figure 6.8: Difference between modelled linear spring stiffness and actual movement

The simulation shows that the wheel balances the tensions in both lines when the distance between the FOWT and the FOWT change. As a result, the catenary chain between the anchor and the FOWT slightly changes length and hence the tension.

The static simulation is run at the end of the pre-tensioning operation. In the dynamic model, the effective stiffness for the line between the AHV and the FOWT at the end of the process is $k_{3,x} = 2.3E6$ N/m. Then, the situation is modelled with slightly altered distances between the AHV and FOWT. For example, for a one-meter difference, it was observed that the horizontal component of the line tension at the FOWT has changed 5.57 kN. The effective stiffness $k_{3,x}$ is then calculated accordingly:

$$k_{3,x} = \frac{\partial H}{\partial x} = \frac{5.57}{1} = 5.57[\text{kN}] \tag{6.4}$$

This altered stiffness is then adjusted, and a dynamic simulation is performed. Because it was already observed that the motions of the floater hardly change during fairlead tensioning, only the dynamic line tensions are shown:

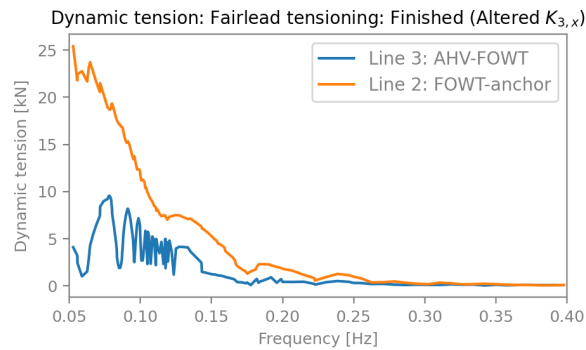


Figure 6.9: Dynamic tensions while fairlead tensioning using altered stiffness matrix

The dynamic tension for the line segment between the AHV and the FOWT has decreased significantly. It would require more operational information to validate whether gypsy wheels truly oscillate with the wave frequency, but based on the tension difference at the wheel, it seems realistic. In the RAO of the AHV, it can be seen that the surge motion at low wave ($\omega < 0.10$ Hz) is 1 m/m, and the FOWT surge motion is between 0.6 and 0.8 m/m. Hence the maximum dynamic distance between the AHV and the FOWT is a maximum of 1.8, assuming opposite motion. When multiplied with the altered stiffness, it matches the maximum dynamic tension at 8 kN. However, this calculation assumes frictionless instant rotation at the fairlead and does not incorporate the variable stiffness of the lines based on the changing line lengths.

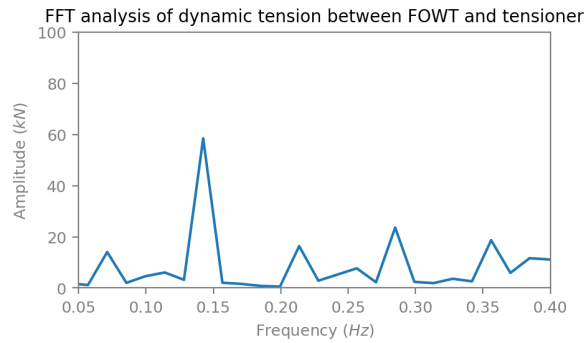
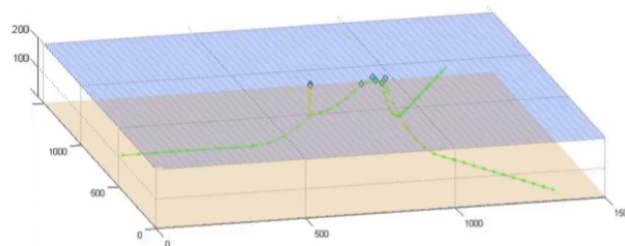


Figure 6.11: FFT analysis on the dynamic tensions between the FOWT and the tensioner

6.4.2. Assumption of catenary shape verification

At the beginning of this chapter, the developed frequency model was compared to the time-domain model from the University of Maine. This comparison helped validate the FOWT-related dynamics. Together with Aqitec, the static and dynamic modelling results are compared to their in-house mooring simulation software. The software package is a lumped mass model in the time-domain that contributes to the development of cultivation arrangements for aquaculture[48]. A simulation is set up to compare the model results for the final phase of inline tensioning. The floating bodies' line and dynamic properties are modelled precisely as in the model developed in this study. The main difference lies in the fact that the model from Aqitec simulates the mooring line as a lumped mass as described by paper from V.J. Kurian et al. [49]. One simulation of 70 seconds is run for a regular wave of 1 meter with a wave period of 7 seconds.

The simulation results can be used for verification in three ways: Firstly, the static tension can be compared against the means of the tensions. Secondly, the dominant frequencies can be identified from the time series by the FFT method. That helps to determine whether any dynamic behaviour that is not covered in the frequency model, and finally, the amplitude of the tension oscillation at the wave frequency can be identified.



For academic use only | © Aqitec Projects B.V. 2022

Figure 6.10: Validation study performed by Aqitec to show catenary motion

The results from the static analysis are compared to the means for the dynamic tensions of the model. For the interpretation of the dynamic tension, an FFT analysis is performed on the dynamic tensions.

As can be seen, distinct peaks show at exactly the wave frequency: $1/7 = 0.124$ Hz with an amplitude of 60 kN. The full comparison between the frequency domain and time domain model is shown below:

	Units	Developed model	Validation by Aqitec	Difference
Static tension in FOWT chain	kN	1 396	1 445	3.5%
Static tension in AHV line	kN	1 196	1 270	5.8%
Dynamic tension in FOWT chain	kN	75	62	21%
Dynamic tension in AHV line	kN	93	61	50%

As can be seen, the static tensions match accurately between the two models. As expected, the dynamic tensions in the frequency domain are overestimated by an average of 35%. This can be explained by the fact that the hydrodynamic damping on the mooring lines is not included. Furthermore, the run was too short of appropriately identifying the motions at the eigenfrequencies. These periods are around 120 seconds and would require longer simulation times.

Practical implications and pre-tension trade-off

In this chapter, the goal is to compare the seabed-, inline- and fairlead tensioners by merging the results of the static and dynamic analyses and discussing the practicalities of installing offshore wind turbines.

7.1. Seabed tensioning

The seabed tensioner has been used in a few pilot projects, including the TetraSpar demonstrator[21]. One of the properties of this tensioner is that the weight of the suspended mooring line only marginally influences pre-tension requirements for the AHV. As specified in section 2.2.1, modern mooring designs have heavier sections on the seabed and dipping section. This increased weight on the seabed leads to more drag and is unfavourable for seabed tensioning. Sumer et al. (2021)[50] suggest that seabed scours around the tensioner are possible, concluding that the tensioner will sink a bit. Still, this approach is heavily dependent on the local seabed conditions.

After the FOWT is hooked up, the work wire of the AHV can easily be connected to the seabed tensioner, which sits steadily on the seabed. The work wire is tensioned, as is the mooring line, which starts at 65 t of wire tension at the AHV and gradually increases to 150 t before the end of the operation. As found in the static analysis, a strong relationship exists between the total weight on the seabed between the tensioner and the floater and the required tension to haul in the chain, making clump weights increasingly popular. There is little research into the dynamic behaviour of seabed tensioning due to the seabed interaction. Therefore, the catenary shape and dynamic tension around the tensioner are assumed independent of the FOWT motions. As long as the ROV can be deployed, there are no restrictions on seabed tensioning[18].

7.2. Inline tensioning

Inline tensioning resolves the issue of dragging heavy chains over the seabed that might even contain clump weights. The details of inline tensioning are later in this section. A common advantage of inline tensioning is that it happens vertically. An onboard winch or crane can be used to pull, whereas tensioning from a fairlead requires high bollard pull force.

What can be observed in the static analysis is that the configuration acts as a 2-to-1 pulley system. The tension transferred to the tensioner from the anchor chain, is partially taken on by the line between the tensioner and the floater, and partially by the wire to the AHV.

When the FOWT is finally hooked up, it is considered safe from storms. The mooring system can keep the FOWT in position with a larger offset than when the system would be adequately pre-tensioned. One concern was that the tensioner would move vigorously when the AHV was connected to it to start pre-tensioning. An AHV like the CBO Iguacu operates in sea states up to 2.5 m [3]. Wave frequencies that wind turbine installations can be subjected to vary from region to region and even day to day.

However, frequencies for 2.5 m waves are generally between 6 and 11 seconds. When subjected to 2.5m waves at such frequencies, a FOWT moves less than 25cm (according to the calculated RAOs). When mooring lines are set up with a catenary system, such movements of the tensioner do not pose a problem for the ROV [26].

In the dynamic simulation, it could be seen that the tensioner followed the heave motion of the AHV quite accurately. This can be explained by the fact that the vertical wire has a very high effective stiffness. For most catenary lines, the stiffness is mainly influenced by their catenary shape. However, no catenary flexibility is present for this vertical line, yielding a high degree of stiffness.

7.3. Fairlead tensioning

Tensioning at the fairlead is the most mature method of the three. In 2010, an employee of Principle Power shared their insights on the installation of mooring equipment. [20]. Their perspective was that the tensioning should be performed with chain jacks or winches and that that requires attention when it comes to deck layout. Although the first inline tensioner was already used in 2005[51], most of the moored structures had onboard tensioning devices. Chain jacks or winches are expensive equipment that requires maintenance and are hardly used. Fitting such equipment on the floater can be cumbersome, especially when spar floaters have little deck space. An FPSO or oil rig is usually repositioned a couple of times in its lifetime, but the expectation is that FOWTs don't have to do so[52]. There is interest in floating turbines to temporary power oil, and gas rigs, yet it is a niche. [53]

Tensions exerted on the AHV, and therefore the bollard pull, depend heavily on the mooring configuration. The original mooring configuration, with only a chain, is heavy and simplistic, making it very unappealing to pre-tension it using a classic pre-tensioner. However, the proposed alternative mooring system already made it much more legitimate to consider this form of tensioning.

For seabed and inline tensioning, the tension could be generated by a crane or winch. In the case of fairlead tensioning, the AHV must use thrust to counteract the horizontal load. To estimate the difference in energy consumption while tensioning, a comparison can be made. Note that the effective work is solely compared, and the auxiliary power requirements are not quantified. The assumptions used to calculate the necessary power to perform a pre-tension operation are detailed below:

- The CBO Iguacu has 12.000 kW of installed engine power and a maximum bollard pull of 220 t. A vessel with very similar length, gross tonnage and installed engine power is the Korean icebreaker Araon. For this vessel, the relation between thrust and engine power is known [54].
- It is assumed that the bollard pull during fairlead tensioning takes 45 minutes[26] and linearly increases from 40 to 100 t bollard pull for the case with inserts.
- For inline tensioning, the tension linearly increases from 60 to 120 t. The energy efficiency of an electrical Huisman winch is determined to be 80%[55]. The inline tension energy requirement is calculated by multiplying the performed work by the winch and the efficiency factor.
- the efficiency from marine gas oil(MGO) to engine power is assumed to be 40% according to the Center for Alternative Fuels, Engines & Emissions [56].
- The specific energy of MGO is 43 MJ per kilo[57].

During a 45-minute bollard pull, a total of 13.5 GJ of engine energy is used. For comparison, inline tensioning requires less than 1% of that: 112.5 MJ. For inline tensions, the energy consumption is calculated by the work performed by the winch and divided by the winch efficiency. It must be noted that auxiliary power is not included in the simulation. The lighting, steering and other systems on board both require power differences for solely hauling in the chain.

This translates into a fuel usage difference of 0.8 t. Although this may seem insignificant, smaller and cheaper vessels have sufficient winch capacity to perform the job. Other cost components of a winch-related method over a bollard pull tensioning might be more significant. However, quantifying the exact cost differences would require more information, such as the day rate of various vessels. The proper selection of the installation vessel is key to making a project economically viable, as has been made clear in the literature [5],[20], [27].

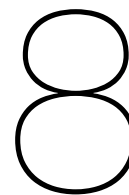
7.4. Trade off

This research contributed to the existing literature on FOWTs by comparing the advantages and disadvantages of different approaches to tensioning. To gain a better understanding of how different pre-tensioning concepts perform relative to one another, all the conclusions are summarised in table 7.1 below:

Table 7.1: Overall comparison of the pre-tension methods to conclude the research outcomes

	Seabed tensioning	Inside tensioning	Fairlead tensioning
Practicalities	<ul style="list-style-type: none"> ▪ New concept, little field experience ▪ Sits steady on the seabed ▪ Smallest cyclic loads 	<ul style="list-style-type: none"> ▪ Favourable angle to use the pulley as 2:1 reduction. 	<ul style="list-style-type: none"> ▪ Requires bollard pull instead of winching ▪ Easiest to hook on, no ROV required
Static tension development at AHV	<ul style="list-style-type: none"> ▪ Up to 170 t for system without inserts ▪ Up to 152 t for system with inserts 	<ul style="list-style-type: none"> ▪ Up to 130 t for system without inserts ▪ Up to 114 t for system with inserts 	<ul style="list-style-type: none"> ▪ Up to 165 t for system without inserts ▪ Up to 103 t for system with inserts
Influence on mooring configuration	<ul style="list-style-type: none"> ▪ Mostly influenced by mooring weight on the seabed 	<ul style="list-style-type: none"> ▪ Possibility to alter the tensioner location to any suspended point 	<ul style="list-style-type: none"> ▪ Strong relationship with suspended line mass
Dynamic behaviour	<ul style="list-style-type: none"> ▪ No interference from floater on tensioner ▪ Not thoroughly investigated in this research 	<ul style="list-style-type: none"> ▪ tensioner motion follows AHV very strongly ▪ No dynamic chain issues after validation 	<ul style="list-style-type: none"> ▪ Hard to draw conclusions based on the used method ▪ Validation led to insight that rolling element will help reduce loads

To determine the most cost-effective method to install a FOWT, one would have to look at the associated costs of the tensioning equipment and the vessels required for installation. In the following chapter, conclusions and recommendations for further research will be outlined in detail.



Conclusion and recommendations

In this chapter, the conclusions and recommendations that have emerged from this dissertation are presented. The purpose of the conclusion is to answer the main research question and associated sub-questions that were introduced in Chapter 1. Then, in section 8.2, recommendations are set out for further research and the practical application of this investigation at Huisman. Finally, in section 8.3 the limitations and the scientific contribution of this research are discussed.

8.1. Conclusion

The purpose of this thesis was to examine the practicalities of different tensioning options that are used during the pre-tensioning phase of mooring system installation for semi-submersible based 15-MW offshore wind turbines. The central question to be answered was:

“How do procedures and required equipment influence the pre-tensioning operation to ultimately reduce the duration and cost of installing mooring systems for floating wind?”

To answer the above question, two simulation models were used, and the results were analysed in order to determine the static and dynamic tensions that emerged from the results of the two models. In the following sections, the sub-questions of this investigation are addressed one by one.

8.1.1. Characteristics and problems of pre-tensioning

In this section, the question to be answered is: *What are the details for a typical FOWT pre-tension operation, what critical events must one account for, and how is this different from the oil and gas industry?*

Details of a typical FOWT pre-tension operation

Consultation of different sources provided a big picture of mooring installation systems. To analyse mooring methods that are established in the industry, all possible installation steps were applied to one example of a floating wind turbine and thoroughly examined. It can be concluded that every mooring installation operation has three phases: 1. Anchor installation 2. Mooring line prelay and 3. Hook-up. The prelay operation is often performed right after the anchor installation is complete.

Critical events offshore

It was found that each step in the installation revealed many opportunities for further research and that within the final phase - pre-tensioning - many options exist, namely, the seabed tensioner, inline tensioner and fairlead tensioning, all of which have different characteristics. An analysis of all three of the above tensioning methods was carried out to answer the research questions as thoroughly as possible. One of the critical moments of a pre-tensioning operation is the tension exerted on the AHV wire. Mooring systems are designed for tensions that remain intact in extreme sea-states, but the AHV and connective equipment are only used during the installation. In this research, the mooring tension

at the fairlead can go up to 6 000kN, while the tensions during pre-tensioning remained under 1 700 kN at the AHV.

Relation with oil and gas industry

The oil and gas industry has created a solid knowledge base of mooring behaviour and installation, with fleets of dedicated vessels for anchor and mooring installations present worldwide. The experiences from the oil and gas industry can be put to good use for floating wind. However, there are three significant differences between mooring installation for floating wind and oil and gas. Firstly, the mass of a 15MW FOWT turbine is 20 000 t, whereas the mass of an oil-gas rig can go up to 100 000 T, with drastic implications for mooring requirements.

Secondly, oil and gas rigs need to be repositioned more often than wind turbines. Therefore, they are equipped with redundant onboard tensioning tools while FOWTs hardly ever need to be repositioned. New methods are necessary for FOWTs with different infrastructural arrangements for hook up and pre-tensioning. Finally, for oil- and gas-related projects, mooring systems and installation techniques were specifically designed for each individual project. The repetition of operations due to a large quantity of FOWTs creates the need for better installation techniques.

8.1.2. Environmental conditions and potentially critical events

In this section, the question to be answered is: *What is the relationship between environmental conditions and potentially critical events? What are the corresponding limiting (response) parameters?*

Modelling approach

Two stages of modelling were used to quantify the motions of the floating bodies and ultimately find the tension in the AHV work wire. First, the three concepts were simulated solely based on static loads and without any time or frequency-dependent variables. As a result, equilibrium can be found as well as the catenary shapes. From them, the tensions at fairleads and inline tensions are found. In order to include rotating and sliding elements at the tensioner, existing modelling had to be used in an altered procedure. The static simulation was validated with the help of the Umaine floater description and the Vryhofs documentation on the Stevadjuster and proved accurate. The mass-spring approach works well for low-fidelity models and simple mooring systems. However, it is complicated to set up for more complex mooring configurations, and the non-linearities around the tensioner yielded overestimated values for fairlead tensioning.

Static tensions

It is shown that the mooring lines can be tensioned over 600 t in extreme sea states and that failure, while pre-tension, of the permanent mooring equipment, was not probable. What also was found is that the proposed mooring configuration involved long suspended segments of the heavy chain. The total mass of the first 200 meters of the mooring line of the three legs is an impressive 411 tons. This, in combination with the industry trend of having synthetic or steel inserts within mooring lines, led to the development of a simplistic alternative mooring system. It must be clearly stated that this mooring system has not undergone further analysis in terms of validity than a restoring force comparison. The proposed configuration led to a 57% decrease in pre-tension and 40% in overall mooring weight. The tensions while pre-tensioning resulted in being very dependent on the mooring configurations. Especially the fairlead tensioning showed a 50% decrease of required bollard pull.

Dynamic behaviour

At sea, the vessel and the floater will undergo the influence of wind, current and waves. The steady wind could be modelled in the static simulation, and current is not considered for this comparative study. The mooring configurations are modelled as linear mass-spring systems that are excited at various frequencies. Two main issues should become apparent after the dynamic analysis.

The analysis of the motions of the tensioner and the FOWT has led to two conclusions: Firstly, The heave motion for the inline tensioner closely follows the heave motion of the stern roller of the AHV. This was explained by the high effective stiffness of the vertical wire primarily tensioned in its axial direction. As a result, the catenary effect is limited, hence the high geometric stiffness. Secondly, the FOWT motions seem hardly influenced by the variations in tensions and dynamics of the other bodies. Within the fairlead tensioning simulation, increased FOWT surge motions can be observed, but this is probably a result of overestimated dynamic tensions and will be discussed later.

The possibility of resonance is studied. The eigenfrequencies and the dynamic simulations show that at the beginning of inline tensioning, the system is particularly vulnerable to excitations at 0.3 Hz. When half of the slack chain is hauled in, this resonance attenuates in magnitude and shifts towards 0.24 Hz. Since hydrodynamic damping on the mooring line and the tensioner is not considered, this extreme motion is likely more damped in reality.

The dynamic tensions are also interpreted: For inline tensioning, dynamic tensions in the line between the FOWT and the tensioner can go up to 710 kN for low-frequency excitations at the end of the operation. The static tension at this point is 1 707 kN. After comparing the results with the time-domain model of Aqitec, the mass-spring approach yielded similar results: The static tension difference was up to 5.8%, and the dynamic tension difference was up to 50%. The dynamic modelling of the fairlead tensioning showed that if the fairlead gypsy wheel does not rotate with the wave frequency, the tensions difference on both sides of the wheel goes up to 3; 000 kN, and it is unrealistic that the wheel will try to equalise the tensions on both sides of the wheel. When simulating the dynamic behaviour as if the wheel can rotate, the dynamic tension between the AHV and the FOWT is around 60kN and is much more realistic.

Two validation studies have been performed: In collaboration with Huisman and Aqitec, a full dynamic simulation has been performed to understand whether the chain would show behaviour that is not covered in the first-order model. This was needed to validate the linear stiffness assumption where chain whipping is not considered.

Limiting parameters

This research shows the conceptual differences of pre-tensioners, including static and dynamic tensions of the loads. After this research, issues are found for each tensioning mechanism. The seabed tensioner leads to no dynamics on the fairlead and, by its method of operation, can be executed in the highest seas. While inline tensioning, the tensioner follows the heave motion of the vessel very closely. The tensioner does not move vigorously, but it should be investigated up to what sea state the ROV would be able to disconnect the work wire from the active chain. Finally, for fairlead tensioning, the used simulation technique in combination with the available data could not predict whether the AHV motion would lead to forceful rotations.

Zhen et al. presented a good method to obtain workability for offshore operations[58]. However, more criteria should be investigated to translate the static and dynamic tensions and motions into limiting environmental conditions.

8.1.3. Suggested improvements for pre-tensioning

The question states *To decrease the overall installation time of a mooring system, what type of pre-tensioning improvements show the highest potential?*

From a load perspective

As concluded in this research, the decision on what pre-tensioning method is favourable is a complex one where one needs to consider maintenance, purchase costs, installation duration and equipment and personnel safety. The work wire tension at the AHV is smallest when using the inline tensioner. Also, when it comes to just mentioned criteria, the inline tensioner performs well, as discussed in chapter 7.

Efficient tension transfer from FOWT to AHV

Fairlead tensioning, as performed with Hywind Scotland, requires significant bollard pull. However, there are practical advantages when a chain could be pulled from the FOWT, locked and left. The pre-tensioning can start right after the last mooring line is hooked up, and no ROV is required. It would be an interesting research to see how the chain could be tensioned best from the floater. Options could include having temporary windlasses on the floater pulling the chain or fastening the AHV to the FOWT so that the winch can be used to haul in the chain.

Finally, to reduce the cost of pre-tension operations, it would be wise to not only analyse tensions but also logistical decision-making. The exact recommendations to contribute further to the developments in this field are presented in the next section.

8.2. Recommendations

This section describes the recommendations for continuing the scientific research and the recommendations for further research and recommendations to leverage the value of this research at Huisman.

8.2.1. Recommendations for scientific research

Simulation of logistical procedure When this research started, a significant focus on logistical simulation was envisioned. However, performing such simulations requires a lot of assumptions on costs of equipment and vessels, duration of operations and reliability of materials used. It is hard to justify research with so much unverified and variable data from an MSc thesis perspective. Nevertheless, cooperating with suitable stakeholders could still result in valuable research: Bourbon has installed the most FOWT projects, and Boskalis and Skandi are also options. Furthermore, logistical studies might also have more theory on incorporating uncertainty in such analysis. Heerema Engineer Solutions recently published that they hold such a tool in esteem.

Investigate the influence of a gypsy wheel further

The oscillation of line length at wave frequencies is still hard to determine. The chain behaviour around the rotational joint is uncertain in the current model. It was shown that this is not expected to happen for seabed and inline tensioning. The question for further research would be whether the rolling under high tension could form a workability criterion.

investigate extreme ballasting

For tensioning of TLP platforms, it is common to sink the TLP below the operational draft, hook it up, and tension the floater by reducing the ballast. By increasing the draught 15 m, the static tensions eased from 1; 313 kN to 838 kN. Could the temporary sinking of the floater make pre-tensioning unnecessary?

8.2.2. Recommendations for Huisman

Investigate the option of the most efficient tension transfer to a FOWT.

Huisman's engineering expertise is varied: Hydraulics systems, cable tensioning equipment, winches and cranes have all been designed before. Therefore, it would be interesting to see what would be possible to transfer the tension from the FOWT to the AHV. In addition, the feasibility of mooring the AHV alongside a FOWT should be investigated. This could go simultaneously with the current 'Wind turbine Installation Vessel'(WIV) to FOWT lifting research. Alternatively, when the WIV is used to install turbines on floaters offshore, the WIV could also pre-tension the system at the fairlead.

Perform similar research for other installation steps to identify more potential installation gains

This research was required to fully understand pre-tensioning. After being involved nine months it was possible to grasp the pre-tensioning considerations. During conversations with Huisman colleagues, new ideas were born that could also lead to faster, safer or cheaper installation of FOWTs. One of those them was the offshore 'drop off' of a floating substructure. When semi-submersible transport vessels could unload the floaters offshore at site, the transport time could be reduced. Limitations on current offloading operations should be investigated and potentially design equipment to mitigate those limits.

8.3. Discussion

This thesis is a preliminary design and will serve as basis for further development of the pre-tension operations. In this discussion section of this research, the limitations to the research and the scientific contributions are discussed.

8.3.1. Limitations

The results of the inline tensioning are within the expectations. However, there are numerous nonlinear properties of FOWT mooring that are critical but unclear yet. Here are the limitations of the modelling presented on a hypothetical relevance order:

The mass-spring approach works really well for low fidelity and simple mooring systems, for more complex mooring systems, it is relatively complex to set up and many effects are not possible to incorporate or hard to quantify. Those will be mentioned below.

Linear mooring stiffness was shown to be a good assumption for the majority of the mooring lines. However, in the case of tight lines near the rotational element, the linear stiffness would be heavily overestimated. This was validated by computing the true relation between tension and vessel distance in a series of static simulations. For further research, this stiffness could be tuned but as stated, continuing with a complex mass-spring system is not recommended.

Uncoupled AHV motions has led to unreliable dynamic results for the final phase of fairlead tensioning. Within the current simulation framework, it would be viable to simulate the AHV in a similar manner as the FOWT. Such a hydrodynamic database was not available at the time of the research.

Different waves approach angles and changing vessel heading. The reasoning behind the orientation of the vessel and the floater was to reduce a 3D problem to a 2D problem.

Hydrodynamic damping from the mooring line, which is mainly induced by the drag force on the line. Not including the line damping most likely leads to an overestimation of the motions and therefore the tensions.[46]

Reflected waves are not considered in the calculations. Possibly, this could lead to enhanced motions. However, when the distance between the floater and the AHV remains 100 m + while tensioning, and the significant wave height does not exceed 2.5 m, the effects might be small.

Tensioner rotations

8.3.2. Scientific contributions

Develop code to quickly compare pre-tension statics including rotational joints.

The developed code is built in an object-orientated manner and can be easily adapted to fit more purposes within mooring load estimation. In total, over 2000 lines are written in order to find the conclusions presented in this thesis. It is publicly available through GitHub without the AHV RAOs, which are not publicly available. The code could contribute to any mooring optimisation or operation study that requires fast results.

Investigating dynamic modelling approach for complex mooring situations.

This thesis explored the viability of simulating the complex mooring configurations with multiple floating bodies as a multi-degree of freedom mass-spring system. Within the time constraints of the thesis, more hydrodynamic effects could have been taken into account with more off-the-shelf software packages. However, by building the model, a lot of fundamental knowledge has been touched upon.

Side by side comparison of pre-tensioning devices

The information about pre-tension operation is scattered over a variety of papers and books. This thesis presented a side-by-side comparison of static, dynamic and practical issues.

Bibliography

- [1] Center for Sustainable Systems and University of Michigan. "Wind Energy Factsheet." In: (2021).
- [2] Ryan Wiser, Karen Jenni, Joachim Seel, Erin Baker, Maureen Hand, Eric Lantz, and Aaron Smith. "Expert elicitation survey on future wind energy costs". In: *Nature Energy* 1.10 (2016). ISSN: 20587546. DOI: 10.1038/nenergy.2016.135.
- [3] Kai-Tung Ma Yong Luo Chi-Tat Thomas Kwan Yongyan Wu. *Mooring Systems Engineering for Offshore Structures*. Vol. 148. 2019, pp. 148–162. ISBN: 9780128185513.
- [4] Georgios Katsouris and Andrew Marina. "Cost Modelling of Floating Wind Farms". In: March (2016), p. 36. ISSN: 0197-3533.
- [5] Anders Myhr, Catho Bjerkseter, Anders Ågotnes, and Tor A. Nygaard. "Levelised cost of energy for offshore floating wind turbines in a lifecycle perspective". In: *Renewable Energy* 66 (2014), pp. 714–728. ISSN: 09601481. DOI: 10.1016/j.renene.2014.01.017. URL: <http://dx.doi.org/10.1016/j.renene.2014.01.017>.
- [6] Dan Kyle Spearman, Sam Strivens, Denis Matha, Nicolai Cosack, Alan Macleay, Jeroen Regelink, Darren Patel, and Tim Walsh. "Phase I- Summary Report - Floating Wind Joint Industry Project". In: *Carbon Trust* (2018).
- [7] Carlos Eduardo Silva de Souza, Nuno Fonseca, Petter Andreas Berthelsen, and Maxime Thys. "Calibration of a time-domain hydrodynamic model for a 12 MW semi-submersible floating wind turbine". In: *Proceedings of the International Conference on Offshore Mechanics and Arctic Engineering - OMAE 9* (2021), pp. 1–12. DOI: 10.1115/OMAE2021-62857.
- [8] Touhidul Islam. "Design , numerical modelling and analysis of a Semi-submersible floater supporting the DTU 10MW wind turbine". In: *Norwegian University of Science and Technology* (2016). URL: core.ac.uk/download/pdf/154676062.pdf.
- [9] Xu Wenfe. "Design , numerical modelling and analysis of a spars floater supporting the DTU 10MW wind turbine". In: *Gh June* (2017), pp. 1–109. URL: core.ac.uk/download/pdf/154676062.pdf.
- [10] Xiaoshuang Tian. "Design , numerical modelling and analysis of a TLP floater supporting the DTU 10MW wind turbine". In: *Norwegian University of Science and Technology* (2016). URL: core.ac.uk/download/pdf/154676062.pdf.
- [11] Maria Ikhennicheu, Mattias Lynch, Siobhan Doole, and Friedemann Borisade. "Review of the state of the art of mooring and anchoring designs, technical challenges and identification of relevant DLCs". In: *Corewind* February (2020), p. 88. URL: http://files/95/R_2020_COREWIND-D2.1-Review-of-the-state-of-the-art-of-mooring-and-anchoring-designs.pdf.
- [12] Kate Freeman, Ciaran Frost, Giles Hundleby, and Colin Walsh. *Our energy, our future*. Tech. rep. WindEurope, 2019.
- [13] Dan Kyle Spearman, Sam Strivens, Denis Martha, Nicolai Cosack, Alan Macleay, Jeroen Regelink, Darren Patel, and Tim Walsh. "Phase II - Summary Report - Floating Wind Joint Industry Project". In: *Carbon Trust* (2020).
- [14] Vryhof. *The Guide To Anchoring*. 2018. ISBN: 9789090288017.
- [15] Oregon Wave Energy Trust. "Advanced Anchoring and Mooring Study". In: *Oregon Wave Energy Trust* (2009). URL: <http://ir.library.oregonstate.edu/xmlui/handle/1957/19177>.
- [16] Madeleine Tholen, Richard Auckland, Bridget Randall-Smith, Lilja Valtonen, James Berntal Hooker, Mocca Yiping, and Bonning-Schmitt. *4C Offshore: Global Floating Wind Progress Update 2022*. Tech. rep. 2022.
- [17] Kjell Larsen. *TMR4225 Marine Operations Lectures*. 2021.
- [18] Eirini Papapanagiotou and Kevin Nomen. *Discussion with Vryhof about mooring equipment*. Schiedam, Jan. 2022.

- [19] Vryhof. *Stevadjuster® Installation Procedure*. Tech. rep. Carbon Trust Floating Wind Technology Acceleration Competition, 2021.
- [20] Dominique Roddier, Christian Cermelli, Alexia Aubault, and Alla Weinstein. “WindFloat: A floating foundation for offshore wind turbines”. In: *Journal of Renewable and Sustainable Energy* 2.3 (2010), p. 33104.
- [21] Michael Borg, Morten Walkusch Jensen, Scott Urquhart, Morten Thøtt Andersen, Jonas Bjerg Thomsen, and Henrik Stiesdal. “Technical definition of the tetraspar demonstrator floating wind turbine foundation”. In: *Energies* 13.18 (Sept. 2020). ISSN: 19961073. DOI: 10.3390/en13184911.
- [22] Leif Delp. “Hywind Scotland Pilot Park – Marine Operations”. In: *Subsea Operations Conference 2016* (2016).
- [23] K. E. Steen. “Hywind Scotland - status and plans”. In: *EERA DeepWind 2015* (2015). URL: https://www.sintef.no/globalassets/project/eera-deepwind-2015/presentations/closing/rune-yttervik_statoil.pdf.
- [24] Dock90, Vryhof, Principle Power, and Bourbon Subsea Services. *Installation Floating Wind serie*. 2020. URL: <https://youtu.be/aS4iY-cFmlU>.
- [25] Q FWE. *Map Floating Wind Energy Projects of the World*. Tech. rep. 2020, p. 1.
- [26] Reinier van Rossum. *Discussion with Heerema Engineering Solutions about installation techniques*. Delft, Feb. 2022.
- [27] Dan Kyle Spearman, Sam Strivens, Denis Matha, Nicolai Cosack, Alan Macleay, Jeroen Regelink, Darren Patel, and Tim Walsh. “Phase III - Summary Report - Floating Wind Joint Industry Project”. In: *Carbon Trust* (2020).
- [28] Carl Petter Halvorsen. *Mooring Solutions*. Feb. 2021.
- [29] Ideal Offshore. “Ideol, A breakthrough floating foundation”. In: (2021).
- [30] K. E. Steen. “Hywind Scotland - status and plans”. In: *EERA DeepWind 2016* (2016). URL: https://www.sintef.no/globalassets/project/eera-deepwind-2015/presentations/closing/rune-yttervik_statoil.pdf.
- [31] H. Irvine. *Cable Structures*. MIT Press Series. Vol. I. Massachusetts Institute of Technology, 1992.
- [32] Subrata K Chakrabarti. *Handbook of Offshore Engineering*. Vol. II. 2005. ISBN: 9780080445687.
- [33] Marco Masciola, Jason M Jonkman, and Amy N Robertson. “Implementation of a Multisegmented, Quasi-Static Cable Model”. In: 2013.
- [34] Mathew Hall, Stein Housner, Senu Srinivas, and Samuel Wilson. *MoorPy (Quasi-Static Mooring Analysis in Python)*. June 2021.
- [35] A H Pevrot and A M Goulois. “Analysis of cable structures”. In: *Computers & Structures* 10.5 (1979), pp. 805–813. ISSN: 0045-7949. DOI: [https://doi.org/10.1016/0045-7949\(79\)90044-0](https://doi.org/10.1016/0045-7949(79)90044-0). URL: <https://www.sciencedirect.com/science/article/pii/0045794979900440>.
- [36] Stefan C Endres, Carl Sandrock, and Walter W Focke. “A simplicial homology algorithm for Lipschitz optimisation”. In: *Journal of Global Optimization* 72.2 (2018), pp. 181–217. ISSN: 1573-2916. DOI: 10.1007/s10898-018-0645-y. URL: <https://doi.org/10.1007/s10898-018-0645-y>.
- [37] Hugo Kerckhoffs. *Mooring systems: literature study*. Tech. rep. 2022.
- [38] Jinsong Liu, Edwin Thomas, Lance Manuel, D Griffith, Kelley Ruehl, and Matthew Barone. “Integrated System Design for a Large Wind Turbine Supported on a Moored Semi-Submersible Platform [59]”. In: *Journal of Marine Science and Engineering* 6 (June 2018), p. 9. DOI: 10.3390/jmse6010009.
- [39] Christopher Allen, Anthony Viselli, Habib Dagher, Andrew Goupee, Evan Gaertner, Nikhar Abbas, Matthew Hall, and Garrett Barter. “Definition of the UMaine VoltornUS-S Reference Platform Developed for the IEA Wind 15-Megawatt Offshore Reference Wind Turbine”. In: (2020), p. 41.
- [40] Andrew Clayson. “Developments in Subsea Tensioning of Mooring Lines”. In: *SNAME Offshore Symposium* (Feb. 2018).
- [41] Robert Garrity and William Fronzaglia. “The use of HMPE mooring lines in deepwater MODU mooring systems”. In: *OCEANS 2008*. 2008, pp. 1–4. DOI: 10.1109/OCEANS.2008.5151912.
- [42] Josh Davidson and John Ringwood. “Mathematical Modelling of Mooring Systems for Wave Energy Converters—A Review”. In: *Energies* 10 (June 2017). DOI: 10.3390/en10050666.
- [43] Frederico Cerveira, Nuno Fonseca, and Ricardo Pascoal. “Mooring system influence on the efficiency of wave energy converters”. In: *International Journal of Marine Energy* 3-4 (2013), pp. 65–

81. ISSN: 2214-1669. DOI: <https://doi.org/10.1016/j.ijome.2013.11.006>. URL: <https://www.sciencedirect.com/science/article/pii/S2214166913000325>.
- [44] Lixian Zhang, Wei Shi, Madjid Karimirad, Constantine Michailides, and Zhiyu Jiang. "Second-order hydrodynamic effects on the response of three semisubmersible floating offshore wind turbines". In: *Ocean Engineering* 207 (2020), p. 107371. ISSN: 0029-8018. DOI: <https://doi.org/10.1016/j.oceaneng.2020.107371>. URL: <https://www.sciencedirect.com/science/article/pii/S0029801820304029>.
- [45] Christopher Allen, Anthony Viselli, Habib Dagher, Andrew Goupee, Evan Gaertner, Nikhar Abbas, Matthew Hall, and Garrett Barter. *15MW reference wind turbine repository developed in conjunction with IEA Wind*. 2020.
- [46] Halvor Lie, Zhen Gao, and Torgeir Moan. "Mooring Line Damping Estimation by a Simplified Dynamic Model". In: *Proceedings of the International Conference on Offshore Mechanics and Arctic Engineering - OMAE*. Vol. 1. May 2007. DOI: 10.1115/OMAE2007-29155.
- [47] Sebastian Schreier. *OE44100 Floating Structures and Offshore moorings*. Delft, 2021.
- [48] Idtz Wieling. *Website of Aqitec Engineering*. 2022.
- [49] V J Kurian, Yassir Abbas, C Y Ng, and Indra Harahap. "Nonlinear Dynamic Analysis of Multi-component Mooring Lines Incorporating Line-seabed Interaction". In: *Research Journal of Applied Sciences, Engineering and Technology* 6 (June 2013), pp. 1428–1445. DOI: 10.19026/rjaset.6.3967.
- [50] B Mutlu Sumer and Veysel Sadan Ozgur Kirca. "Scour and liquefaction issues for anchors and other subsea structures in floating offshore wind farms: A review". In: *Water Science and Engineering* 15.1 (2022), pp. 3–14. ISSN: 1674-2370. DOI: <https://doi.org/10.1016/j.wse.2021.11.002>. URL: <https://www.sciencedirect.com/science/article/pii/S1674237021001174>.
- [51] Carlyle Webb and Marco van Vugt. "Offshore Construction – Installing the World’s Deepest FPSO Development". In: 2017.
- [52] Dan Kyle Spearman, Sam Strivens, Denis Matha, Nicolai Cosack, Alan Macleay, Jeroen Regelink, Darren Patel, and Tim Walsh. "Phase I- Summary Report - Floating Wind Joint Industry Project". In: *Carbon Trust* (2018).
- [53] Tom Quinn. "Using floating offshore wind to power oil and gas platforms". In: *Catapult Offshore Renewable Energy* (2021).
- [54] Hyun Soo Kim, Seong Yeob Jeong, Sun Hong Woo, and Donghwa Han. "Study on the procedure to obtain an attainable speed in pack ice". In: *International Journal of Naval Architecture and Ocean Engineering* 10.4 (July 2018), pp. 491–498. ISSN: 20926790. DOI: 10.1016/j.ijnaoe.2017.09.004.
- [55] Matthijs Stofregen. *Interview with Matthijs Stofregen, Dynamic simulation engineer*. 2022.
- [56] Arvind Thiruvengadam, Saroj Pradhan, Pragalath Thiruvengadam, Marc Besch, Daniel Carder, and Oscar Delgado. *Efficiency Evaluation and Energy Audit Final Report The International Council on Clean Transportation*. Tech. rep. 2014.
- [57] Raimonds Aronietis, Christa Sys, Edwin van Hassel, and Thierry Vanelislander. "Forecasting port-level demand for LNG as a ship fuel: the case of the port of Antwerp". In: *Journal of Shipping and Trade* 1 (May 2016). DOI: 10.1186/s41072-016-0007-1.
- [58] Wilson Guachamin Acero, Lin Li, Zhen Gao, and Torgeir Moan. "Methodology for assessment of the operational limits and operability of marine operations". In: *Ocean Engineering* 125 (2016), pp. 308–327. ISSN: 00298018. DOI: 10.1016/j.oceaneng.2016.08.015. URL: <http://dx.doi.org/10.1016/j.oceaneng.2016.08.015>.

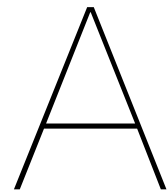
List of Figures

2.1	Mooring concepts: Taut moorings, catenary moorings and their combination: Semi-taut	7
2.2	Mooring system lay-out for Hywind Scotland	9
2.3	Procedure for chain attachment to the suction bucket. [22]	9
2.4	Mooring attachment detail. [23]	9
2.5	Mooring system lay-out for Hywind Tampen	10
2.6	Mooring system lay-out for Windfloat Atlantic	10
2.7	Stiesdal Tetraspar floating substructure concept. Original from Tetraspar description [21]	11
2.8	Mooring systematic overview of different components	12
2.9	Drag anchor installation	13
2.10	Ground chain lay out on the seabed and proof loading of anchor	13
2.11	Preload operation of mooring line. For one the of the three legs, the seabed tensioner is deployed too.	14
2.12	Towing of the FOWT, arrival at site and transfer of messenger line to prepare hook-up. .	14
2.13	Hooking up the three mooring lines to the FOWT to create a storm-safe situation	15
2.14	Pre-tensioning operation using a seabed tensioner	15
2.15	Seabed tensioning	16
2.16	Inline tensioning	16
2.17	Fairlead tensioning	17
2.18	Single line definitions for a hanging catenary. Altered symbol for wet specific weight of mooring line. Original from Irvine[31]	18
2.19	Single line definitions for a catenary touching a bottom boundary with friction. Symbol γ is added. Original from Irvine[31]	19
3.1	Architecture of the model code.	23
3.2	Flowchart of the building process of a complete system	24
3.3	Illustration of the relation between bodies, lines and points in the static model	25
3.4	Schematic overview of the forces during a pre-tension operation using a fairlead tensioner.	27
3.5	Methodology of including a sliding point in the mooring system	27
3.6	Tension differences at the wheel for a range of x	28
3.7	The UMaine VoltturnUS-S reference platform[39]	29
3.8	Mooring system	30
3.9	Anchor handling vessel 'CBO Iguacu'	31
3.10	Tensioning configurations for three tensioners at the beginning and the end of the operation.	32
4.1	Simulation of the mooring system of the Umaine VoltturnUS-S.	34
4.2	Static tensions while tensioning using a seabed tensioner	36
4.3	Static tensions while tensioning using an inline tensioner	36
4.4	Static tensions while tensioning using a fairlead tensioner	37
4.5	Mooring configuration with inserts visualisation and restoring force comparison	39
4.6	Configurations during the start and finish of the seabed pre-tensioning with inserts	40
4.7	Configurations during the start and finish of the inline pre-tensioning with inserts	40
4.8	Configurations during the start and finish of the fairlead pre-tensioning with inserts	40
5.1	Kinetic diagrams for dynamic simulation	43
5.2	Added mass entries for the Umaine semi-submersible floater	45
5.3	Radiation damping for the Umaine semi-submersible floater	45
5.4	Wave induced force coefficients	46
5.5	Surge, heave and pitch motion for the CBO Iguacu	47

5.6	Non-linear relation between FOWT surge and restoring force of a mooring line. However, for small oscillation movement, the curve is more linear.	49
5.7	Spring configuration of inline tensioning	49
5.8	Spring configuration of fairlead tensioning	50
5.9	Code structure for dynamic simulations and tension quantification	53
6.1	Validation of motion responses for the FOWT	55
6.2	Dynamic behaviour while begin of inline tensioning	56
6.3	Dynamic behaviour while halfway of inline tensioning	57
6.4	Dynamic behaviour while end of inline tensioning	57
6.5	Dynamic behaviour while begin of fairlead tensioning	58
6.6	Dynamic behaviour while halfway of fairlead tensioning	58
6.7	Dynamic behaviour while end of fairlead tensioning	59
6.8	Difference between modelled linear spring stiffness and actual movement	60
6.9	Dynamic tensions while fairlead tensioning using altered stiffness matrix	60
6.11	FFT analysis on the dynamic tensions between the FOWT and the tensioner	61
6.10	Validation study performed by Aqitec to show catenary motion	61
A.1	Added mass matrix and damping matrix entries for translation modes	77
A.2	Added mass matrix and damping matrix entries for moment rotation modes	77
A.3	Added mass matrix and damping matrix entries for Force translation and moment rotation modes	78
A.4	First-order wave excitation coefficients for forces in surge and heave direction	78
A.5	First-order wave excitation coefficients for moment in pitch direction	78
A.6	First-order wave excitation coefficients for motion and phase in surge and heave direction of the AHV	79
A.7	First-order wave excitation coefficients for motion and phase in pitch direction of the AHV	79

List of Tables

2.1	Overview of floating substructure concepts	6
2.2	Summary of the results of three NTNU researches to compare substructure types	6
2.3	FOWT mooring installation characteristics, critical events and comparison with oil and gas.	20
3.1	Introduction of the parameters used to construct a mooring simulation	23
3.2	Information of UMaine 15 MW floater[39]	30
3.3	Information of Umaine mooring system	31
3.4	Information of CBO Iguacu	32
3.5	Information on the pre-tensioning cases	32
4.1	Validation of model results against Umaine platform description	35
4.2	Results of pre-tensioning operation static simulation with original mooring system	37
4.3	Information of the alternative mooring configuration for the Umaine floater with Dyneema inserts	39
4.4	Results of pre-tensioning operation static simulation with mooring system with inserts	41
6.1	Model validation by comparing the natural frequencies, calculated by the model, with the specified natural frequencies in the Umaine description	55
7.1	Overall comparison of the pre-tension methods to conclude the research outcomes	65



Complete RAO descriptions

A.1. FOWT

Added mass and damping:

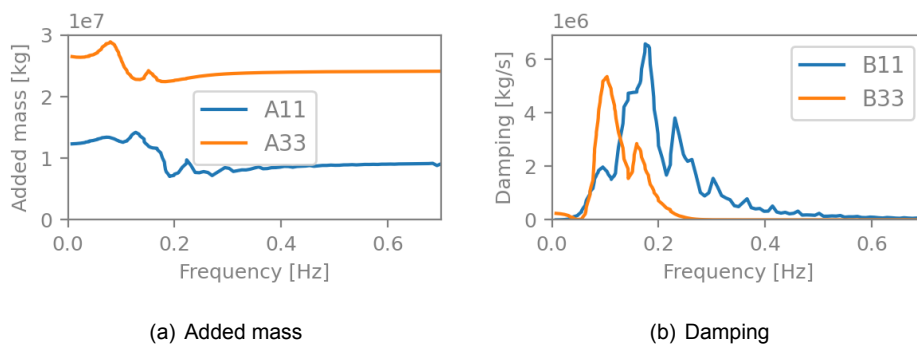


Figure A.1: Added mass matrix and damping matrix entries for translation modes

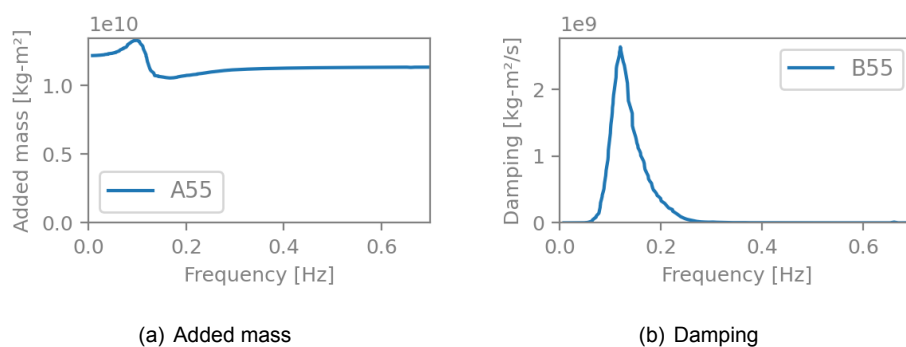


Figure A.2: Added mass matrix and damping matrix entries for moment rotation modes

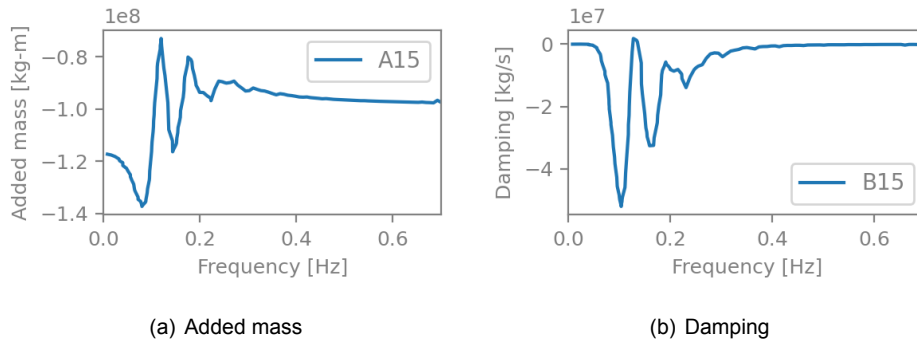


Figure A.3: Added mass matrix and damping matrix entries for Force translation and moment rotation modes

Wave forcing:

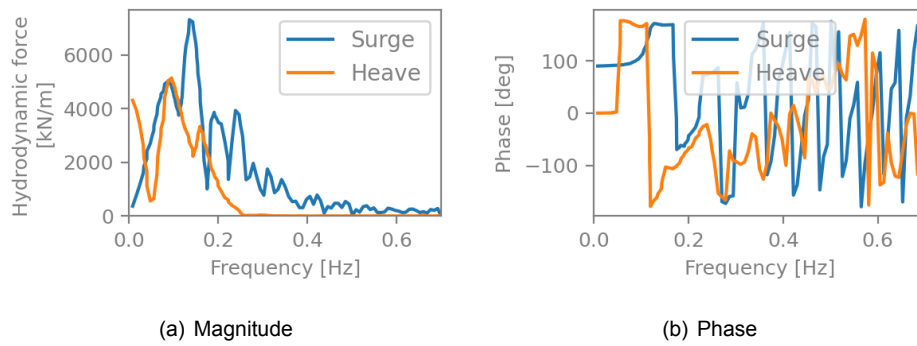


Figure A.4: First-order wave excitation coefficients for forces in surge and heave direction

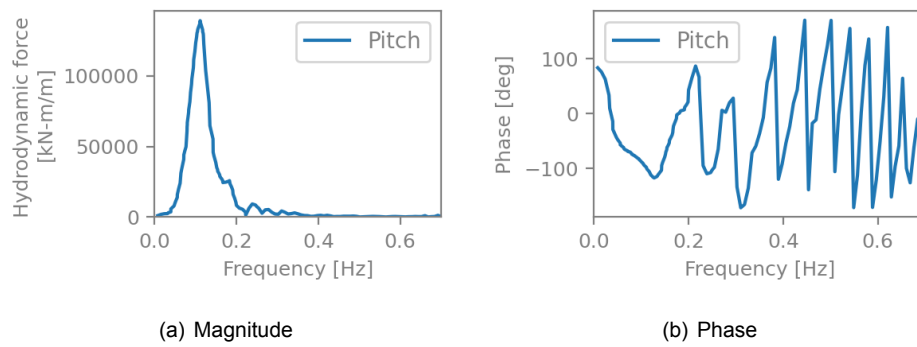


Figure A.5: First-order wave excitation coefficients for moment in pitch direction

A.2. AHV

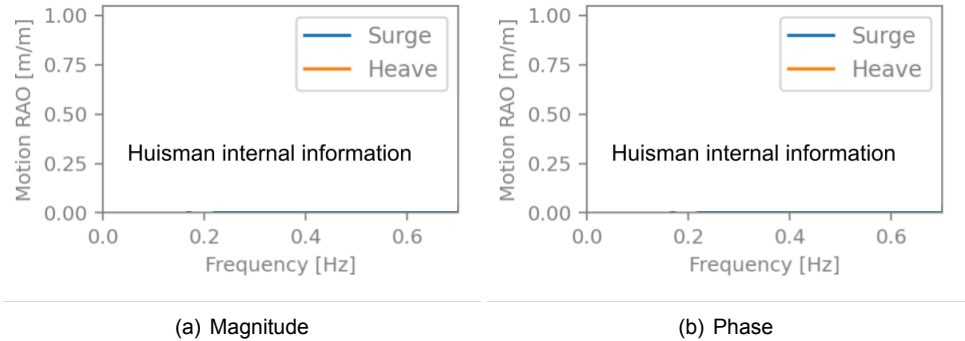


Figure A.6: First-order wave excitation coefficients for motion and phase in surge and heave direction of the AHV

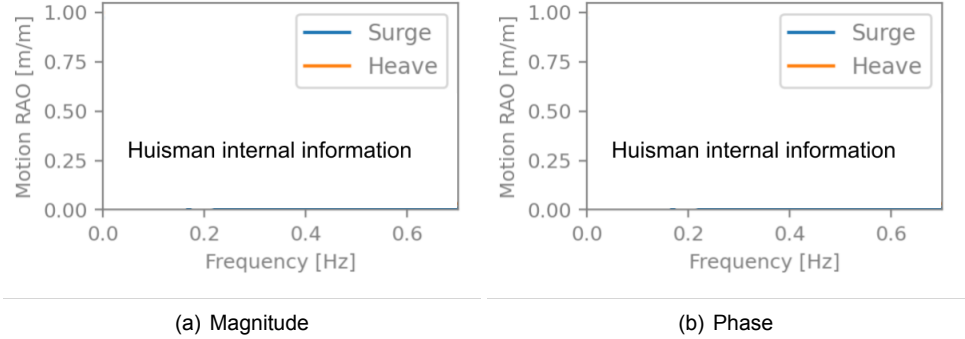


Figure A.7: First-order wave excitation coefficients for motion and phase in pitch direction of the AHV

B

Matrix specifications

B.1. Inline tensioning

The mass and added mass matrix, with the added mass terms as specified in appendix A.1

$$(M + A) = \begin{bmatrix} m_f + A_{11}(\omega) & 0 & A_{15}(\omega) & 0 & 0 \\ 0 & m_f + A_{33}(\omega) & 0 & 0 & 0 \\ A_{15}(\omega) & 0 & J_f + A_{55}(\omega) & 0 & 0 \\ 0 & 0 & 0 & 1.51m_t & 0 \\ 0 & 0 & 0 & 0 & 1.51m_t \end{bmatrix} \quad (\text{B.1})$$

The damping matrix is the sum of the viscous damping, as specified in matrix 5.8 and the ration damping, as specified in appendix A.1.

$$B = \begin{bmatrix} 9.225\text{E}5 + B_{11}(\omega) & 0 & -8.918\text{E}6 + B_{15}(\omega) & 0 & 0 \\ 0 & 2.296\text{E}6 + B_{33}(\omega) & 0 & 0 & 0 \\ -8.918\text{E}6 + B_{15}(\omega) & 0 & 1.676\text{E}10 + B_{55}(\omega) & 0 & 0 \\ 0 & 0 & 0 & 0 & 0 \\ 0 & 0 & 0 & 0 & 0 \end{bmatrix} \quad (\text{B.2})$$

The stiffness matrix is the sum of the hydrostatic stiffness for the FOWT, as specified in matrix 5.10, and the restoring forces of the mooring lines, as specified in matrix 5.15.

$$K = \begin{bmatrix} k_{1,x} + k_{4,x} & 0 & -8.91\text{E}6 & -k_{4,x} & 0 \\ 0 & 4.47\text{E}6 + k_{1,z} + k_{4,z} & k_{1,z}r_l - k_{4,z}r_r & -k_{4,z} & 0 \\ -8.91\text{E}6 & k_{1,z}r_r - k_{4,z}r_l & 2.19\text{E}9 + k_{1,z}r_r^2 + k_{4,z}r_l^2 & k_{4,z}r_l & 0 \\ k_{2,x} - k_{4,x} & 0 & 0 & k_{3,x} + k_{4,x} & 0 \\ 0 & -k_{4,z} & k_{4,z}r_l & k_{4,z} & k_{3,z} \end{bmatrix} \quad (\text{B.3})$$

The force matrix, which has components due to hydrodynamic forcing on the FOWT, as specified in section 5.2.1 and external forcing due to implied AHV motion as described in section 5.2.3.

$$F = \begin{bmatrix} F_{f,hydr,x}(\omega) \\ F_{f,hydr,z}(\omega) \\ M_{f,hydr}(\omega) \\ k_{3,x} x_v \\ k_{3,z} x_z \end{bmatrix} \quad (\text{B.4})$$

B.2. Fairlead tensioning

The mass and added mass matrix, with the added mass terms as specified in appendix A.1

$$(M + A) = \begin{bmatrix} m_f + A_{11}(\omega) & 0 & A_{15}(\omega) \\ 0 & m_f + A_{33}(\omega) & 0 \\ A_{51}(\omega) & 0 & J_f + A_{55}(\omega) \end{bmatrix} \quad (\text{B.5})$$

The damping matrix is the sum of the viscous damping, as specified in matrix 5.8 and the ration damping, as specified in appendix A.1.

$$B = \begin{bmatrix} 9.225\text{E}5 + B_{11}(\omega) & 0 & -8.918\text{E}6 + B_{15}(\omega) \\ 0 & 2.296\text{E}6 + B_{33}(\omega) & 0 \\ -8.918\text{E}6 + B_{51}(\omega) & 0 & 1.676\text{E}10 + B_{55}(\omega) \end{bmatrix} \quad (\text{B.6})$$

The stiffness matrix is the sum of the hydrostatic stiffness for the FOWT, as specified in matrix 5.10, and the restoring forces of the mooring lines, as specified in matrix 5.16.

$$K = \begin{bmatrix} k_{1,x} + k_{2,x} + k_{3,x} & 0 & 0 \\ 0 & k_{1,z} + k_{2,z} & k_{1,z}r_r - k_{2,z}r_l \\ 0 & k_{1,z}r_r - k_{2,z}r_l & k_{1,z}r_r^2 + k_{2,z}r_l^2 \end{bmatrix} \begin{bmatrix} x_f \\ z_f \\ \theta_f \end{bmatrix} \quad (\text{B.7})$$

The force matrix, which has components due to hydrodynamic forcing on the FOWT, as specified in section 5.2.1 and external forcing due to implied AHV motion as described in section 5.2.3.

$$F = \begin{bmatrix} F_{f,hydr,x}(\omega) + k_{3,x}x_v \\ F_{f,hydr,z}(\omega) \\ M_{f,hydr}(\omega) \end{bmatrix} \quad (\text{B.8})$$